CHAPERONE LIMITATIONS IN PRION CURING

by

Xuezhen Ge

A Dissertation Submitted to the Faculty of the

DEPARTMENT OF MOLECULAR AND CELLULAR BIOLOGY

In Partial Fulfillment of the Requirements

For the Degree of

DOCTOR OF PHILOSOPHY

In the Graduate College

THE UNIVERSITY OF ARIZONA

2019

THE UNIVERSITY OF ARIZONA
GRADUATE COLLEGE

As members of the Dissertation Committee, we certify that we have read the dissertation prepared by Xuezhen Ge, titled Chaperone Limitations In Prion Curing and recommend that it be accepted as fulfilling the dissertation requirement for the Degree of Doctor of Philosophy.

Dr. Andrew Capaldi — Date: 8/23/19

Dr. Tricia Serio — Date: 8/23/19

Dr. Ross Buchan — Date: 8/23/19

Dr. Eli Chapman — Date: 8/23/19

Dr. Carol Dieckman — Date: 8/23/19

Final approval and acceptance of this dissertation is contingent upon the candidate's submission of the final copies of the dissertation to the Graduate College.

I hereby certify that I have read this dissertation prepared under my direction and recommend that it be accepted as fulfilling the dissertation requirement.

Andrew P Capaldi (Dec 5, 2019) — Date: Dec 5, 2019

Dr. Andrew Capaldi
Dissertation Committee Chair
Department of Molecular and Cellular Biology

2

ACKNOWLEDGEMENTS

First, I would like to thank my thesis advisor, Dr. Tricia Serio, for her guidance and support in my training. She gives me the freedom to pursue the topic I am excited about, allows me to make mistakes and learn from them, and leads me when I navigate through unproductive routes. I learn from her how to conduct research in a rigorous way and review literature critically and get inspired frequently by her passion for research. She truly leads me to the door of scientific research.

I would also like to thank my committee members, Dr. Andrew Capaldi, Dr. Ross Buchan, Dr. Eli Chapman, and Dr. Carol Dieckman for their help throughout my training. Their critical feedback always motivates me to think harder and be aware of potential caveats and alternative explanations. Besides, I would like to thank Dr. Jeff Laney, Dr. Peter Chien, Dr. Eric Strieter, and Dr. Margaret Stratton for their advice and scientific suggestions.

Furthermore, I have to thank everyone in the Serio lab; Wes, Courtney, Christine, Jenny, Fen, Teal, Nicole, and Afua. They have not only given me a lot of help but also offered great friendships. Because of them, working in the lab and attending seminars is fun and exciting, and fun activities with them outside the lab make life colorful.

Lastly, I would like to thank my family, especially my wife Luwen, for their encouragement and unconditional love. Their confidence in me gives me the courage to pursue what I love.

TABLE OF CONTENTS

LIST OF TABLES

Chapter 2:

Chapter 3:

LIST OF FIGURES

Chapter 1:

Chapter 2:

Abstract

Amyloid promotes a dramatic transition in protein conformation that perpetuates, giving rise to a broad variety of distinct phenotypes, ranging from pathological disorders to dynamic heritable traits. Amyloid has long been thought to be resistant to clearance by the proteostasis network, but increasing evidence is challenging this view. For example, heat shock disassembles yeast prion amyloids, revealing *in vivo* solubilization of these aggregates. However, the exact proteostatic niche that promotes amyloid clearance is largely unknown. We identified several environmental stresses leading to prion curing via the same mechanism as heat shock and further showed that a shared characteristic was the activation of the transcription factor heat shock factor 1 (Hsf1). Strikingly, artificial Hsf1 activation interfered with heat shock-mediated prion curing, presumably due to overexpression of a nucleotide exchange factor Sse1. Limiting Sse1, which decelerates the Hsp70 cycle, promoted chaperone loading on prion aggregates and enabled artificial Hsf1 activation to resolve prion aggregates; in contrast, it impaired resolution of stress-induced aggregates and cell growth at elevated temperature. Thus, our study demonstrates that the proteostasis network, fine-tuned for optimal dissolution of non-amyloid aggregates, can be reconfigured for solubilization of amyloid by modulating the Hsp70 cycle.

Chapter 1:

Introduction

The Prion Hypothesis

The traditional view that phenotypes are exclusively encoded in nucleic acids was challenged when the prion hypothesis was proposed. According to this hypothesis, a protein-based infectious agent underlies a group of diseases known as the transmissible spongiform encephalopathies (TSEs) (Griffith, 1967; Prusiner, 1982). Although these diseases, such as mad cow disease in cattle, scrape in sheep, kuru and Creutzfeldt-Jakob disease (CJD) in humans, exist across multiple species with diverse pathologies, a common feature is that the causative agent is resistant to methods known to destroy nucleic acids and becomes inert only by methods that denature protein (Alper et al., 1967; Prusiner, 1982). These observations imply a distinct nature of the infectious element - protein-only.

The once heretical concept of a proteinaceous infectious agent has been supported by numerous studies and gradually accepted as the basis of these transmissible pathologies. The prion that correlates with scrapie infectivity was first identified from scrapie-infected hamster brain (Bolton et al., 1982) and designated PrP for proteinaceous infectious particle (McKinley et al., 1983). The observation that animals with no PrP protein are resistant to TSEs confirms the crucial role of PrP protein in the development of these diseases (Büeler et al., 1993; Prusiner et al., 1993; Sailer et al., 1994).

According to the hypothesis, the prion protein has two forms, one form with native conformation (PrP^{C}) and another with the infectious or prion conformation (PrP^{Sc}), which

is only present in animals with TSE. PrP^{Sc} has the ability to convert PrP^{C} into the prion form, allowing the infectious conformation to self-replicate and conferring the novel biological outcomes associated with this state (Prusiner, 1998). This conversion process can be recapitulated *in vitro* using substantially purified components, suggesting that specific PrP^{C}-PrP^{Sc} interactions mediate the conformational replication of PrP^{Sc} (Kocisko et al., 1994). Furthermore, an *in vitro* technique known as cyclic amplification of protein misfolding, in which PrP^{C} is iteratively added to PrP^{Sc} after repeated rounds of sonication, increases the efficiency of *in vitro* conversion to the point that sufficient material can be generated to evoke the pathologies of scrapie when inoculated into wild-type hamsters (Castilla et al., 2005; Saborio et al., 2001; Wang et al., 2010). Thus, the hypothesis that prions are the causative agent of TSEs is firmly established.

Yeast Prions

The discovery of yeast prions not only bolsters the prion hypothesis but also expands its relevance from disease-causing agents to epigenetic regulators of phenotypes (Tuite and Serio, 2010). The first confirmed yeast prion was [*URE3*], a prion form of Ure2 protein, a negative regulator of nitrogen metabolism (Wickner, 1994), and in this work, the author proposed that another yeast epigenetic phenotype [*PSI*$^{+}$] was also a prion. Shortly after that, [*PSI*$^{+}$] was demonstrated to be a self-replicating conformation of the translation termination factor Sup35 through differential centrifugation analysis and microscopy of a Sup35-GFP fusion (Patino et al., 1996; Paushkin et al., 1996). Remarkably, a systematic proteome-wide survey using bioinformatics and experimental validation identified 19

potential yeast prions, revealing the prevalence of self-perpetuating protein conformations in yeast (Alberti et al., 2009). These diverse prion proteins offer a tractable experimental system to elucidate the processes necessary to create protein-based elements encoding heritable traits, ranging from its *de novo* formation and propagation to destabilization and clearance.

Although it is still unclear how the mammalian prion PrP^{Sc} causes diseases in mammals, yeast prions explicitly demonstrate how alternative self-replicating conformations lead to distinct phenotypes, especially for [*PSI*$^{+}$] and [*URE3*]. For example, [*PSI*$^{+}$] is formed by a translation termination factor Sup35. The N-terminal domain (N; aa 1-125) enriched in glutamine and asparagine along with middle domain (M; aa 126-254) is sufficient to maintain the prion state while C-terminal domain (C; aa 255-685) is responsible for translation termination and required for viability (Derkatch et al., 1996; Liu et al., 2002; Patino et al., 1996; Ter-Avanesyan et al., 1993). In a strain background with a pre-mature stop-codon in the *ADE1* or *ADE2* gene, translation of Ade1/2 is disrupted, leading to buildup of an intermediate with red pigment and consequently red colonies (Chernoff et al., 1995; Cox, 1965; Fisher, 1969). In [*PSI*$^{+}$] cells, the conformational conversion of Sup35 promotes its incorporation into aggregates retaining limited function (Pezza et al., 2014). As a consequence, stop codons are read through, a process known as nonsense suppression, and this event allows the complete synthesis of Ade1/2 and eliminates the production of red pigment, resulting in white colonies. In the case of the [*URE3*] phenotype, Ure2, which is involved in nitrogen metabolism, also becomes aggregated, leading to the loss of its normal function to restrict the use of poor nitrogen sources during growth

(Wickner, 1994). As a consequence, [*URE3*] strains grow on ureidosuccinate in the presence of glutamate, while [*ure-o*] strains cannot.

Besides these well-studied prions, a number of additional yeast proteins have also been characterized as prion proteins. [*PIN*$^+$] is formed by the prion protein Rnq1 (Sondheimer and Lindquist, 2000). It is still unknown what is the exact function of this protein; however, [*PIN*$^+$] is required for the *de novo* formation of other yeast prions, a gain-of-function phenotype (Derkatch et al., 1997, 2001). [*SWI*$^+$], formed by conformational conversion of Swi1, a factor involved in the chromatin remodeling complex, is reported to form prion aggregates, causing a partial loss-of-function phenotype and changes in transcriptional regulation (Du et al., 2008). [*OCT*$^+$] and [*MOT3*$^+$], formed by unique conformations of the global transcription co-repressor Cyc8 and the globally acting transcription factor Mot3 respectively, are involved in remodeling of transcriptional states (Alberti et al., 2009; Patel et al., 2009). Together with [*PSI*$^+$] and [*URE3*], the diverse proteins exhibiting functional regulation through a prion mechanism suggest that this pathway is a potentially universal mechanism of epigenetic regulation. Without modifying the genome, organisms can create phenotypic diversity readily by adopting a self-replicating conformation, perhaps offering some advantages for adaptability (True and Lindquist, 2000).

Conformational Self-Replication

Generally speaking, elements of inheritance must satisfy two criteria. First, the information encoding a trait must be replicated readily so that extra copies are available

for transmission; second, the information must be passed on to re-establish the phenotype in a new individual. The prion hypothesis posits that the prion form of a protein must convert like proteins of the native form to the prion state, ensuring the replication of the prion phenotype. For the mammalian prion protein PrP, PrP^C can be converted to a protease-resistant form, a property of PrP^{Sc}, both *in vivo* and *in vitro* (Kocisko et al., 1994; Saborio et al., 2001). The *in vitro*-generated protease-resistant form assembles into linear aggregates known as fibers, which share similar biochemical and structural properties with the *ex vivo* scrapie agent and can be inoculated into healthy animals to induce a scrapie disease, indicating faithful replication (Castilla et al., 2005). Likewise, Sup35 fibers efficiently convert soluble Sup35 to the prion form *in vitro* (Glover et al., 1997; King et al., 1997; Serio et al., 2000; Taylor et al., 1999). Introducing *in vitro*-generated Sup35 fibers, generated from an *ex vivo* template, into yeast cells leads to the development of a prion phenotype that is indistinguishable from that of initial prions (King and Diaz-Avalos, 2004). Furthermore, fibers formed from Sup35, Ure2, and Rnq1, can also be spontaneously formed *in vitro* and give rise to *de novo* prion phenotypes once transformed into prion-free yeast cells (Brachmann et al., 2005; King and Diaz-Avalos, 2004; Patel and Liebman, 2007; Tanaka et al., 2004). These studies illustrate the robust conversion and replication of the prion conformation.

The structural characteristics of the fibers themselves confers the capability to recruit and convert like proteins to the prion conformation. Scrapie-associated forms of PrP adopt the amyloid structure, enriched in cross-β sheets that exhibit apple-green birefringence under polarized light (Dearmond et al., 1985). The mechanism by which amyloidogenic proteins,

including prion proteins, polymerize has been extensively examined, revealing a nucleated growth mechanism (Naiki et al., 1991; Pedersen et al., 2004; Serio et al., 2000; Uversky et al., 2002). Specifically, a thermodynamically stable aggregate of minimum size (i.e. the nucleus) is assembled during a lag phase, and this aggregate grows through the incorporation of non-prion protein onto fiber ends during a rapid exponential growth phase. The lag phase can be shortened or eliminated by adding preformed seeds. This shared self-replication process underlies the link between amyloidogenic proteins and prion proteins.

Despite the structural and conformational self-replication similarities, the second criterion - transmissibility - separates prion proteins from non-prion amyloids. Mammalian prions spread throughout the central nervous system readily (Baldauf et al., 1998; Fraser, 1982) and to new individuals infectiously (Prusiner, 1998). Spreading of non-prion amyloid is rather limited, such as to neighboring cells (Nath et al., 2012); however, it has recently been proposed that human amyloid-β associated with cerebral amyloid angiopathy can be transmitted in a prion-like manner albeit through an iatrogenic route (Jaunmuktane et al., 2015). While more evidence is needed to substantiate the claim, the idea that non-prion amyloids can be transmitted infectiously may lead to an expansion of the impact of protein-based traits in biology.

Prion Propagation in vivo

Moving from conformational self-replication *in vitro* to prion persistence *in vivo*, there are several steps, some common and some unique to the cellular environment, that must take place (Figure 1). As is the case *in vitro*, the first step of prion propagation *in vivo* is conversion, allowing replication of the prion conformation and thereby altering the function of associated protein and creating the prion-associated phenotype (Tuite and Serio, 2010). The next step - fragmentation - is essential to prion propagation as it creates more templates for conversion, which substantially increases the conversion rate (Tuite and Serio, 2010). This event also reduces the size of prion aggregates and improves their mobility (Tuite and Serio, 2010). Lastly, prion aggregates must be transmitted to progeny/other individuals to faithfully establish the phenotype in the next generation or another host (Tuite and Serio, 2010). Here, I will detail the current understanding of these processes and their underlying mechanisms.

Conversion is an essential step to increase the amount of protein present in a prion conformation, and its efficiency is not only determined by the specific amyloid structure but also by the number of ends of the amyloid fibrils, where soluble monomers can join. Conversion *in vitro* has been discussed earlier. The *in vivo* process has also been reported. PrP conversion *in vivo* is indirectly inferred by the observation that PrP^{Sc} is synthesized and degraded much slower than PrP^{C} assayed by pulse-chase experiments (Borchelt, 1990; Caughey and Raymond, 1991). For the yeast prion protein Sup35, conversion of pre-existing soluble prion protein occurs, and this conformational change is simultaneously accompanied by a phenotypic change, directly demonstrating *in vivo*

conversion and its relevance to the emergence of prion traits (Satpute-Krishnan and Serio, 2005).

Fragmentation is critical for prion propagation in several ways. First, it breaks apart the prion fibrils and creates more aggregates for conversion and transmission (Cox et al., 2003; Ness et al., 2002; Satpute-Krishnan et al., 2007). Second, it reduces prion aggregate size and facilitates transmission of prion aggregates (Derdowski et al., 2010). Earlier work has reported that breaking apart PrP fibrils either through adding detergent and phospholipids or sonication in the case of cyclic amplification of protein misfolding can greatly increase infectivity, indicating the significance of fragmentation (Gabizon et al., 1987; Saborio et al., 2001). Although the mechanism by which mammalian prions are fragmented remains unclear, mathematical modeling suggests such a step is required for the spread of the disease (Hall and Edskes, 2004; Masel et al., 1999), and several mammalian disaggregation systems have been proposed, which may be involved in processing prion aggregates (Nillegoda et al., 2018). Like PrP, sonicating Sup35 fibrils generated *in vitro* can also enhance conversion rates (Glover et al., 1997; Serio et al., 2000; Taylor et al., 1999). Unlike PrP, the machinery fragmenting yeast prions *in vivo* has been extensively studied. The molecular chaperones Hsp104, Hsp70, Hsp40 work together to carry out this crucial activity and modulate prion propagation (Chernoff et al., 1995; Higurashi et al., 2008; Jung et al., 2000; Ness et al., 2002; Satpute-Krishnan et al., 2007; Tipton et al., 2008). Of these, the AAA+ ATPase Hsp104 acts as the fragmentase and is required for prion propagation, as deletion of the gene or inactivation of the protein by treatment with GdnHCl eliminates all amyloid-associated yeast prions (Alberti et al.,

2009; Chernoff et al., 1995; Du et al., 2008; Moriyama et al., 2000; Ness et al., 2002; Patel et al., 2009; Rogoza et al., 2010). When Hsp104 is inhibited, prion aggregate size increases, assayed by either semi-denaturing detergent gel electrophoresis (SDD-AGE) or fluorescence microscopy, consistent with a role for Hsp104 in prion aggregate fragmentation (Kryndushkin et al., 2003; Satpute-Krishnan et al., 2007; Wegrzyn et al., 2001). Not surprisingly, as a result of Hsp104 inactivation, prion aggregates become immobile; their amplification ceases, and they are diluted in a population, resulting in the loss of prions from a growing population of cells (Cox et al., 2003; Ness et al., 2002; Satpute-Krishnan et al., 2007). Thus, the crucial roles of Hsp104 in promoting prion propagation are increasing the number of prion aggregates and reducing prion aggregate size.

To ensure spreading of the prion phenotype, the last step - transmission - is required. The spreading of infectivity in scrapie diseases through iatrogenic and consumption routes is well documented (Baldauf et al., 1998; Fraser, 1982), and PrP infectivity peaks with masses equivalent to 14-28 PrP molecules instead of large fibrils, indicating a size dependency (Silveira et al., 2005). For yeast prions, it has been proposed that the transmission of prion aggregates is a passive process that occurs through cell division or mating, with the amount of heritable prion aggregates (propagons) transmitted to daughter cells reflecting the relative volumes of mother and daughter cells (Byrne et al., 2009). Notably, prion aggregate size is linked to transmission efficiency, with smaller prion aggregates being more readily transmitted (Derdowski et al., 2010). Thus, cellular

pathways modulating the prion aggregate size are essential to ensure the transmissibility of prion phenotypes.

These processes act together to determine the phenotypic traits of a prion conformation. Prion proteins, such as Sup35, are usually able to form distinct self-replicating conformations with varying rates of conversion and fragmentation, thereby leading to different distribution of prion aggregate size and presumably different frequency of transmission (Tanaka et al., 2006). These variations lead to heritable and/or transmission differences in the severity and stability of prion phenotypes, known as variants, highlighting the heterogeneity and diversity of the prion phenotypes. Taken together, the *in vivo* propagation of prion aggregates requires the coordination of conversion, fragmentation and transmission, and all of these steps combined generate various spectrums of prion aggregates and thereby phenotypic diversity.

The Interplay Between the Proteostasis Network and Prion Propagation

Prion propagation *in vivo* is the consequence of the physical properties of prion aggregates and the processing by the protein quality control network, especially on the step of fragmentation. The fragmentation machinery is part of a global proteostasis network, designated PN, which has evolved to protect the integrity of the proteome from protein misfolding and aggregation (Morimoto, 2008). Remarkably, increasing studies are unraveling the interplay between the proteostasis network and prion propagation. To fully understand the cellular control of prion propagation through amyloid dynamics, I will first

review the major players of the proteostasis network and then the intricate connections between both.

The Integral Proteostasis Network

A comprehensive proteostasis network composed of molecular chaperones and proteases modulates every step of a protein's life, from protein synthesis to degradation.

Among all the factors, Hsp70 is perhaps the most abundant and versatile chaperone, playing a role in almost every aspect of protein quality control including the *de novo* folding of newly synthesized polypeptides, protein refolding, protein translocation across organelle membranes, the resolution of protein aggregates, and protein triage (Saibil, 2013). The substrate binding and release capabilities of Hsp70, supported by its unique structure, dictates its function, and these activities are finely tuned by Hsp70 regulators, including Hsp40s and nucleotide exchange factors (NEFs). Hsp70 is composed of an N-terminal nucleotide binding domain (NBD), a C-terminal substrate binding domain (SBD) including a β-sheet substrate binding pocket and an α-helical lid, and a flexible linker connecting the two domains, thus mediating allosteric regulation (Rosenzweig et al., 2019). When the NBD is bound by ATP, the lid of the SBD is open, priming Hsp70 for substrate binding (Zhu et al., 1996). When substrate is bound at the binding pocket, usually coupled with binding of Hsp40s at or near the linker between NBD and SBD, ATP hydrolysis will be accelerated, resulting in a conformational change of the lid and stabilization of substrate binding to the ADP-bound Hsp70 (Jiang et al., 2007; Kampinga

and Craig, 2010). Following substrate binding and ATP hydrolysis, nucleotide exchange and allosteric conformational change is facilitated by NEFs, resulting in the release of substrate and recycling Hsp70 for a new cycle (Polier et al., 2008; Schuermann et al., 2008). The substrate will be released to fold freely or transferred to downstream chaperones or proteases (Balchin et al., 2016).

How Hsp70 facilitates protein folding is partially known. Hsp70 recognizes roughly seven -residue segments enriched in hydrophobic amino acids, which are usually hidden in natively folded proteins and exposed in misfolded or unfolded proteins (Rüdiger et al., 1997). Thus, Hsp70 interacts with misfolded or unfolded proteins preferentially and prevents their aggregation, as aggregation is largely driven by hydrophobic forces (Chiti et al., 2003). Although a large number of polypeptides can collapse into their native fold in free solution spontaneously, some chaperone-dependent molecules have to cross substantial kinetic barriers during folding (Frydman, 2001). Hsp70 may bind to kinetically trapped intermediates in the folding process to overcome these kinetic barriers (Sharma et al., 2010), especially for chaperone-dependent protein folding. Thus, Hsp70 acts to stabilize folding intermediates, thus preventing protein misfolding or aggregation and promoting the on-pathway folding processes.

One key factor of the proteostasis network in budding yeast is Hsp104, a disaggregase rescuing misfolded proteins from aggregates (Parsell et al., 1994). This activity is vital for the cells to respond to a variety of stresses (Sanchez et al., 1992), as degradation of protein aggregates is not sufficient for survival following heat stress (Tessarz et al., 2008).

Hsp104 homologues exist in plants (Hsp101), in *E. coli.* (ClpB) and in mitochondria (Hsp78); however, there is no Hsp104 homologue in mammals (Doyle et al., 2013). Among this group, ClpB is the most extensively studied, and these observations provide mechanistic insight into protein disaggregation by Hsp104. Hsp104 is composed of an N-terminal domain (N), two AAA+ ATPase domains (NBD1 and NBD2), a middle domain (M) and a C-terminal (C) domain. The N-terminal domain has been proposed to confer plasticity and potentiation especially for ordered aggregates like amyloids (Sweeny et al., 2015). The conserved AAA+ ATPase domains are sites for ATP binding and hydrolysis and also mediate the oligomerization of Hsp104 monomers into a ring-like hexamer to create a substrate-threading channel. The M-domain controls the Hsp104 ATPase cycle and coordinates the function of Hsp104 and Hsp70 (Mogk et al., 2015). The C-domain is proposed to be involved in oligomerization and the interaction with co-chaperones (Mackay et al., 2008).

Threading polypeptide through its central channel is essential to the function of Hsp104. Engineering Hsp104 to interact with a bacterial ring-like protease ClpP in the yeast cytosol leads to the degradation of unfolded luciferase and prion fibrils, albeit inefficiently, and luciferase and prion protein is detected in $ClpP_{trap}$, an inactive ClpP variant which encapsulates substrates instead of degrading them. Furthermore, the Hsp104 variants with reduced threading activity exhibit impaired protein disaggregation and prion propagation. These data support the idea that Hsp104 can thread misfolded protein substrates from disordered aggregates and prion proteins from amyloid aggregates (Tessarz et al., 2008). With the mechanical force generated by this threading capability,

Hsp104 can extract polypeptide from aggregates, and the released polypeptide can refold into its native conformation spontaneously or with the help of other chaperones (Maillard et al., 2011).

Allosteric regulation of ATP hydrolysis has been extensively studied. The ATPase activities of NBD1 and NBD2 result in conformational changes necessary to generate the force for the threading processes, while the exact mechanism is still being elucidated. Mixtures of ATP and ATP-γS (a slowly hydrolyzable ATP analog) unexpectedly unleash disaggregation and unfolding activity of Hsp104 independent of cochaperones, and ATPase domain mutations also show that impaired hydrolysis at individual NBDs unleashes the remodeling activity of Hsp104 (Doyle et al., 2007). Together, these observations suggest that asymmetric deceleration of Hsp104 ATPase activity promotes its protein remodeling activity. In line with this idea, using different ratios of wild-type & mutant Hsp104 subunits enables the chaperone to disaggregate a diverse repertoire of clients (DeSantis et al., 2012). Hsp104 subunits use probabilistic substrate binding and ATP hydrolysis to resolve disordered aggregates; while several subunits cooperatively engage substrate and hydrolyze ATP to disaggregate ordered aggregates, such as amyloids (DeSantis et al., 2012). Thus, coordination of ATP hydrolysis among the subunits is key to the disaggregation function of Hsp104.

Although Hsp104 can disassemble aggregates independently in special cases, such as in the presence of a mixture of ATP and ATP-γS, it is well accepted that the cooperation of Hsp70 and Hsp104 is mandatory for the disaggregation activities of Hsp104 under

standard conditions *in vitro* and *in vivo*. This framework was first proposed as a genetic interaction and later demonstrated in an *in vitro* study showing that Hsp104 along with Hsp70 can disassemble protein aggregates (Glover and Lindquist, 1998; Sanchez et al., 1993), and numerous studies have confirmed the cooperation of Hsp104 and Hsp70. The M-domain is proposed to be the Hsp70 binding site on Hsp104 (Sielaff and Tsai, 2010), and its positioning at the exterior of the Hsp104 hexameric ring supports the possibility of this interaction (Lee et al., 2007). Hsp104 and its *E. coli.* homologue ClpB collaborate with eukaryotic Hsp70 and *E. coli.* DnaK (i.e. Hsp70) chaperone systems, respectively, to rescue proteins from aggregates (Glover and Lindquist, 1998; Motohashi et al., 1999). However, Hsp104 cannot function in bacteria, and ClpB cannot function in yeast. Chimeric ClpB, having the Hsp104 M-domain, can collaborate with eukaryotic Hsp70, and chimeric Hsp104 with the ClpB M-domain can collaborate with DnaK, revealing the species-specific cooperation of Hsp104 and Hsp70 and the role of M-domain (Miot et al., 2011; Sielaff and Tsai, 2010). Hsp70 targets Hsp104 to heat-induced aggregates and prion aggregates *in vivo,* revealing the collaboration for disaggregation of amorphous and ordered aggregates (Winkler et al., 2012a). Thus, Hsp70 functions upstream to bind substrates and target Hsp104 to its substrates.

Besides Hsp70 and Hsp104, there are also other classes of chaperones in the proteostasis network, such as Hsp90 chaperones, which facilitate the folding of specific substrates (for example, transcriptional factors), small heat shock proteins that function as holdases to prevent protein aggregation, and Hsp60s or chaperonins with a completely isolated chamber for substrates to fold (Kim et al., 2013). All these factors constitute a

comprehensive surveillance system to ensure the native folds of proteins and the integrity of the proteome.

The Adaptability of the Network

The capacity of the protein quality control network is tuned to the needs of the cell. Therefore, the buffering capacity increases in response to environmental stresses. A variety of environmental stresses have been shown to induce a global change of cytoprotective genes, including genes involved in protein folding, degradation and DNA damage repair (Gasch, 2002; Gasch et al., 2000; Verghese et al., 2012). Such activation is mediated by the master transcription factor heat shock factor 1 (Hsf1) and environmental stress response factors Msn2/4 (multicopy suppressor of *snf*) (Verghese et al., 2012). These factors recognize cognate transcriptional regulatory elements in the promoters of their target genes: heat shock element (HSE) and stress response element (STRE), respectively (Verghese et al., 2012).

How does the cell sense proteotoxic conditions and activate stress responses? Hsf1 is conserved from budding yeast to mammals (Anckar and Sistonen, 2011). It has been shown that titration of chaperones serving as repressors of Hsf1 by stress-induced aggregates and phosphorylation are the main mechanisms regulating the activity of mammalian Hsf1, which are also believed to be applicable to yeast Hsf1 (Anckar and Sistonen, 2011). However, a recent study demonstrates that titration of Hsp70 away from Hsf1 by stress-induced aggregates plays a pivotal role in activating Hsf1 while

phosphorylation only positively tunes the extent of Hsf1 activation (Zheng et al., 2016). Activation of Msn2/4 targets under stress conditions is achieved through nuclear import of Msn2/4 (Gorner et al., 1998). Under non-stress conditions, the glucose-responsive cyclic AMP-protein kinase A signaling pathway phosphorylates Msn2/4 to keep them from entering the nucleus, thus repressing their transcriptional activity, while under low glucose conditions, low cAMP-PKA activity allows Msn2/4 to translocate to the nucleus to activate its target genes (Gorner et al., 1998). However, activation of Msn2/4 by heat shock is still poorly understood.

Despite this mechanism to sense misfolded protein aggregates, it is still unclear whether the proteostasis network can detect and respond to the emergence of ordered aggregates, such as prion aggregates. Studies have shown that the presence of prion aggregates either does not elicit a transcriptional response in the case of [*URE3*] or does not change the expression of Hsp104 in the case of [*PSI*$^{+}$] (Eaglestone et al., 1999; Ross and Wickner, 2004). Therefore, it is tempting to speculate that prion aggregates under physiological conditions fail to activate the proteostasis network and therefore evade protein quality control systems.

The Burden of Prion/Amyloid Persistence on the PN

While in most instances, the presence of prion aggregates seems to confer increased tolerance to environmental stress (Eaglestone et al., 1999), there are cases where these aggregates become problematic and impede cell growth. One well-studied case is that

[*PSI*+] makes yeast cells vulnerable to Sup35 overexpression (Dagkesamanskaya and Ter-Avanesyan, 1991; Derkatch et al., 1996). This outcome is the consequence of loss of Sup35 function when the NM domain of Sup35 is overexpressed or sequestration of another essential translation termination factor Sup45 when Sup35 is overexpressed (Pezza et al., 2014; Vishveshwara et al., 2009). Moreover, [*PSI*+] cells have a growth defect when a certain function of Hsp40 Sis1 is missing (Kirkland et al., 2011). Furthermore, the growth defect associated with disruption of the N-terminal acetyltransferase NatA is exacerbated by the [*PSI*+] state (Holmes et al., 2014). Finally, a recent study shows that Ssa1 overexpression causes toxicity in [*PSI*+] cells, perhaps due to competition for cofactors (Keefer and True, 2017). Overall, despite undetectable fitness costs associated with prion aggregates under normal conditions, such costs likely manifest when the protein folding environment is somehow compromised.

As shown earlier, amyloid aggregates have many shared characteristics with prion aggregates. The toxicity of amyloid aggregates has been well studied and involves a multitude of alterations, such as sequestration of essential cellular factors or proteostasis regulators, physical damage to membranes, blocking intracellular trafficking, translation impairment, which all lead to secondary loss-of-function (Mogk et al., 2018).

The first alteration is the most well-studied. Sequestration of essential cellular factors by amyloids was detected using quantitative proteomics to globally monitor the amyloid-affected proteome (Olzscha et al., 2011). Strikingly, the sequestered proteins are relatively large in size and enriched in predicted unstructured regions, likely occupying

hub positions in cellular protein networks. Consequently, a variety of key functions may be affected, eventually resulting in fatal network collapse. Sequestration of proteostasis regulators or alteration to the proteostasis network have also been shown. Polyglutamine protein aggregates in *C. elegans* disrupt protein folding quality control, resulting in loss of function of metastable proteins with destabilizing temperature-sensitive mutations (Gidalevitz et al., 2006). Expression of amyloid-like fibrils leads to a deficiency of the normal cytosolic stress response, limiting the capacity of cells to mount an effective defense (Olzscha et al., 2011). Polyglutamine protein aggregates sequester Sis1 chaperone and interfere with nuclear degradation of cytosolic proteins (Park et al., 2013) and inhibit clathrin-mediated endocytosis in mammalian cells via sequestering Hsc70 (Yu et al., 2014). In summary, amyloid aggregates can highly engage chaperone machinery and titrate chaperones away from their original targets, thus interfering with the protein quality control network and causing more severe folding defects.

The Modulation of Prion Propagation by the PN

The most well-studied proteostasis regulator of prion maintenance is Hsp104 (Figure 2). It was first linked to prion maintenance by the observation that deletion of the gene causes [*PSI*$^{+}$] prion loss (Chernoff et al., 1995), and chemical inhibition of Hsp104 with guanidine HCl also blocks propagation of the [*PSI*$^{+}$] prion, indicating it is required for prion maintenance (Eaglestone et al., 2000; Jung et al., 2002; Tuite et al., 1981). Hsp104 is also required for the propagation of all other known amyloid-associated yeast prions (Alberti et al., 2009; Du et al., 2008; Moriyama et al., 2000; Patel et al., 2009). The current

understanding of the role of Hsp104 in [*PSI*+] prion propagation is that it severs prion aggregates by pulling out Sup35 monomers from the middle of prion fibrils, resulting in an increased number and reduced steady-state size of aggregates. For example, when Hsp104 is inhibited, the amplification of heritable prion aggregates (propagons) is blocked, indicating that Hsp104 is responsible for increasing the number of prion aggregates (Cox et al., 2003; Ness et al., 2002). Moreover, upon Hsp104 inactivation, prion aggregate size increases (Kawai-Noma et al., 2009; Kryndushkin et al., 2003; Satpute-Krishnan et al., 2007; Wegrzyn et al., 2001), consistent with a role in fragmentation. Normal aggregate dynamics mediated by Hsp104 are critical for prion propagation: increased aggregate number promotes conversion by providing additional fiber ends for templating (Satpute-Krishnan et al., 2007), and reduced aggregate size promotes transmission likely through diffusion through the bud neck (Derdowski et al., 2010).

Studies on the effect of deletion or inactivation of Hsp104 under normal growth conditions are straightforward to mechanistically dissect because Hsp104 is not essential for viability, and its loss does not activate a stress response on its own (Sanchez et al., 1993). In contrast, other manipulations of Hsp104 and of other chaperones, which function together in the proteostasis network, are more challenging to mechanistically interpret because imbalance in the system leads to compensatory changes, which complicate interpretations (Brandman et al., 2012). Nonetheless, numerous studies have linked various components of the proteostasis network to efficient prion propagation, and these studies do provide insight into the integration of protein quality control pathways and the forces that destabilize the prion state *in vivo*.

A clear example of these challenges is evident in the large body of work on the impact of Hsp104 overexpression on [*PSI*+] propagation. Strikingly, Hsp104 overexpression alone was linked to [*PSI*+] prion loss decades ago (Chernoff et al., 1995), yet the mechanism underlying this type of curing is still under debate (Astor et al., 2018; Cox and Tuite, 2018; Greene et al., 2018; Matveenko et al., 2018). Existing models suggest fragmentation inhibition, malpartitioning of prion aggregates in a sub-population of cells and dissolution of prion aggregates (Ness et al., 2017; Park et al., 2014; Winkler et al., 2012a). Fragmentation inhibition appears to be the model most consistent with all available observations. Curing by Hsp104 overexpression is associated with an increase in prion aggregate size (Kryndushkin et al., 2003) and a decrease in prion aggregate mobility (Winkler et al., 2012a). These observations are in line with the notion that Hsp104 overexpression leads to inhibition of its fragmentation activity (Winkler et al., 2012). Non-productive binding between Hsp104 and prion aggregates is thought to occur in the absence of Hsp70 due to the imbalance in these factors created by Hsp104 overexpression, and this configuration is proposed to inhibit Hsp104 activity (Winkler et al., 2012a). Consistent with this idea, a short segment of the middle domain of Sup35 identified as an Hsp104 binding site is necessary for prion curing through Hsp104 overexpression (Helsen and Glover, 2012). In contrast, the malpartitioning model suggests that [*PSI*+] heritable units (propagons) are not appropriately distributed between mother and daughter cells in a subset of cells during cell division, leading to the emergence of cells without aggregates (Ness et al., 2017). However, the mechanism of such malpartitioning is largely unknown, and this mechanism fails to explain the observed

increase in prion aggregate size upon Hsp104 overexpression. Similarly, the dissolution model proposes that Hsp104 disassembles aggregates through a second trimming activity (i.e. removal of monomers from fibril ends), although this model was proposed to explain observations of yeast cells transferred to water, which may complicate the analysis (Park et al., 2014). Additionally, contradicting the trimming model, resolubilization of prion aggregates is not observed upon Hsp104 overexpression (Ness et al., 2017).

If the balance between Hsp104 and its co-chaperones is necessary to maintain productive fragmentation, imbalance in these factors might also be predicted to impact prion propagation. Several observations support this idea. For example, Hsp70 (Ssa1) is responsible for targeting Hsp104 to substrates, including prion aggregates (Winkler et al., 2012a); *ssa1* mutants destabilize [*PSI*+] (Jung et al., 2000), and overexpression of Ssa1 promotes *de novo* prion formation (Allen et al., 2005). Moreover, overexpression of Ssa1 prevents prion curing caused by Hsp104 overexpression (Newnam et al., 1999). Ssa1 overexpression is believed to destabilize [*PSI*+] by increasing aggregate size, consistent with the idea that chaperone balance is crucial for efficient fragmentation (Newnam et al., 1999; Mathur et al., 2009).

Besides Hsp70s, Hsp70 cofactors are also implicated in prion propagation (Figure 2). Hsp40s act as stimulators of ATPase activity of Hsp70, and Sis1 is required for the propagation of multiple yeast prions, [*PSI*+] [*PIN*+] [*URE3*] (Higurashi et al., 2008; Sondheimer, 2001). Sis1 has been proposed to function upstream of fragmentation by Hsp104, likely presenting the substrate to the fragmentase (Tipton et al., 2008); indeed

deletion of Sis1 is associated with an increase in [*PIN*+] prion aggregate size, revealing its effect on fragmentation (Aron et al., 2007). Despite these observations, recent studies suggest that Sis1 may have multiple biochemically distinct functions that are required for the maintenance of distinct prion variants, revealing a complicated involvement of this factor in modulating prion propagation (Harris et al., 2014; Killian et al., 2019; Stein and True, 2014). Nonetheless, balanced Sis1 expression is important for prion propagation, as overexpression of Sis1 promotes prion curing (Kryndushkin et al., 2011); certain functions of Sis1 are required for prion curing mediated by Hsp104 overexpression (Kirkland et al., 2011), and overexpression of the chaperone-sorting factors, Btn2 and Cur1, promotes relocalization of Sis1 (Barbitoff et al., 2017; Matveenko et al., 2018), likely explaining the associated loss of [*URE3*] (Kryndushkin et al., 2008).

Another class of Hsp70 cofactors, the nucleotide exchange factors (NEFs), facilitate nucleotide exchange on Hsp70 and substrate release and are also involved in prion propagation (Figure 2). Changes in Sse1 availability and function mediate its effects, suggesting that it is a key contributor to the creation of distinct prion niches through chaperone balance. Deletion of Sse1 reduces [*PSI*+] propagation and inhibits [*PIN*+] propagation (Fan et al., 2007; Kryndushkin and Wickner, 2007; Sadlish et al., 2008), while Sse1 overexpression promotes [*PSI*+] appearance and variant determination (Fan et al., 2007) and inhibits Hsp104-mediated prion curing (Sadlish et al., 2008). The nucleotide exchange function of Sse1 has been linked to the effects; however, how and if this function modulates the fragmentation activity is largely unknown.

Hsp90 is required for the prion curing by Hsp104 overexpression (Moosavi et al., 2010; Reidy and Masison, 2010). Besides, deleting a Hsp70-Hsp90 cofactor Sti1 inhibits Hsp104-mediated prion curing, although the mechanism is unknown (Moosavi et al., 2010; Reidy and Masison, 2010).

The role of co-chaperone balance in prion propagation has also been indirectly suggested by competitive interactions between Hsp70s. For example, overexpression of another Hsp70, the ribosome-associated Ssb1, promotes prion curing by Hsp104 over-expression (Chernoff et al., 1999). In addition, overexpressing Ssb1 destabilizes prion propagation, and deletion of Ssb1 promotes prion propagation (Chacinska et al., 2001; Kushnirov et al., 2000). These effects appear to be mediated by Ssb1 action on nascent chains, as other members of the ribosome-associated complex (RAC) are also reported to affect prion propagation or prion formation (Amor et al., 2015; Kiktev et al., 2015). The opposing effects of Ssa1 and Ssb1 on prion propagation are dependent on the specificity conferred by their respective peptide binding domains (Allen et al., 2005).

All these observations demonstrate the broad involvement of heat shock proteins in the regulation of prion propagation *in vivo*, either under normal conditions or perturbed conditions, such as Hsp104 overexpression and also reveal the complexity of these genetic connections. The fragmentation process mediated by Hsp104 and cofactors, Hsp70 and Hsp40, has been well established by numerous studies employing a variety of assays. However, the roles of additional factors in prion propagation remain to be

delineated beyond these genetic links, demanding thorough characterization of the system.

Amyloid Dissolution in Metazoa

Due to the toxicity of amyloid aggregates, considerable attention has been extended to understand whether these complexes can be resolved under physiological conditions. According to the prion hypothesis, fragmentation of prion fibrils is required for the replication of these species (Masel et al., 1999); however, metazoans lack an Hsp104 homolog (Doyle et al., 2013). Nonetheless, recent work has revealed a variety of disaggregation systems in metazoa that can disassemble amyloid fibrils. The most extensively studied disaggregation machinery in metazoa is the Hsp70/Hsc70 based complex. Hsp110, a member of the Hsp70 family, can function as a *bona fide* chaperone to utilize ATP to solubilize protein aggregates in an *in vitro* assay (Mattoo et al., 2013). However, its significant contribution appears to be the facilitation of the disaggregation of heat-denatured aggregates *in vitro* or in cell lysates by mammalian Hsp70-Hsp40 by promoting nucleotide exchange, although this disaggregation activity is limited (Rampelt et al., 2012; Shorter, 2011). Later, it was shown that adding both types of J-proteins, class A and B, enables the Hsp70 chaperone complex to more efficiently disentangle protein aggregates *in vitro* (Nillegoda et al., 2015), while only one class of J-protein - the class B J-protein DNAJB1, is necessary for Hsc70 chaperone and nucleotide exchange factor together to disassemble amyloid α-synuclein fibrils into small oligomers and monomers *in vitro* (Gao et al., 2015). While most of the early studies had been conducted *in vitro*,

the disaggregation system comprised of both types of J-proteins was shown to be able to resolve aggregates formed by the amyloidogenic polyQ-containing proteins in *C. elegans*, indicating its potential in disassembling *in vivo* (Kirstein et al., 2017). A more recent work shows that a trimeric chaperone complex comprised of Hsc70, J-protein DNAJB1 and Hsp110 resolubilizes fibrils *in vitro*, and depletion of the members enhances the toxicity of polyQ aggregation, revealing its biological significance (Scior et al., 2018).

Other disaggregation systems have also been reported. The valosin-containing hexamic AAA+ protein VCP/p97 has been shown to modulate the fibrillogenesis of a pathogenic form of a polyglutamine protein ataxin-3 (Atx-3) and the aggregation of huntingtin exon1 containing expanded polyQ repeat and reduce the cytotoxicity in *Drosophila melanogaster* and *C. elegans* (Boeddrich et al., 2006; Nishikori et al., 2008). However, it remains unknown whether it can directly disaggregate amyloid-like assemblies. Another human AAA+ ATPase RuvBL1/2 partially represses the seeding of amyloid Aβ fibrillation and shows limited disaggregation activity on insulin fibers (Zaarur et al., 2015). Moreover, the PDZ protease HTRA1 can solubilize amyloid fibrils in an ATP-dependent manner (Poepsel et al., 2015), and human cyclophilin 40 (CyP40), a peptidyl-prolyl isomerases (PPIases) solubilizes tau amyloids *in vitro* through an interaction with tau at sites enriched in proline residues (Baker et al., 2017). Together, these observations suggest that the machinery exists to clear amyloids from metazoans; the challenge is to understand the limitations on these factors that prevent them from normally doing so.

Prion Resolubilization in Budding Yeast

Prion curing can be caused by inhibition of fragmentation, which leads to an increase in aggregate size and retention of large aggregates in mother cells (Kawai-Noma et al., 2009; Kryndushkin et al., 2003; Satpute-Krishnan et al., 2007; Wegrzyn et al., 2001). As such, new daughter cells fail to acquire prion aggregates before division, leading to the creating of prion-free cells in a growing population. In addition to this mechanism, several studies have shown that disassembly of yeast prion aggregates can also occur *in vivo* through the action of the well-studied Hsp104/Hsp70/Hsp40 system. DiSalvo, *et. al.* first revealed that incorporation of the G58D mutant of Sup35 into wildtype prion aggregates led to excessive processing of these aggregates and destabilization of [*PSI*$^{+}$] (DiSalvo et al., 2011). By inhibiting protein synthesis and tracking the amount of soluble Sup35, the authors demonstrated an increase in soluble Sup35 in G58D-containing strains, indicating resolubilization of prion aggregates. Later, it was shown that this effect could be extended to different prion variants, albeit with differential sensitivities (Pei et al., 2017). Another example of amyloid disassembly is that a transient heat shock of [*PSI*$^{+}$] cells leads to resolubilization of prion aggregates (Klaips et al., 2014). This outcome is dependent on the activity of Hsp104, and the release of soluble Sup35 from prion aggregate is also observed in this case. In both cases, prion aggregates decrease in size, and previously aggregated protein is released in a soluble form, indicating that prion loss occurs through resolubilization of prion aggregates.

However, as mentioned earlier, Hsp104 overexpression alone does not promote prion loss through disassembly (Winkler et al., 2012a). Strikingly, such treatment has been

proposed to inhibit the processing of prion aggregates due to lack of Hsp104 cofactor – Hsp70, leading to an increase in prion aggregate size (Winkler et al., 2012a). However, upon heat shock, Hsp104 and its cofactors, including Hsp70 and Hsp40, are overexpressed, and the processing of prion aggregates is enhanced (Klaips et al., 2014). One explanation is that expressing Hsp104 cofactors can help restore the proper balance between Hsp104 and such cofactors and rescue the activity of Hsp104, which remains to be tested directly.

There are some limitations of current approaches to establishing the relationships between chaperone manipulations and phenotypic changes in prion dynamics. First, there is a gap in knowledge to connect prion curing – a genetic observation to changes in Sup35 aggregate dynamics. Multiple mechanisms with distinct effects on aggregate fragmentation can account for the same genetic observation. For example, the prion curing phenotype can result from inhibition of fragmentation, such as GdnHCl treatment, or enhancement of fragmentation, such as heat shock (Klaips et al., 2014; Ness et al., 2002). Therefore, without a thorough examination of the prion dynamics, the role of the identified factor or treatment in these studies can hardly be defined. Second, common approaches for manipulating individual factors, such as gene deletion, may lead to perturbation of the protein quality control network, a secondary effect which could complicate the phenotypic outcome. These issues need to be properly addressed or at least taken into consideration in interpreting the observations.

Summary of Dissertation Studies

In Chapter 2, I first sought to test whether co-overexpression of Hsp104 co-factors, including Hsp70 (Ssa1) and Hsp40 (Sis1), could restore the fragmentation activity of Hsp104 and observed larger aggregates, indicating that the fragmentation activity was inhibited. To determine additional Hsp104 co-factors involved in heat shock-mediated prion curing, I screened Hsf1-controlled heat shock proteins and identified several factors that differentially affect curing efficiency, including Ssa2, Sse1, and Sti1. However, none of these factors seem to be limited for fragmentation upon Hsp104 overexpression. Although further characterization of the roles of these factors in solubilizing prion aggregates upon heat shock is needed, the findings suggest that there is critical regulation of chaperone activity upon heat shock that modulates the outcome of fragmentation.

Then, in Chapter 3, to define the exact proteostatic niche that promotes amyloid clearance, I explored a range of environmental stresses, identified several conditions leading to prion curing via the same mechanism as heat shock, and further showed that a shared characteristic was the activation of the transcription factor - heat shock factor 1 (Hsf1). Strikingly, artificial Hsf1 activation interfered with heat shock-mediated prion curing, presumably due to overexpression of Sse1, a nucleotide exchange factor of Hsp70. Limiting Sse1, which decelerates the Hsp70 cycle, promoted chaperone loading on prion aggregates and enabled artificial Hsf1 activation to resolve prion aggregates. Unexpectedly, it impaired the resolution of stress-induced aggregates and cell growth at elevated temperatures. Thus, our study demonstrates that the proteostasis network, fine-

tuned for optimal dissolution of non-amyloid aggregates, can be reconfigured for solubilization of amyloid by modulating the Hsp70 cycle.

References

Alberti, S., Halfmann, R., King, O., Kapila, A., and Lindquist, S. (2009). A Systematic Survey Identifies Prions and Illuminates Sequence Features of Prionogenic Proteins. Cell *137*, 146–158.

Allen, K.D., Wegrzyn, R.D., Chernova, T. a, Müller, S., Newnam, G.P., Winslett, P. a, Wittich, K.B., Wilkinson, K.D., and Chernoff, Y.O. (2005). Hsp70 chaperones as modulators of prion life cycle: novel effects of Ssa and Ssb on the Saccharomyces cerevisiae prion [PSI+]. Genetics *169*, 1227–1242.

Alper, T., Cramp, W.A., Haig, D.A., and Clarke, M.C. (1967). Does the agent of scrapie replicate without nucleic acid? Nature *214*, 764–766.

Amor, A.J., Castanzo, D.T., Delany, S.P., Selechnik, D.M., van Ooy, A., and Cameron, D.M. (2015). The ribosome-associated complex antagonizes prion formation in yeast. Prion *9*, 144–164.

Anckar, J., and Sistonen, L. (2011). Regulation of HSF1 function in the heat stress response: implications in aging and disease. Annu. Rev. Biochem. *80*, 1089–1115.

Aron, R., Higurashi, T., Sahi, C., and Craig, E.A. (2007). J-protein co-chaperone Sis1 required for generation of [RNQ+] seeds necessary for prion propagation. EMBO J. *26*, 3794–3803.

Astor, M.T., Kamiya, E., Sporn, Z.A., Berger, S.E., and Hines, J.K. (2018). Variant-specific and reciprocal Hsp40 functions in Hsp104-mediated prion elimination. Mol. Microbiol. *00*, 1–22.

Baker, J.D., Shelton, L.B., Zheng, D., Favretto, F., Nordhues, B.A., Darling, A., Sullivan, L.E., Sun, Z., Solanki, P.K., Martin, M.D., et al. (2017). Human cyclophilin 40 unravels neurotoxic amyloids. PLoS Biol. *15*, 1–22.

Balchin, D., Hayer-Hartl, M., and Hartl, F.U. (2016). In vivo aspects of protein folding and quality control. Science (80-.). *353*, aac4354–aac4354.

Baldauf, E., McBride, P.A., and Beekes, M. (1998). Cerebral targeting indicates vagal spread of infection in hamsters fed with scrapie. J. Gen. Virol. *79*, 601–607.

Barbitoff, Y.A., Matveenko, A.G., Moskalenko, S.E., Zemlyanko, O.M., Newnam, G.P., Patel, A., Chernova, T.A., Chernoff, Y.O., and Zhouravleva, G.A. (2017). To CURe or not to CURe? Differential effects of the chaperone sorting factor Cur1 on yeast prions are mediated by the chaperone Sis1. Mol. Microbiol. *105*, 242–257.

Boeddrich, A., Gaumer, S., Haacke, A., Tzvetkov, N., Albrecht, M., Evert, B.O., Müller, E.C., Lurz, R., Breuer, P., Schugardt, N., et al. (2006). An arginine/lysine-rich motif is crucial for VCP/p97-mediated modulation of ataxin-3 fibrillogenesis. EMBO J. *25*, 1547–1558.

Bolton, D., McKinley, M., and Prusiner, S. (1982). Identification of a protein that purifies with the scrapie prion. Science (80-.). *218*, 1309–1311.

Borchelt, D.R. (1990). Scrapie and cellular prion proteins differ in their kinetics of

synthesis and topology in cultured cells. J. Cell Biol. *110*, 743–752.

Brachmann, A., Baxa, U., and Wickner, R.B. (2005). Prion generation in vitro: amyloid of Ure2p is infectious. EMBO J. *24*, 3082–3092.

Brandman, O., Stewart-Ornstein, J., Wong, D., Larson, A., Williams, C.C., Li, G.-W., Zhou, S., King, D., Shen, P.S., Weibezahn, J., et al. (2012). A Ribosome-Bound Quality Control Complex Triggers Degradation of Nascent Peptides and Signals Translation Stress. Cell *151*, 1042–1054.

Büeler, H., Aguzzi, A., Sailer, A., Greiner, R.-A., Autenried, P., Aguet, M., and Weissmann, C. (1993). Mice devoid of PrP are resistant to scrapie. Cell *73*, 1339–1347.

Byrne, L.J., Cole, D.J., Cox, B.S., Ridout, M.S., Morgan, B.J.T., and Tuite, M.F. (2009). The number and transmission of [PSI+] prion seeds (propagons) in the yeast Saccharomyces cerevisiae. PLoS One *4*.

Castilla, J., Saá, P., Hetz, C., and Soto, C. (2005). In Vitro Generation of Infectious Scrapie Prions. Cell *121*, 195–206.

Caughey, B., and Raymond, G.J. (1991). The scrapie-associated form of PrP is made from a cell surface precursor that is both protease- and phospholipase-sensitive. J. Biol. Chem. *266*, 18217–18223.

Chacinska, A., Szczesniak, B., Kochneva-Pervukhova, N. V., Kushnirov, V. V., Ter-Avanesyan, M.D., and Boguta, M. (2001). Ssb1 chaperone is a [PSI +] prion-curing factor. Curr. Genet. *39*, 62–67.

Chernoff, Y.O., Lindquist, S.L., Ono, B., Inge-Vechtomov, S.G., and Liebman, S.W. (1995). Role of the chaperone protein Hsp104 in propagation of the yeast prion-like factor [psi+]. Science *268*, 880–884.

Chernoff, Y.O., Newnam, G.P., Kumar, J., Allen, K., and Zink, A.D. (1999). Evidence for a protein mutator in yeast: role of the Hsp70-related chaperone ssb in formation, stability, and toxicity of the [PSI] prion. Mol. Cell. Biol. *19*, 8103–8112.

Chiti, F., Stefani, M., Taddei, N., Ramponi, G., and Dobson, C.M. (2003). Rationalization of the effects of mutations on peptide and protein aggregation rates. Nature *424*, 805–808.

Cox, B.S. (1965). Ψ, A cytoplasmic suppressor of super-suppressor in yeast. Heredity (Edinb). *20*, 505–521.

Cox, B., and Tuite, M. (2018). The life of [PSI]. Curr. Genet. *64*, 1–8.

Cox, B., Ness, F., and Tuite, M. (2003). Analysis of the generation and segregation of propagons: Entities that propagate the [PSI+] prion in yeast. Genetics *165*, 23–33.

Dagkesamanskaya, A.R., and Ter-Avanesyan, M.D. (1991). Interaction of the yeast omnipotent suppressors SUP1(SUP45) and SUP2(SUP35) with non-mendelian factors. Genetics *128*, 513–520.

Dearmond, S.J., McKinley, M.P., Barry, R.A., Braunfeld, M.B., McColloch, J.R., and Prusinert, S.B. (1985). Identification of prion amyloid filaments in scrapie-infected brain. Cell *41*, 221–235.

Derdowski, A., Sindi, S.S., Klaips, C.L., DiSalvo, S., and Serio, T.R. (2010). A size threshold limits prion transmission and establishes phenotypic diversity. Science *330*, 680–683.

Derkatch, I.L., Chernoff, Y.O., Kushnirov, V. V, Inge-Vechtomov, S.G., and Liebman, S.W. (1996). Genesis and variability of [PSI] prion factors in Saccharomyces cerevisiae. Genetics *144*, 1375–1386.

Derkatch, I.L., Bradley, M.E., Zhou, P., Chernoff, Y.O., and Liebman, S.W. (1997). Genetic and environmental factors affecting the de novo appearance of the [PSI+] prion in Saccharomyces cerevisiae. Genetics *147*, 507–519.

Derkatch, I.L., Bradley, M.E., Hong, J.Y., and Liebman, S.W. (2001). Prions affect the appearance of other prions: the story of [PIN(+)]. Cell *106*, 171–182.

DeSantis, M.E., Leung, E.H., Sweeny, E.A., Jackrel, M.E., Cushman-Nick, M., Neuhaus-Follini, A., Vashist, S., Sochor, M.A., Knight, M.N., and Shorter, J. (2012). Operational plasticity enables hsp104 to disaggregate diverse amyloid and nonamyloid clients. Cell *151*, 778–793.

DiSalvo, S., Derdowski, A., Pezza, J.A., and Serio, T.R. (2011). Dominant prion mutants induce curing through pathways that promote chaperone-mediated disaggregation. Nat. Struct. Mol. Biol. *18*, 486–492.

Doyle, S.M., Shorter, J., Zolkiewski, M., Hoskins, J.R., Lindquist, S., and Wickner, S. (2007). Asymmetric deceleration of ClpB or Hsp104 ATPase activity unleashes protein-remodeling activity. Nat. Struct. Mol. Biol. *14*, 114–122.

Doyle, S.M., Genest, O., and Wickner, S. (2013). Protein rescue from aggregates by powerful molecular chaperone machines. Nat. Rev. Mol. Cell Biol. *14*, 617–629.

Du, Z., Park, K.W., Yu, H., Fan, Q., and Li, L. (2008). Newly identified prion linked to the chromatin-remodeling factor Swi1 in Saccharomyces cerevisiae. Nat. Genet. *40*, 460–465.

Eaglestone, S.S., Cox, B.S., and Tuite, M.F. (1999). Translation termination efficiency can be regulated in Saccharomyces cerevisiae by environmental stress through a prion-mediated mechanism. Eur. Mol. Biol. Organ. J. *18*, 1974–1981.

Eaglestone, S.S., Ruddock, L.W., Cox, B.S., and Tuite, M.F. (2000). Guanidine hydrochloride blocks a critical step in the propagation of the prion-like determinant [PSI(+)] of Saccharomyces cerevisiae. Proc. Natl. Acad. Sci. U. S. A. *97*, 240–244.

Fan, Q., Park, K.-W., Du, Z., Morano, K. a, and Li, L. (2007). The role of Sse1 in the de novo formation and variant determination of the [PSI+] prion. Genetics *177*, 1583–1593.

Fisher, C.R. (1969). Enzymology of the pigmented adenine-requiring mutants of Saccharomyces and Schizosaccharomyces. Biochem. Biophys. Res. Commun. *34*, 306–310.

Fraser, H. (1982). Neuronal spread of scrapie agent and targeting of lesions within the retino-tectal pathway. Nature *295*, 149–150.

Frydman, J. (2001). Folding of Newly Translated Proteins In Vivo: The Role of Molecular

Chaperones. Annu. Rev. Biochem. *70*, 603–647.

Gabizon, R., McKinley, M.P., and Prusiner, S.B. (1987). Purified prion proteins and scrapie infectivity copartition into liposomes. Proc. Natl. Acad. Sci. *84*, 4017–4021.

Gao, X., Carroni, M., Helen, R., Mayer, M.P., and Bukau, B. (2015). Human Hsp70 Disaggregase Reverses Parkinson ' s-Linked a -Synuclein Amyloid Fibrils. Mol. Cell *59*, 781–793.

Gasch, A.P. (2002). The environmental stress response : a common yeast response to diverse environmental stresses. Top. Curr. Genet. *1*, 11–70.

Gasch, a P., Spellman, P.T., Kao, C.M., Carmel-Harel, O., Eisen, M.B., Storz, G., Botstein, D., and Brown, P.O. (2000). Genomic expression programs in the response of yeast cells to environmental changes. Mol. Biol. Cell *11*, 4241–4257.

Gidalevitz, T., Ben-Zvi, A., Ho, K.H., Brignull, H.R., and Morimoto, R.I. (2006). Progressive disruption of cellular protein folding in models of polyglutamine diseases. Science *311*, 1471–1474.

Glover, J.R., and Lindquist, S. (1998). Hsp104, Hsp70, and Hsp40: a novel chaperone system that rescues previously aggregated proteins. Cell *94*, 73–82.

Glover, J.R., Kowal, A.S., Schirmer, E.C., Patino, M.M., Liu, J.-J., and Lindquist, S. (1997). Self-Seeded Fibers Formed by Sup35, the Protein Determinant of [PSI+], a Heritable Prion-like Factor of S. cerevisiae. Cell *89*, 811–819.

Gorner, W., Durchschlag, E., Martinez-Pastor, M.T., Estruch, F., Ammerer, G., Hamilton, B., Ruis, H., and Schuller, C. (1998). Nuclear localization of the C2H2 zinc finger protein Msn2p is regulated by stress and protein kinase A activity. Genes Dev. *12*, 586–597.

Greene, L.E., Zhao, X., and Eisenberg, E. (2018). Curing of [PSI +] by Hsp104 Overexpression: Clues to solving the puzzle. Prion *12*, 9–15.

Griffith, J.S. (1967). Self-replication and scrapie. Nature *215*, 1043–1044.

Hall, D., and Edskes, H. (2004). Silent Prions Lying in Wait: A Two-hit Model of Prion/Amyloid Formation and Infection. J. Mol. Biol. *336*, 775–786.

Harris, J.M., Nguyen, P.P., Patel, M.J., Sporn, Z. a, and Hines, J.K. (2014). Functional diversification of hsp40: distinct j-protein functional requirements for two prions allow for chaperone-dependent prion selection. PLoS Genet. *10*, e1004510.

Helsen, C.W., and Glover, J.R. (2012). Insight into molecular basis of curing of [PSI+] prion by overexpression of 104-kDa heat shock protein (Hsp104). J. Biol. Chem. *287*, 542–556.

Higurashi, T., Hines, J.K., Sahi, C., Aron, R., and Craig, E.A. (2008). Specificity of the J-protein Sis1 in the propagation of 3 yeast prions. Proc. Natl. Acad. Sci. U. S. A. *105*, 16596–16601.

Holmes, W.M., Mannakee, B.K., Gutenkunst, R.N., and Serio, T.R. (2014). Loss of amino-terminal acetylation suppresses a prion phenotype by modulating global protein folding. Nat. Commun. *5*, 4383.

Jaunmuktane, Z., Mead, S., Ellis, M., Wadsworth, J.D.F., Nicoll, A.J., Kenny, J., Launchbury, F., Linehan, J., Richard-Loendt, A., Walker, a S., et al. (2015). Evidence for human transmission of amyloid-β pathology and cerebral amyloid angiopathy. Nature *525*, 247–250.

Jiang, J., Maes, E.G., Taylor, A.B., Wang, L., Hinck, A.P., Lafer, E.M., and Sousa, R. (2007). Structural basis of J cochaperone binding and regulation of Hsp70. Mol. Cell *28*, 422–433.

Jung, G., Jones, G., Wegrzyn, R.D., and Masison, D.C. (2000). A role for cytosolic hsp70 in yeast [PSI(+)] prion propagation and [PSI(+)] as a cellular stress. Genetics *156*, 559–570.

Jung, G., Jones, G., and Masison, D.C. (2002). Amino acid residue 184 of yeast Hsp104 chaperone is critical for prion-curing by guanidine, prion propagation, and thermotolerance. Proc. Natl. Acad. Sci. U. S. A. *99*, 9936–9941.

Kampinga, H.H., and Craig, E.A. (2010). The HSP70 chaperone machinery: J proteins as drivers of functional specificity. Nat. Rev. Mol. Cell Biol. *11*, 579–592.

Kawai-Noma, S., Pack, C.-G., Tsuji, T., Kinjo, M., and Taguchi, H. (2009). Single mother-daughter pair analysis to clarify the diffusion properties of yeast prion Sup35 in guanidine-HCl-treated [PSI +] cells. Genes to Cells *14*, 1045–1054.

Keefer, K.M., and True, H.L. (2017). A toxic imbalance of Hsp70s in Saccharomyces cerevisiae is caused by competition for cofactors. Mol. Microbiol. *105*, 860–868.

Kiktev, D.A., Melomed, M.M., Lu, C.D., Newnam, G.P., and Chernoff, Y.O. (2015). Feedback control of prion formation and propagation by the ribosome-associated chaperone complex. *96*, 621–632.

Killian, A.N., Miller, S.C., and Hines, J.K. (2019). Impact of Amyloid Polymorphism on Prion-Chaperone Interactions in Yeast. Viruses *11*, 349.

Kim, Y.E., Hipp, M.S., Bracher, A., Hayer-Hartl, M., and Hartl, F.U. (2013). Molecular chaperone functions in protein folding and proteostasis.

King, C.-Y., and Diaz-Avalos, R. (2004). Protein-only transmission of three yeast prion strains. Nature *428*, 319–323.

King, C.-Y., Tittmann, P., Gross, H., Gebert, R., Aebi, M., and Wuthrich, K. (1997). Prion-inducing domain 2-114 of yeast Sup35 protein transforms in vitro into amyloid-like filaments. Proc. Natl. Acad. Sci. *94*, 6618–6622.

Kirkland, P.A., Reidy, M., and Masison, D.C. (2011). Functions of yeast Hsp40 chaperone Sis1p dispensable for prion propagation but important for prion curing and protection from prion toxicity. Genetics *188*, 565–577.

Kirstein, J., Arnsburg, K., Scior, A., Szlachcic, A., Guilbride, D.L., Morimoto, R.I., Bukau, B., and Nillegoda, N.B. (2017). In vivo properties of the disaggregase function of J-proteins and Hsc70 in Caenorhabditis elegans stress and aging. Aging Cell *16*, 1414–1424.

Klaips, C.L., Hochstrasser, M.L., Langlois, C.R., and Serio, T.R. (2014). Spatial quality

control bypasses cell-based limitations on proteostasis to promote prion curing. Elife *3*, e04288.

Kocisko, D.A., Come, J.H., Priola, S.A., Chesebro, B., Raymond, G.J., Lansbury, P.T., and Caughey, B. (1994). Cell-free formation of protease-resistant prion protein. Nature *370*, 471–474.

Kryndushkin, D., and Wickner, R.B. (2007). Nucleotide exchange factors for Hsp70s are required for [URE3] prion propagation in Saccharomyces cerevisiae. Mol. Biol. Cell *18*, 2149–2154.

Kryndushkin, D.S., Alexandrov, I.M., Ter-Avanesyan, M.D., and Kushnirov, V. V (2003). Yeast [PSI+] prion aggregates are formed by small Sup35 polymers fragmented by Hsp104. J. Biol. Chem. *278*, 49636–49643.

Kryndushkin, D.S., Shewmaker, F., and Wickner, R.B. (2008). Curing of the [URE3] prion by Btn2p, a Batten disease-related protein. EMBO J. *27*, 2725–2735.

Kryndushkin, D.S., Engel, A., Edskes, H., and Wickner, R.B. (2011). Molecular chaperone Hsp104 can promote yeast prion generation. Genetics *188*, 339–348.

Kushnirov, V. V, Kryndushkin, D.S., Boguta, M., Smirnov, V.N., and Ter-Avanesyan, M.D. (2000). Chaperones that cure yeast artificial [PSI+] and their prion-specific effects. Curr. Biol. *10*, 1443–1446.

Lee, S., Choi, J.-M., and Tsai, F.T.F. (2007). Visualizing the ATPase Cycle in a Protein Disaggregating Machine: Structural Basis for Substrate Binding by ClpB. Mol. Cell *25*, 261–271.

Liu, J.-J., Sondheimer, N., and Lindquist, S.L. (2002). Changes in the middle region of Sup35 profoundly alter the nature of epigenetic inheritance for the yeast prion [PSI+]. Proc. Natl. Acad. Sci. *99*, 16446–16453.

Mackay, R.G., Helsen, C.W., Tkach, J.M., and Glover, J.R. (2008). The C-terminal extension of Saccharomyces cerevisiae Hsp104 plays a role in oligomer assembly. Biochemistry *47*, 1918–1927.

Maillard, R.A., Chistol, G., Sen, M., Righini, M., Tan, J., Kaiser, C.M., Hodges, C., Martin, A., and Bustamante, C. (2011). ClpX(P) Generates Mechanical Force to Unfold and Translocate Its Protein Substrates. Cell *145*, 459–469.

Masel, J., Jansen, V.A., and Nowak, M.A. (1999). Quantifying the kinetic parameters of prion replication. Biophys. Chem. *77*, 139–152.

Mathur, V., Hong, J.Y., and Liebman, S.W. (2009). Ssa1 overexpression and [PIN(+)] variants cure [PSI(+)] by dilution of aggregates. J. Mol. Biol. *390*, 155–167.

Mattoo, R.U.H., Sharma, S.K., Priya, S., Finka, A., and Goloubinoff, P. (2013). Hsp110 is a bona fide chaperone using ATP to unfold stable misfolded polypeptides and reciprocally collaborate with Hsp70 to solubilize protein aggregates. J. Biol. Chem. *288*, 21399–21411.

Matveenko, A.G., Barbitoff, Y.A., Jay-Garcia, L.M., Chernoff, Y.O., and Zhouravleva, G.A. (2018). Differential effects of chaperones on yeast prions: CURrent view. Curr. Genet. *64*, 317–325.

McKinley, M.P., Bolton, D.C., and Prusiner, S.B. (1983). A protease-resistant protein is a structural component of the Scrapie prion. Cell *35*, 57–62.

Miot, M., Reidy, M., Doyle, S.M., Hoskins, J.R., Johnston, D.M., Genest, O., Vitery, M.-C., Masison, D.C., and Wickner, S. (2011). Species-specific collaboration of heat shock proteins (Hsp) 70 and 100 in thermotolerance and protein disaggregation. Proc. Natl. Acad. Sci. U. S. A. *108*, 6915–6920.

Mogk, A., Kummer, E., and Bukau, B. (2015). Cooperation of Hsp70 and Hsp100 chaperone machines in protein disaggregation. Front. Mol. Biosci. *2*, 22.

Mogk, A., Bukau, B., and Kampinga, H.H. (2018). Cellular Handling of Protein Aggregates by Disaggregation Machines. Mol. Cell *69*, 214–226.

Moosavi, B., Wongwigkarn, J., and Tuite, M.F. (2010). Hsp70/Hsp90 co-chaperones are required for efficient Hsp104-mediated elimination of the yeast [PSI(+)] prion but not for prion propagation. Yeast *27*, 167–179.

Morimoto, R.I. (2008). Proteotoxic stress and inducible chaperone networks in neurodegenerative disease and aging. Genes Dev. *22*, 1427–1438.

Moriyama, H., Edskes, H.K., and Wickner, R.B. (2000). [URE3] prion propagation in Saccharomyces cerevisiae: requirement for chaperone Hsp104 and curing by overexpressed chaperone Ydj1p. Mol. Cell. Biol. *20*, 8916–8922.

Motohashi, K., Watanabe, Y., Yohda, M., and Yoshida, M. (1999). Heat-inactivated proteins are rescued by the DnaK.J-GrpE set and ClpB chaperones. Proc. Natl. Acad. Sci. U. S. A. *96*, 7184–7189.

Naiki, H., Higuchi, K., Nakakuki, K., and Takeda, T. (1991). Kinetic analysis of amyloid fibril polymerization in vitro. Lab. Invest. *65*, 104–110.

Nath, S., Agholme, L., Kurudenkandy, F.R., Granseth, B., Marcusson, J., and Hallbeck, M. (2012). Spreading of Neurodegenerative Pathology via Neuron-to-Neuron Transmission of -Amyloid. J. Neurosci. *32*, 8767–8777.

Ness, F., Ferreira, P., Cox, B.S., and Tuite, M.F. (2002). Guanidine hydrochloride inhibits the generation of prion “seeds” but not prion protein aggregation in yeast. Mol. Cell. Biol. *22*, 5593–5605.

Ness, F., Cox, B.S., Wongwigkarn, J., Naeimi, W.R., and Tuite, M.F. (2017). Over-expression of the molecular chaperone Hsp104 in *Saccharomyces cerevisiae* results in the malpartition of [*PSI* +] propagons. Mol. Microbiol. *00*.

Newnam, G.P., Wegrzyn, R.D., Lindquist, S.L., and Chernoff, Y.O. (1999). Antagonistic interactions between yeast chaperones Hsp104 and Hsp70 in prion curing. Mol. Cell. Biol. *19*, 1325–1333.

Nillegoda, N.B., Kirstein, J., Szlachcic, A., Berynskyy, M., Stank, A., Stengel, F., Arnsburg, K., Gao, X., Scior, A., Aebersold, R., et al. (2015). Crucial HSP70 co-chaperone complex unlocks metazoan protein disaggregation. Nature.

Nillegoda, N.B., Wentink, A.S., and Bukau, B. (2018). Protein Disaggregation in Multicellular Organisms. Trends Biochem. Sci. *43*, 285–300.

Nishikori, S., Yamanaka, K., Sakurai, T., Esaki, M., and Ogura, T. (2008). p97 homologs from Caenorhabditis elegans, CDC-48.1 and CDC-48.2, suppress the aggregate formation of huntingtin exon1 containing expanded polyQ repeat. Genes to Cells *13*, 827–838.

Olzscha, H., Schermann, S.M., Woerner, A.C., Pinkert, S., Hecht, M.H., Tartaglia, G.G., Vendruscolo, M., Hayer-Hartl, M., Hartl, F.U., and Vabulas, R.M. (2011). Amyloid-like aggregates sequester numerous metastable proteins with essential cellular functions. Cell *144*, 67–78.

Park, S.-H., Kukushkin, Y., Gupta, R., Chen, T., Konagai, A., Hipp, M.S., Hayer-Hartl, M., and Hartl, F.U. (2013). PolyQ proteins interfere with nuclear degradation of cytosolic proteins by sequestering the Sis1p chaperone. Cell *154*, 134–145.

Park, Y.-N., Zhao, X., Yim, Y.-I., Todor, H., Ellerbrock, R., Reidy, M., Eisenberg, E., Masison, D.C., and Greene, L.E. (2014). Hsp104 overexpression cures yeast [PSI+] by causing dissolution of the prion seeds. Eukaryot. Cell.

Parsell, D.A., Kowal, A.S., Singer, M.A., and Lindquist, S. (1994). Protein disaggregation mediated by heat-shock protein Hsp104. Nature *372*, 475–478.

Patel, B.K., and Liebman, S.W. (2007). “Prion-proof” for [PIN+]: Infection with In Vitro-made Amyloid Aggregates of Rnq1p-(132–405) Induces [PIN+]. J. Mol. Biol. *365*, 773–782.

Patel, B.K., Gavin-Smyth, J., and Liebman, S.W. (2009). The yeast global transcriptional co-repressor protein Cyc8 can propagate as a prion. Nat. Cell Biol. *11*, 344–349.

Patino, M.M., Liu, J.J., Glover, J.R., and Lindquist, S. (1996). Support for the prion hypothesis for inheritance of a phenotypic trait in yeast. Science *273*, 622–626.

Paushkin, S. V, Kushnirov, V. V, Smirnov, V.N., and Ter-Avanesyan, M.D. (1996). Propagation of the yeast prion-like [psi+] determinant is mediated by oligomerization of the SUP35-encoded polypeptide chain release factor. EMBO J. *15*, 3127–3134.

Pedersen, J.S., Christensen, G., and Otzen, D.E. (2004). Modulation of S6 Fibrillation by Unfolding Rates and Gatekeeper Residues. J. Mol. Biol. *341*, 575–588.

Pei, F., DiSalvo, S., Sindi, S.S., and Serio, T.R. (2017). A dominant-negative mutant inhibits multiple prion variants through a common mechanism. PLoS Genet. *13*, e1007085.

Pezza, J. a, Villali, J., Sindi, S.S., and Serio, T.R. (2014). Amyloid-associated activity contributes to the severity and toxicity of a prion phenotype. Nat. Commun. *5*, 4384.

Poepsel, S., Sprengel, A., Sacca, B., Kaschani, F., Kaiser, M., Gatsogiannis, C., Raunser, S., Clausen, T., and Ehrmann, M. (2015). Determinants of amyloid fibril degradation by the PDZ protease HTRA1. Nat. Chem. Biol. *11*, 862–869.

Polier, S., Dragovic, Z., Hartl, F.U., and Bracher, A. (2008). Structural basis for the cooperation of Hsp70 and Hsp110 chaperones in protein folding. Cell *133*, 1068–1079.

Prusiner, S.B. (1982). Novel proteinaceous infectious particles cause scrapie. Science *216*, 136–144.

Prusiner, S.B. (1998). Nobel Lecture: Prions. Proc. Natl. Acad. Sci. *95*, 13363–13383.

Prusiner, S.B., Groth, D., Serban, A., Koehler, R., Foster, D., Torchia, M., Burton, D., Yang, S.L., and DeArmond, S.J. (1993). Ablation of the prion protein (PrP) gene in mice prevents scrapie and facilitates production of anti-PrP antibodies. Proc. Natl. Acad. Sci. U. S. A. *90*, 10608–10612.

Prusiner, S.B., Woerman, A.L., Mordes, D. a., Watts, J.C., Rampersaud, R., Berry, D.B., Patel, S., Oehler, A., Lowe, J.K., Kravitz, S.N., et al. (2015). Evidence for α-synuclein prions causing multiple system atrophy in humans with parkinsonism. Proc. Natl. Acad. Sci. *112*, E5308–E5317.

Rampelt, H., Kirstein-Miles, J., Nillegoda, N.B., Chi, K., Scholz, S.R., Morimoto, R.I., and Bukau, B. (2012). Metazoan Hsp70 machines use Hsp110 to power protein disaggregation. EMBO J. *31*, 4221–4235.

Reidy, M., and Masison, D.C. (2010). Sti1 regulation of Hsp70 and Hsp90 is critical for curing of Saccharomyces cerevisiae [PSI+] prions by Hsp104. Mol. Cell. Biol. *30*, 3542–3552.

Rogoza, T., Goginashvili, A., Rodionova, S., Ivanov, M., Viktorovskaya, O., Rubel, A., Volkov, K., and Mironova, L. (2010). Non-Mendelian determinant [ISP+] in yeast is a nuclear-residing prion form of the global transcriptional regulator Sfp1. Proc. Natl. Acad. Sci. *107*, 10573–10577.

Rosenzweig, R., Nillegoda, N.B., Mayer, M.P., and Bukau, B. (2019). The Hsp70 chaperone network. Nat. Rev. Mol. Cell Biol. (under revision).

Ross, E.D., and Wickner, R.B. (2004). Prions of yeast fail to elicit a transcriptional response. Yeast *21*, 963–972.

Rüdiger, S., Germeroth, L., Schneider-Mergener, J., and Bukau, B. (1997). Substrate specificity of the DnaK chaperone determined by screening cellulose-bound peptide libraries. EMBO J. *16*, 1501–1507.

Saborio, G.P., Permanne, B., and Soto, C. (2001). Sensitive detection of pathological prion protein by cyclic amplification of protein misfolding. Nature *411*, 810–813.

Sadlish, H., Rampelt, H., Shorter, J., Wegrzyn, R.D., Andréasson, C., Lindquist, S., and Bukau, B. (2008). Hsp110 chaperones regulate prion formation and propagation in S. cerevisiae by two discrete activities. PLoS One *3*, e1763.

Saibil, H. (2013). Chaperone machines for protein folding, unfolding and disaggregation. Nat. Rev. Mol. Cell Biol. *14*, 630–642.

Sailer, A., Büeler, H., Fischer, M., Aguzzi, A., and Weissmann, C. (1994). No propagation of prions in mice devoid of PrP. Cell *77*, 967–968.

Sanchez, Y., Taulien, J., Borkovich, K.A., and Lindquist, S. (1992). Hsp104 is required for tolerance to many forms of stress. EMBO J. *11*, 2357–2364.

Sanchez, Y., Parsell, D. a, Taulien, J., Vogel, J.L., Craig, E. a, and Lindquist, S. (1993). Genetic evidence for a functional relationship between Hsp104 and Hsp70. J. Bacteriol. *175*, 6484–6491.

Satpute-Krishnan, P., and Serio, T.R. (2005). Prion protein remodelling confers an immediate phenotypic switch. Nature *437*, 262–265.

Satpute-Krishnan, P., Langseth, S.X., and Serio, T.R. (2007). Hsp104-dependent remodeling of prion complexes mediates protein-only inheritance. PLoS Biol. *5*, e24.

Schuermann, J.P., Jiang, J., Cuellar, J., Llorca, O., Wang, L., Gimenez, L.E., Jin, S., Taylor, A.B., Demeler, B., Morano, K. a, et al. (2008). Structure of the Hsp110:Hsc70 nucleotide exchange machine. Mol. Cell *31*, 232–243.

Scior, A., Buntru, A., Arnsburg, K., Ast, A., Iburg, M., Juenemann, K., Pigazzini, M.L., Mlody, B., Puchkov, D., Priller, J., et al. (2018). Complete suppression of Htt fibrilization and disaggregation of Htt fibrils by a trimeric chaperone complex. EMBO J. *37*, 282–299.

Serio, T.R., Cashikar, A.G., Kowal, A.S., Sawicki, G.J., Moslehi, J.J., Serpell, L., Arnsdorf, M.F., and Lindquist, S.L. (2000). Nucleated conformational conversion and the replication of conformational information by a prion determinant. Science *289*, 1317–1321.

Sharma, S.K., De los Rios, P., Christen, P., Lustig, A., and Goloubinoff, P. (2010). The kinetic parameters and energy cost of the Hsp70 chaperone as a polypeptide unfoldase. Nat. Chem. Biol. *6*, 914–920.

Shorter, J. (2011). The mammalian disaggregase machinery: Hsp110 synergizes with Hsp70 and Hsp40 to catalyze protein disaggregation and reactivation in a cell-free system. PLoS One *6*, e26319.

Sielaff, B., and Tsai, F.T.F. (2010). The M-domain controls Hsp104 protein remodeling activity in an Hsp70/Hsp40-dependent manner. J. Mol. Biol. *402*, 30–37.

Silveira, J.R., Raymond, G.J., Hughson, A.G., Race, R.E., Sim, V.L., Hayes, S.F., and Caughey, B. (2005). The most infectious prion protein particles. Nature *437*, 257–261.

Sondheimer, N. (2001). The role of Sis1 in the maintenance of the [RNQ+] prion. EMBO J. *20*, 2435–2442.

Sondheimer, N., and Lindquist, S. (2000). Rnq1: an epigenetic modifier of protein function in yeast. Mol. Cell *5*, 163–172.

Stein, K.C., and True, H.L. (2014). Structural variants of yeast prions show conformer-specific requirements for chaperone activity. Mol. Microbiol. *93*, n/a-n/a.

Sweeny, E. a, Jackrel, M.E., Go, M.S., Sochor, M. a, Razzo, B.M., DeSantis, M.E., Gupta, K., and Shorter, J. (2015). The Hsp104 N-Terminal Domain Enables Disaggregase Plasticity and Potentiation. Mol. Cell *57*, 1–14.

Tanaka, M., Chien, P., Naber, N., Cooke, R., and Weissman, J.S. (2004). Conformational variations in an infectious protein determine prion strain differences. Nature *428*, 323–328.

Tanaka, M., Collins, S.R., Toyama, B.H., and Weissman, J.S. (2006). The physical basis of how prion conformations determine strain phenotypes. Nature *442*, 585–589.

Taylor, K.L., Cheng, N., Williams, R.W., Steven, A.C., and Wickner, R.B. (1999). Prion domain initiation of amyloid formation in vitro from native Ure2p. Science *283*, 1339–1343.

Ter-Avanesyan, M.D., Kushnirov, V. V., Dagkesamanskaya, A.R., Didichenko, S.A., Chernoff, Y.O., Inge-Vechtomov, S.G., and Smirnov, V.N. (1993). Deletion analysis of the SUP35 gene of the yeast Saccharomyces cerevisiae reveals two non-overlapping functional regions in the encoded protein. Mol. Microbiol. *7*, 683–692.

Tessarz, P., Mogk, A., and Bukau, B. (2008). Substrate threading through the central pore of the Hsp104 chaperone as a common mechanism for protein disaggregation and prion propagation. Mol. Microbiol. *68*, 87–97.

Tipton, K., Verges, K., and Weissman, J. (2008). In vivo monitoring of the prion replication cycle reveals a critical role for Sis1 in delivering substrates to Hsp104. Mol. Cell *32*, 584–591.

True, H.L., and Lindquist, S.L. (2000). A yeast prion provides a mechanism for genetic variation and phenotypic diversity. Nature *407*, 477–483.

Tuite, M.F., and Serio, T.R. (2010). The prion hypothesis: from biological anomaly to basic regulatory mechanism. Nat. Rev. Mol. Cell Biol. *11*, 823–833.

Tuite, M.F., Mundy, C.R., and Cox, B.S. (1981). Agents that cause a high frequency of genetic change from [psi+] to [psi-] in Saccharomyces cerevisiae. Genetics *98*, 691–711.

Uversky, V.N., Li, J., Souillac, P., Millett, I.S., Doniach, S., Jakes, R., Goedert, M., and Fink, A.L. (2002). Biophysical Properties of the Synucleins and Their Propensities to Fibrillate. J. Biol. Chem. *277*, 11970–11978.

Verghese, J., Abrams, J., Wang, Y., and Morano, K. a (2012). Biology of the heat shock response and protein chaperones: budding yeast (Saccharomyces cerevisiae) as a model system. Microbiol. Mol. Biol. Rev. *76*, 115–158.

Vishveshwara, N., Bradley, M.E., and Liebman, S.W. (2009). Sequestration of essential proteins causes prion associated toxicity in yeast. Mol. Microbiol. *73*, 1101–1114.

Wang, F., Wang, X., Yuan, C.-G., and Ma, J. (2010). Generating a prion with bacterially expressed recombinant prion protein. Science *327*, 1132–1135.

Wegrzyn, R.D., Bapat, K., Newnam, G.P., Zink, A.D., and Chernoff, Y.O. (2001). Mechanism of Prion Loss after Hsp104 Inactivation in Yeast. Mol. Cell. Biol. *21*, 4656–4669.

Wickner, R.B. (1994). [URE3] as an altered URE2 protein: evidence for a prion analog in Saccharomyces cerevisiae. Science *264*, 566–569.

Winkler, J., Tyedmers, J., Bukau, B., and Mogk, A. (2012). Hsp70 targets Hsp100 chaperones to substrates for protein disaggregation and prion fragmentation. J. Cell Biol. *198*, 387–404.

Yu, A., Shibata, Y., Shah, B., Calamini, B., Lo, D.C., and Morimoto, R.I. (2014). Protein aggregation can inhibit clathrin-mediated endocytosis by chaperone competition. Proc. Natl. Acad. Sci. U. S. A. *111*, E1481-90.

Zaarur, N., Xu, X., Lestienne, P., Meriin, A.B., McComb, M., Costello, C.E., Newnam, G.P., Ganti, R., Romanova, N. V, Shanmugasundaram, M., et al. (2015). RuvbL1 and RuvbL2 enhance aggresome formation and disaggregate amyloid fibrils. EMBO J. *34*,

2363–2382.

Zheng, X., Krakowiak, J., Patel, N., Beyzavi, A., Ezike, J., Khalil, A.S., and Pincus, D. (2016). Dynamic control of Hsf1 during heat shock by a chaperone switch and phosphorylation. Elife *5*, e18638.

Zhu, X., Zhao, X., Burkholder, W.F., Gragerov, A., Ogata, C.M., Gottesman, M.E., and Hendrickson, W.A. (1996). Structural analysis of substrate binding by the molecular chaperone DnaK. Science *272*, 1606–1614.

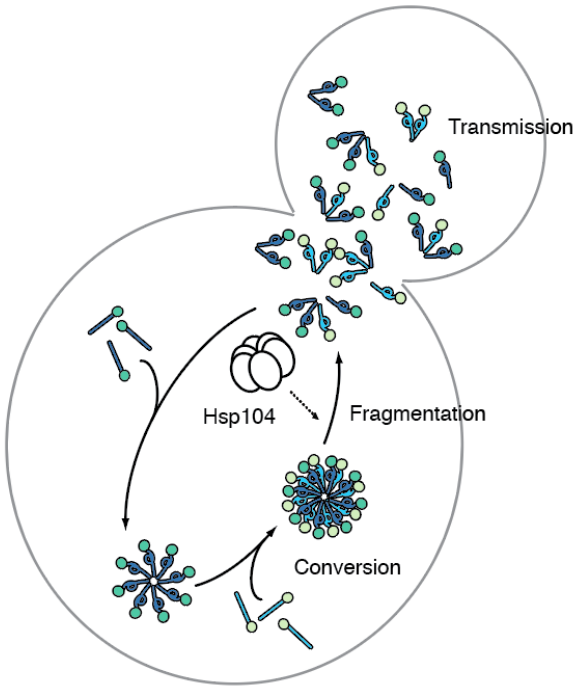

Figure 1. Prion propagation *in vivo* in budding yeast.

Prion propagates *in vivo* via a three-step process. First, newly synthesized prion proteins are incorporated into the existing aggregates via conformational conversion. Next, the Hsp104-dependent step fragments prion aggregates into smaller complexes. Lastly, prion aggregates are transmitted to daughter cells for the inheritance of the prion state. Adapted from (Sindi and Serio, 2009).

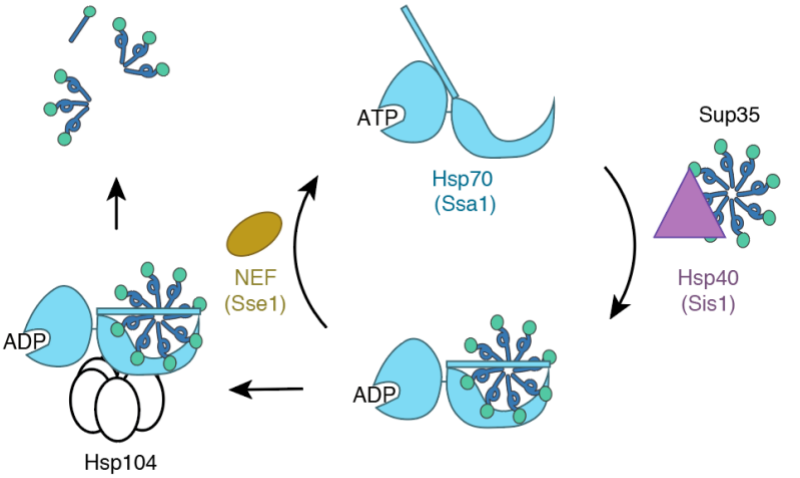

Figure 2. Chaperone-dependent fragmentation of prion aggregates in budding yeast.

The substrate binding and release capabilities of Hsp70 are finely tuned by its cofactors, including Hsp40s and nucleotide exchange factors (NEFs). Hsp40 catalyzes ATP hydrolysis and substrate binding, while NEF facilitates nucleotide exchange and substrate release. Hsp70 (Ssa1), together with its cofactors, recruits prion aggregates to the fragmentase – Hsp104, which fragments prion aggregates into smaller complexes.

Chapter 2:

Screening Heat Shock Proteins for Involvement in Heat Shock-Mediated Prion Curing

Abstract

Despite their thermodynamic stability and ability to convert like proteins of native conformation to the self-replicating state, prion aggregates are effectively resolubilized upon heat shock, revealing a unique proteostatic niche that shifts the balance between amyloid assembly and disassembly through fragmentation toward dissolution. High levels of Hsp104 are tightly linked to heat shock-mediated prion curing; however, Hsp104 overexpression *per se* has been proposed to result in fragmentation inhibition, the opposite outcome of heat shock. The differences in the balance of Hsp104 and its co-factors may account for this striking distinction in curing mechanism. However, overexpressing Hsp70 (Ssa1) and Hsp40 (Sis1), co-factors required for fragmentation, with Hsp104 failed to restore Hsp104 activity as larger aggregates were still observed under these conditions. Extending the search for factors promoting heat shock-mediated prion curing through disassembly to Hsf1-controlled heat shock proteins, we identified several factors that differentially affect curing efficiency, including Ssa2, Sse1 and Sti1. However, none of these factors seem to be limited for fragmentation upon Hsp104 overexpression. Although further characterization of the roles of these factors in solubilizing prion aggregates upon heat shock is needed, the findings suggest that there is critical regulation of chaperone activity upon heat shock that modulates the outcome of fragmentation.

Introduction

Yeast prions are generally regarded as self-perpetuating protein conformations that persist stably under physiological conditions due to the kinetic stability of the amyloid aggregates into which they assembly and the ability of these complexes to convert like proteins of native conformation to the prion state (Chiti and Dobson, 2006; Satpute-Krishnan and Serio, 2005; Serio et al., 2000). However, emerging evidence suggests that resolution of prion amyloids *in vivo* is not insurmountable but rather mechanistically plausible, as exemplified by the cases of a mutant form of the prion protein Sup35 (G58D) that renders its prion amyloid form known as [*PSI*$^{+}$] unstable or that of elevated temperature (DiSalvo et al., 2011; Klaips et al., 2014; Pei et al., 2017). In both cases, prion aggregates decrease in size, and previously aggregated protein is released in a soluble form, indicating that prion loss occurs through the resolubilizaton of prion aggregates. Remarkably, a transient heat shock represents a unique proteostatic niche resulting from a natural activation of the protein quality control network and shifting the balance between amyloid assembly and disassembly towards resolubilization of [*PSI*$^{+}$] prion aggregates. Furthermore, this outcome is stringently dependent on high levels of the fragmentation catalyst Hsp104, both through increased protein synthesis and its asymmetric retention during cell division. Thus, Hsp104 plays a critical role in amyloid clearance *in vivo* (Klaips et al., 2014).

Hsp104 catalyzes the fragmentation of prion aggregates under standard growth conditions, creating new templates (e.g. aggregate ends) for prion conversion and reducing the steady-state size of aggregates to promote their transmission (Derdowski et

al., 2010; Satpute-Krishnan et al., 2007). Strikingly, Hsp104 overexpression alone was linked to [*PSI*+] prion loss decades ago (Chernoff et al., 1995), yet the mechanism underlying this type of curing is still under debate (Astor et al., 2018; Cox and Tuite, 2018; Greene et al., 2018; Matveenko et al., 2018). Existing models suggest fragmentation inhibition, malpartitioning of prion aggregates in a sub-population of cells and dissolution of prion aggregates (Ness et al., 2017; Park et al., 2014; Winkler et al., 2012a). Fragmentation inhibition appears to be the model most consistent with all available observations. Curing by Hsp104 overexpression is associated with an increase in prion aggregate size (Kryndushkin et al., 2003) and a decrease in prion aggregate mobility (Winkler et al., 2012a). These observations are in line with the notion that Hsp104 overexpression leads to inhibition of its fragmentation activity (Winkler et al., 2012). Non-productive binding between Hsp104 and prion aggregates is thought to occur in the absence of Hsp70 due to the imbalance in these factors created by Hsp104 overexpression, and this configuration is proposed to inhibit Hsp104 activity (Winkler et al., 2012a). However, there are remaining questions regarding the fragmentation inhibition model, such as whether increasing the expression of the Hsp104 co-factors prevents the non-productive binding and promotes enhanced fragmentation. The reconstitution of such a minimal system would also allow an assessment of these factors during heat shock (HS), providing additional mechanistic insight into prion curing during a physiologically relevant activation of the proteostasis network.

Several critical factors for prion propagation, including Hsp70 (Ssa1) and Hsp40 (Sis1), seem to fit the profile of limiting factors well. First, both factors are shown to be

overexpressed upon heat shock, implying that the amounts at basal levels might be limiting under conditions of excess Hsp104 (Klaips et al., 2014). Second, extensive studies have implicated them in remodeling of prion aggregates, presumably collaborating with Hsp104 and thereby modulating its fragmentation activity (Higurashi et al., 2008; Jones et al., 2004; Song et al., 2005; Tipton et al., 2008; Winkler et al., 2012b). Indeed, Hsp70 is involved in prion propagation, as Ssa1/2 mutants destabilize [*PSI*+], and Sis1 (Hsp40) as a Hsp70 cochaperone is required for Hsp104-mediated threading of Sup35 prion aggregates (Song et al., 2005; Tipton et al., 2008). Given the importance of these Hsp104 co-factors, it is tempting to speculate that restoring the physiological balance among Hsp104/Ssa1/Sis1 might rescue the fragmentation activity of Hsp104 upon its overexpression.

The distinction between HS-mediated prion curing and prion curing by excess Hsp104 may lie in the factors induced in the former condition. The absence of these factors, or their persistence at basal levels, upon Hsp104 overexpression may limit disaggregation activity; while upon heat shock, the expression level of these factors is adjusted along with that of Hsp104 to preserve the proper balance and functionality of this chaperone network, leading to enhanced fragmentation of prion aggregates.

In addition, a large family of proteins is induced upon heat shock, as part of a global change in the proteostasis network in response to environmental insults, and the majority of those factors are controlled by heat shock factor 1 (Hsf1) and Msn2/4 (Boy-Marcotte et al., 1999; Gasch et al., 2000; Solís et al., 2016; Verghese et al., 2012). Work in Chapter

3 shows that Msn2/4 is dispensable for heat shock-induced prion curing, while Hsf1 activation is sufficient for prion loss, which is why I focus on Hsf1 here. Notably, using an anchor-away approach to precisely control Hsf1 activity and RNA sequencing, another research group successfully pinpointed a compact and precise set of Hsf1 targets under basal conditions (Solís et al., 2016), and a follow-up, unpublished study has identified those factors upregulated by Hsf1 upon heat-shock (D. Pincus, personal communication), making it possible to interrogate all the cytosolic heat shock proteins, whose expression is activated directly by Hsf1. Screening potential heat shock proteins for factors involved in heat shock-mediated prion curing can help us to better understand the limitations of Hsp104 overexpression, which lead to a distinct mechanism of prion curing.

In this study, we first demonstrated that overexpression of Ssa1 and Sis1 was not sufficient to rescue Hsp104 fragmentation activity on prion aggregates when Hsp104 was overproduced, implying that additional factors might be involved. Then, extending the search for factors involved in HS-mediated prion curing across a broad range of Hsf1-controlled genes, we identified several factors that either promote or inhibit this outcome. While none of these factors seem to fit the profile of limiting factors for fragmentation upon Hsp104 overexpression, the findings suggest that regulation of chaperone activity can impact the outcome of amyloid disaggregation, warranting further study of these factors.

Results

Overexpression of Ssa1 and Sis1 fails to rescue Hsp104 fragmentation activity upon Hsp104 overexpression

The fragmentation inhibition model proposed to account for prion curing by Hsp104 overexpression posits that Hsp104 outcompetes Hsp70 (Ssa1) for binding to prion aggregates, rendering the Hsp70-independent interaction non-productive (Winkler et al., 2012a). We reasoned if Hsp70 (alone or with the Hsp40 Sis1), is simultaneously overexpressed with Hsp104, this non-productive binding might be prevented, and the Hsp104 fragmentation activity might be preserved and even enhanced. To test the hypothesis, we employed a galactose-inducible system for Hsp104 and Ssa1 overexpression and introduced a Tet-off-driven extra copy of Sis1. This system leads to overexpression of each factor: 2.8-fold for Hsp104, 1.5-fold for Ssa1 and 1.9-fold for Sis1 in the presence of galactose and absence of doxycycline (Figure S1). We next evaluated prion aggregate size in these strains by a well-established assay---semi-denaturing detergent agarose gel electrophoresis (SDD-AGE) (Kryndushkin et al., 2003). Upon Hsp104 overexpression alone, prion aggregates became larger and disappeared after 12 generations of growth (Figure 1), consistent with the prion curing phenotype reported previously (Chernoff et al., 1995). However, neither the Hsp104/Ssa1 overexpression condition nor the Hsp104/Ssa1/Sis1 overexpression condition prevented the prion aggregates from growing larger, implying the Hsp104 fragmentation activity is still inhibited.

Screening Hsf1-controlled genes for factors impacting HS-mediated prion curing

Because the known key factors for prion propagation, Ssa1 and Sis1, cannot restore Hsp104 activity upon its overexpression, the distinction between the two prion curing cases, Hsp104 overexpression and heat shock, may lie in additional factors induced by heat shock. To identify such putative factors, we obtained a list of Hsf1-controlled genes specific to heat shock (D.Pincus, personal communication), which includes the following cytosolic heat shock proteins, Aha1, Hch1, Hsp26, Btn2, Hsp42, Apj1, Cpr6, Cur1, Hsp82, Ssa1, Ssa2, Ssa4, Sse2, Sti1, Sis1, Ydj1, Sse1 and Fes1. To determine the involvement in HS-mediated prion curing of the non-essential genes on this list, we generated null mutants by PCR-mediated disruption and evaluated their curing efficiencies following transient heat shock. Most of these mutants did not affect HS-mediated prion curing, while two factors had dramatic effects: depletion of a Hsp70 Ssa2 significantly promoted prion curing, and depletion of a Hsp70-Hsp90 cofactor Sti1 inhibited prion curing (Figure 2).

For factors that are essential for cell viability (e.g. Sis1 and Ydj1, another Hsp40) (Luke, 1991) or required for prion propagation (e.g. Fes1 and Sse1, nucleotide exchange factors for Hsp70) (Fan et al., 2007; Kryndushkin and Wickner, 2007), we replaced their promoters with those of another gene that is not induced by Hsf1. In so doing, we attempted to match their basal expression level and block its elevation during heat shock. Although the search for the promoter matching the basal expression level is challenging, this approach is superior to basal depletion of a protein in two ways: first, it results in minimal perturbation to the proteostasis network, which often adapts in response to loss of heat-inducible factors; second, it better mimics the condition of Hsp104 overexpression alone, enabling the assessment of whether a factor at its basal level is limited upon

Hsp104 overexpression. Because of these advantages, we also created a promoter replacement for the non-essential gene *STI1*, which our deletion analysis indicated was essential for heat-shock mediated prion curing (Figure 2). With this set of promoter-replaced strains in hand, we then determined if heat-shock-induced expression levels of each factor were individually required for prion curing.

Despite the considerable Hsf1-dependent increase in mRNA for all these genes upon HS (Solís et al., 2016), an increase in protein levels upon heat shock was not observed for Sse1, and the Ydj1 level was slightly increased upon HS in our wildtype strain background (Figure S2). All of the promoter replacement (R) mutants (e.g. Sis1R, Ydj1R, Sse1R, Fes1R, Sti1R) exhibited over fifty percent of WT basal expression at basal conditions and reduced expression levels upon heat shock (Figure S2). All of these strains can stably propagate the [*PSI*$^{+}$]$_{\text{Weak}}$ prion in the absence of stress (Figure S3). The reduction of Sis1, Ydj1, and Fes1 had no effect on heat shock-mediated prion curing (Figure 3). Sti1R exhibited slightly less prion curing compared with WT, and the extent to which Sti1 perturbation affects prion curing was dramatically reduced from ~80% in Δ*sti1* to ~20% in Sti1R (Figure 2, 3), indicating that basal level of Sti1 is sufficient for supporting heat shock-mediated prion curing. Strikingly, Sse1R promoted prion curing significantly, suggesting its normal expression pattern under heat shock inhibits prion curing (Figure 3). Thus, our deletion and promoter replacement analysis have identified three factors with pronounced effects on HS-mediated prion curing: *SSA2* (negative regulator), *STI1* (positive regulator), and *SSE1* (negative regulator).

Characterization of the mutants regulating HS-mediated prion curing

To determine whether the heat shock-mediated prion curing observed in the mutants is through the same mechanism as observed for wildtype strains (i.e. enhanced fragmentation), we evaluated prion aggregate size by SDD-AGE. At basal conditions, prion aggregates in all the mutants looked similar to WT (Figure 4). At HS, prion aggregates became smaller in all strains; however, partial loss of prion aggregates was only observed for Δ*ssa2* and Sse1R, consistent with the increase in curing for these strains (Figure 2-4). These findings indicate that these mutants, like wildtype, are likely cured through enhanced fragmentation following heat shock.

We next assessed whether the effect on prion curing could be attributed to changes in chaperone abundance, such as the levels of Hsp104. We evaluated chaperone expression levels in the mutants. At basal conditions, Δ*ssa2* and Δ*sti1* upregulate the expression of Hsp104 and Sis1 (Figure S4A). This observation indicates that both mutants lead to upregulation of general heat shock proteins, presumably due to derepression of Hsf1 when the repressor Hsp70s are titrated away by misfolded proteins (Zheng et al., 2016). At heat shock conditions, Δ*ssa2* accumulates chaperones to similar levels as WT, while Δ*sti1* had reduced levels of Hsp104 accumulation relative to WT (Figure S4B). These perturbations to the proteostasis network may contribute to the phenotypes observed in the mutants. In contrast, a similar perturbation was not observed for Sse1R (Figure S4A). At heat shock conditions, chaperone accumulation in Sse1R was similar to that of WT (Figure S4B), suggesting that the Sse1R effect on prion curing cannot

be explained by the aberrant expression of other chaperones required for prion aggregate fragmentation.

It is intriguing that despite 96% sequence identity between the constitutively expressed Hsp70s Ssa1 and Ssa2 (Werner-Washburne et al., 1987), depletion of Ssa2 but not Ssa1 promotes heat-shock-mediated prion curing. To deconvolute the specific contributions of Ssa2 from those resulting from the perturbation to the proteostasis network, we created a Ssa1-only strain by replacing the *SSA2* ORF with *SSA1* ORF and a Ssa2-only strain by replacing the *SSA1* ORF with *SSA2* ORF. The total amount of Ssa1/2 remained similar among WT, Ssa1-only and Ssa2-only at basal and heat shock conditions (Figure S5A). Surprisingly, the HS curing phenotypes were also similar among those strains (Figure S5B), suggesting that the sequence specificity of Ssa1/2 does not affect heat shock-mediated prion curing. The phenotype of Δ*ssa2* is likely linked to the total protein levels of Ssa1/2 rather than the specific loss of Ssa2. However, the total protein levels of Ssa1/2 between Δ*ssa1* and Δ*ssa2* are similar (Figure S5C), implying that total levels of Hsp70 are finely tuned and/or that additional factors are involved in the phenotypes.

The phenotypic distinction between Δ*sti1* and Sti1R motivated us to further examine the perturbation to the proteostasis network in Δ*sti1*, which may account for the phenotypes in Δ*sti1*. We sought to examine whether Δ*sti1* affects the clearance of stress-induced aggregates. We employed Luciferase-mCherry as a reporter of the state of metastable proteins and Hsp104-GFP as a parallel reporter indicating the presence of misfolded protein aggregates. Upon 90-min HS, both types of foci, Luciferase-mCherry and Hsp104-

GFP formed in both WT and Δ*sti1*, and the foci colocalized (Figure S6A), consistent with a previous report (Klaips et al., 2014). After recovery for two hours, Luciferase-mCherry foci were cleared in 93% of WT cells but only in 60% of Δ*sti1* cells (Figure S6C), indicating impairment of disaggregation in Δ*sti1*. A similar trend existed for the clearance of Hsp104-GFP foci (Figure S6B), suggesting a defect in the clearance of stress-induced aggregates. This delay in resolving stress-denatured aggregates may limit the availability of chaperones, therefore impairing resolubilizing of prion aggregates.

Discussion

Despite the extensive studies suggesting the ability of the Hsp104/Ssa1/Sis1 system to remodel prion amyloids (Shorter and Lindquist, 2008; Winkler et al., 2012b), Ssa1 and Sis1 overexpression cannot restore the fragmentation activity of Hsp104 upon its overexpression. Several experimental differences between the two conditions, heat shock and Hsp104 overexpression, are important to consider in attempting to understand the distinct outcomes of these treatments. First, the overexpression level of Ssa1 during galactose induction (50% increase) is similar to that of heat shock (Klaips et al., 2014), but we cannot rule out slight variations created by differences in substrate engagement under these conditions. Second, the prion variants used for heat shock and for Hsp104 overexpression-mediated prion curing are [*PSI*$^{+}$]$_{\text{Weak}}$ and [*PSI*$^{+}$]$_{\text{Strong}}$, respectively, which may complicate the analysis. The effect of the Hsp104/Ssa1/Sis1 co-overexpression on [*PSI*$^{+}$]$_{\text{Weak}}$ has yet to be examined. There is an increasing awareness that the mechanisms of Hsp104-mediated prion curing in [*PSI*$^{+}$]$_{\text{Weak}}$ and [*PSI*$^{+}$]$_{\text{Strong}}$ might be different, as

depletion of the Hsp40 Apj1 only affects the latter (Astor et al., 2018). Future studies should keep the prion variant consistent. Third, the carbon source switch required for galactose induction is known to globally modify the transcriptome (Roth et al., 2004), which might cause unexpected effects on the dynamics of prion aggregates. Alternative means to overexpress Hsp104, such as Tet-on system, should be assessed in future endeavors. Lastly, the inability of co-overexpresson of Ssa1 and Sis1 to restore Hsp104-mediated fragmentation might simply be the consequence of additional missing or limiting factors required for efficient Hsp104-mediated fragmentation.

Despite the limitations, it is evident that Hsp104 overexpression with co-overexpression of Ssa1 and Sis1 leads to prion curing through a distinct mechanism from that of heat shock. Prion aggregates increase in size before prion curing, likely impeding the transmission of these aggregates and leading to a defect in aggregate partitioning (Derdowski et al., 2010; Ness et al., 2017).

Pursuing the hypothesis that the fragmentation differences can be explained by missing or limiting factors, the screening of Hsf1-controlled heat shock proteins for potential regulators of HS-mediated prion curing identified several factors, Ssa2, Sti1 and Sse1. A factor that is limiting for enhanced fragmentation upon Hsp104 overexpression should satisfy the following criterion: the factor should be overexpressed upon heat shock; such overexpression is necessary as basal/reduced expression of the protein impairs HS-mediated prion curing. Based on this prediction, none of the identified factors appears to serve in this role. First, Sse1 is not overexpressed upon heat shock (Figure S2), and

reducing its expression by promoter replacement (SseR) promotes heat-shock mediated prion curing, an observation that is opposite of the predicted dependency. Second, basal expression of Sti1 is sufficient for HS-mediated prion curing (Figure 3). Third, Δ*ssa2* promotes HS-mediated prion curing, an observation that is opposite of the predicted dependency (Figure 2). Therefore, the screening does not offer promising candidates for limiting factors for fragmentation upon Hsp104 overexpression.

Although the mutants (Δ*ssa2*, Δ*sti1*, Sse1R) have dramatic effects on HS-mediated prion curing, further characterization of the mutants indicate that only the effect of Sse1R might be directly linked to the specific protein, while the effects of Δ*ssa2* and Δ*sti1* should be viewed with caution. In the case of Ssa2, Δ*ssa2* perturbs the protein folding environment substantially at basal conditions, and the possibility that this constitutive activation of a stress response modulates prion propagation and curing cannot be ruled out. The follow-up experiment using Ssa1-only and Ssa2-only strains to avoid the perturbation of PN clearly shows that removing *SSA1* or *SSA2* without changing the total level of Ssa1/2 does not affect HS-mediated prion curing (Figure S5). Therefore, Δ*ssa2* should be interpreted as reduction in Ssa1/2 rather than missing Ssa2. An experimental system allowing transient depletion of Ssa1/2 without perturbing PN will be required to conclude whether reduction in Ssa1/2 promotes HS-mediated prion curing. It was reported that Δ*ssa2* does not significantly affect Hsp104-mediated prion curing (Moosavi et al., 2010); however, given the perturbation of PN in Δ*ssa2*, such an effect may need to be reexamined. In the case of Δ*sti1*, several lines of evidence suggest that the effects of Δ*sti1* might be indirect. First, Δ*sti1* perturbs the PN at basal conditions by upregulating

heat shock proteins. Second, Δ*sti1* perturbs the PN during heat shock by slightly reducing the expression of Hsp104 and impairing the clearance of stress-induced misfolded protein aggregates. However, the Sti1R strain demonstrate that basal expression of Sti1, which does not induces a stress response, is sufficient for heat shock-induced prion curing. Thus, the previous observation that Δ*sti1* was shown to inhibit Hsp104-mediated prion curing (Moosavi et al., 2010; Reidy and Masison, 2010), could reasonably be reinterpreted to implicate perturbations to the PN rather than the direct loss of Sti1 in the inhibition of prion curing.

Although the specific role of Ssa2 and Sti1 in heat shock-mediated prion curing is unclear, the isolation of three factors impacting the Hsp70 chaperone cycle as potential regulators of this process is striking. The substrate binding and release capabilities of Hsp70, supported by its unique structure, dictates its function, and these activities are finely tuned by Hsp70 regulators, including Hsp40s and nucleotide exchange factors (NEFs). ATP-bound Hsp70 has low affinity for substrates, and ATP hydrolysis facilitated by Hsp40 stabilizes Hsp70-substrate interaction, while nucleotide exchange facilitated by NEFs on Hsp70 promotes substrate release. Several lines of evidence implicate Hsp70 in prion propagation: *ssa1* mutants destabilize [*PSI*$^{+}$] (Jung et al., 2000); overexpression of Ssa1 promotes *de novo* prion formation (Allen et al., 2005); Hsp70 and Hsp40 render Sup35 fibers formed *in vitro* more susceptible to Hsp104-dependent remodeling (Shorter and Lindquist, 2008); Hsp70 (Ssa1) is responsible for targeting Hsp104 to substrates, including prion aggregates (Winkler et al., 2012a). Moreover, Ssa1 overexpression is believed to destabilize [*PSI*$^{+}$] by increasing aggregate size, suggesting that Ssa1 activity

is finely tuned for prion maintenance (Newnam et al., 1999; Mathur et al., 2009). In line with this idea, the regulators of Hsp70, including Hsp40s (Sis1) and NEFs (Sse1), have been implicated in prion propagation (Aron et al., 2007; Fan et al., 2007; Higurashi et al., 2008; Jones et al., 2004; Masison et al., 2010; Newnam et al., 1999; Sadlish et al., 2008; Song et al., 2005; Tipton et al., 2008), highlighting the significance of Hsp70 functional cycle to prion propagation. The findings here suggest regulation of Hsp70 functional cycle might be key to heat shock-mediated prion curing, demanding future investigation.

The effect of Sse1 reduction on HS-mediated prion curing is particularly striking and demands further investigation. Sse1 has previously been implicated in the appearance and curing of [*PSI*$^{+}$]: deletion of this factor reduces [*PSI*$^{+}$] propagation (Sadlish et al., 2008), and overexpression promotes [*PSI*$^{+}$] appearance and variant determination (Fan et al., 2007). The nucleotide exchange function of Sse1 has been linked to the effects; however, how, and if, this function modulates the fragmentation activity is largely unknown.

We postulate that the mechanism of heat shock-mediated prion curing is overexpression of Hsp104 and its co-factors, thus enhancing fragmentation activity to the extent that exceeds the rate of amyloid assembly. However, a screening of Hsf1-controlled heat shock proteins has not identified putative factors. Alternative models or approaches aimed at addressing the fundamental questions---what constitutes the minimal requirement for the proteostatic niche that can resolubilize prion aggregates and what are the limitations of PN for amyloid dissolution – may provide new insight.

Materials and Methods

Plasmids and yeast strains. All plasmids used in this study are listed in Table S1; all oligonucleotides used in this study are listed in Table S2. All plasmids generated by PCR were confirmed by sequencing.

Plasmids:

SB880 (pCM184-TET-Sis1) was constructed via subcloning a *Bam*HI/*Not*I fragment generated by genomic PCR using primers Sis1 1-19 *Bam*HI and Sis1 1039-1059 *Not*I into a pCM184 vector. SB1186 (pFA6a-KanMX4-P_{APQ12}) was constructed via assembling two fragments, FA6a-Kan and APQ12 promoter, using DNA Assembly (NEB). FA6a-Kan fragment was amplified via PCR using primers FA6a-Kan-F and FA6a-Kan-R and pFA6a-KanMX4-P_{MFA1} (Pezza et al., 2014) as a template. The APQ12 promoter was amplified via PCR using primers APQ12-F and APQ12-R.

Strains:

All yeast strains are derivatives of 74-D694 (Chernoff et al., 1995) unless otherwise specified and are listed in Table S3. The galactose inducible Hsp104 strain (SY2373) was constructed by integration of an *Eco*RI-digested SB598 into SY198 and selection on medium lacking leucine. Expression was confirmed by western blotting. The galactose inducible Hsp104/Ssa1 strain (SY3667) was constructed by integration of *Ppu*MI-digested SB902 into SY2373 and selection on medium lacking uracil. The Hsp104/Ssa1/Sis1 strain (SY3668) was constructed by transforming SY3667 with SB880

followed by transforming a PCR-generated cassette using primers 5 Sis1 KO and 3 Sis1 KO and pFA6a-HphMX4 (Wach et al., 1994) as a template. Disruption was verified via PCR using primer pairs 5 Sis1 KO check/pFA6a and 3 Sis1 KO check/pTEFCH and Sis1 over-expression was confirmed by western blotting. The galactose-inducible strains with Sup35GFP, SY3669, SY3670 and SY3671 were constructed by transforming SY199 with *Eco*47III-digested SB808, followed by mating to SY3668, then sporulation and dissection. Expression was confirmed by western blotting and fluorescence microscopy. All of the [*PSI*$^{+}$]$_{Weak}$ knockout strains were constructed by transformation of a PCR-generated cassette using corresponding primers listed in Table S2 and pFA6a-KanMX4 (Wach et al., 1994) as a template and selection on medium supplemented with G418. Disruptions were verified by PCR using corresponding check primers. The Sis1R strain (SY3665) was constructed by transformation of a PCR-generated fragment using primers Sis1-MFA1 F and Sis1-MFA1 R and SB526 as a template. Promoter replacement was confirmed by PCR using primer pairs Sis1 -700/pFA6a and RC Sis1 100/pTEFCH and western blotting. The SseR strain (SY3639) was constructed by transformation of a PCR-generated fragment using primers Sse1-APQ12 F and Sse1-APQ12 R and SB1186 as a template. Promoter replacement was confirmed by PCR using primer pairs Sse1 -700/pFA6a and RC Sse1 100/pTEFCH and western blotting. The Ydj1R strain (SY3679) was constructed by transformation of a PCR-generated fragment using primers Ydj1-APQ12 F and Ydj1-APQ12 R and SB1186 as a template. Promoter replacement was confirmed by PCR using primer pairs Ydj1 -700/pFA6a and RC Ydj1 100/pTEFCH and western blotting. The Fes1R strain (SY3666) was constructed by transformation of a PCR-generated fragment using primers Fes1-MFA1 F and Fes1-MFA1 R and SB526 as a template. Promoter

replacement was confirmed by PCR using primer pairs Fes1 -700/pFA6a and RC Fes1 100/pTEFCH and western blotting. The Sti1R strain (SY3680) was constructed by transformation of a PCR-generated fragment using primers Sti1-MFA1 F and Sti1-MFA1 R and SB526 as a template. Promoter replacement was confirmed by PCR using primer pairs Sti1 -700/pFA6a and RC Sti1 100/pTEFCH and western blotting. The Ssa1-only strain (SY3640) was constructed by targeting the core module of pCORE to the *SSA2* ORF by transformation of a PCR-generated fragment using primers 5 Ssa2 CORE and 3 Ssa2 CORE and SB583 (Storici et al., 2001) as a template into SLL2600 and selection on medium lacking uracil, followed by transformation of a genomic PCR-generated fragment using primers 5 Ssa1 ORFin Ssa2 and 3 Ssa1 ORFin Ssa2 to replace the CORE cassette. Disruption was confirmed by PCR amplification of genomic DNA and sequencing. The Ssa2-only strain (SY3641) was constructed by targeting the core module of pCORE to the *SSA1* ORF by transformation of a PCR-generated fragment using primers 5 Ssa1 CORE and 3 Ssa1 CORE and SB583 (Storici et al., 2001) as a template into SLL2600 and selection on medium lacking uracil, followed by transformation of a genomic PCR-generated fragment using primers 5 Ssa2 ORFin Ssa1 and 3 Ssa2 ORFin Ssa1 to replace the CORE cassette. Disruption was confirmed by PCR amplification of genomic DNA and sequencing. The *Δsti1* Hsp104-GFP FFL-mCherry strain (SY3485) was constructed by mating SY2125 to SY2343, sporulation and dissection, and selection of a *Δsti1* Hsp104-GFP strain on medium supplemented with G418. Disruption was confirmed by PCR and GFP tagging was confirmed by fluorescence microscopy. Then, this strain was transformed with a *Ppu*MI-digested SB1013. Expression was confirmed by fluorescence microscopy.

Growth conditions and phenotypic analysis. Yeast cultures were grown in rich YPD medium supplemented with 3 mM adenine (YPAD) unless otherwise specified. Cultures were kept at an OD_{600} of less than 0.5 at 30°C for at least 10 doublings to ensure exponential growth. To measure colony color phenotype, aliquots of cultures were diluted and plated on YPD plates. After growth at 30°C and a period of color development at room temperature, each colony was scored based on colony color phenotype: fully cured (red, [*psi-*]), sectored (mixture of red and white), uncured (white, [*PSI*$^{+}$]$_{Weak}$). Unless otherwise indicated, fully cured and sectored colonies were combined in the "cured" category. Galactose induction experiments were performed in glucose-free rich medium containing 3% raffinose supplemented with 3% galactose during induction.

Protein analysis. Semi-denaturing detergent agarose gel electrophoresis (SDD-AGE), SDS-PAGE and quantitative immunoblotting were performed as previously described (Pezza et al., 2009). Quantification of western blots was done using Image Studio Lite (Li-Cor Biosciences).

Microscopy. Imaging was performed in complete SD medium supplemented with 2.5 mM adenine and 2% glucose. Images were obtained on a Zeiss Axio Imager M2 fluorescence light microscope with a 100x objective.

Table S1 Error! Bookmark not defined.**: Plasmids**

Name	Description	Reference
SB598	pRS305-P_{GAL}HSP104	(Klaips et al., 2014)
SB902	pRS306-P_{GAL}SSA1	(Klaips et al., 2014)
SB880	pCM184-TET-Sis1	This work
SB1186	pFA6a-KanMX4-P_{APQ12}	This work
SB526	pFA6a-KanMX4-P_{MFA1}	(Pezza et al., 2014)
SB1013	pRS306-P_{GPD}FFL-mCherry	(Klaips et al., 2014)
SB583	pCORE	(Storici et al., 2001)

Table S2: Oligonucleotide Sequences

Description	Sequence (5'-3')
pTEFCH	GCACGTCAAGACTGTCAAGG
pFA6a	TGCCCAGATGCGAAGTTAAGTG
Sis1 1-19 BamHI	GCCGGATCCATGGTCAAGGAGACAAAAC
Sis1 1039-1059 NotI	GGCGCGGCCGCTTAAAAATTTTCATCTATAGC
FA6a-Kan-F	GATCCGTCGACCTGCAG
FA6a-Kan-R	TGTTTAGCTTGCCTCGTCC
APQ12-F	GGGACGAGGCAAGCTAAACAGGAAGCTTCC TTGAGAGTCC
APQ12-R	ACGCTGCAGGTCGACGGATCTTTTGGGTTGCTCACT TTGC
5 Sis1 KO	TTCACATCAATATAATAGAGTATAGTATACAGAACTAA TACAGCTGAAGCTTCGTACGC
3 Sis1 KO	ATTTATTTGAGTTTATAATTATATTTGCTTAGGATTACT AGCATAGGCCACTAGTGGATCTG
5 Sis1 KO check	CCCTTTTTAAACTTATGCG
3 Sis1 KO check	TCGGTGACCTTCTGTC
5 Aha1 KO	TCTTATTCTT AATCGTTTAT AGTAGCAACA ATATATCAATCAGCTGAAGCTTCGTACGC
3 Aha1 KO	ATTTACGCATACTTTTATTGAAACATGAGAACAATATA TCGCATAGGCCACTAGTGGATC
5 Aha1 KO check	TGTTACCCAG TTCACAATGG
3 Aha1 KO check	TCGGCAATCATTCTAGCAT
5 Hch1 KO	TTGAAACGAT CGGAAAGTTA CAACACATTT ACGATAAAATCAGCTGAAGCTTCGTACGC
3 Hch1 KO	TCTATCTATGCAACGCTCCCCTTTTCGTTACATGAAC ACAGCATAGGCCACTAGTGGATC
5 Hch1 KO check	TGCCATGGAT ACCTTCAAG
3 Hch1 KO check	AGTTATTATGTGACGGGTGGT
5 Hsp26 KO	GGTATCCAAA AAAGCAAACA AACAAACTAA ACAAATTAACCAGCTGAAGCTTCGTACGC
3 Hsp26 KO	GGTCCTCGCGAGAGGGACAACACTATAGAGCCAGGT CACTGCATAGGCCACTAGTGGATC
5 Hsp26 KO check	AACATCCA CAACCAACGA A
3 Hsp26 KO check	TACCGCCATTTCAATACAAA
5 Btn2 KO	CCAAAAGAAA ATAACTAATA GACCCCATTA CAATATAGAACAGCTGAAGCTTCGTACGC
3 Btn2 KO	GCCGTAAAAATGAAAGATGGGGAGTATGTATTATCAC CCAGCATAGGCCACTAGTGGATC
5 Btn2 KO check	TCTTTCG CACCGTCTGT
3 Btn2 KO check	GAGATAATTGTTGGGATTCCAT

5 Hsp42 KO	CCATATCCCA CACAAATTAA GATCATACCA AGCCGAAGCACAGCTGAAGCTTCGTACGC
3 Hsp42 KO	AATATAAATGTATGTATGTGTGTATAAACAGATACGAT ATGCATAGGCCACTAGTGGATC
5 Hsp42 KO check	GGCT CTCGAGAAGA GTAGCA
3 Hsp42 KO check	CGATGATGTAAGATATAATACCCG
5 Cpr6 KO	AAAACTGGTA AGACAATATT CAGGCGATCA AGGAGTAAAACAGCTGAAGCTTCGTACGC
3 Cpr6 KO	TTAGTATTTAAACATATAAGCATATATATAATGCAAGT AAGCATAGGCCACTAGTGGATC
5 Cpr6 KO check	ATGCCGA AACAGGTGAC T
3 Cpr6 KO check	CCGTCTTGTTCCAAATATTGA
5 Cur1 KO	CGAACTCGAT AGGACTGGTC GTAAAACAGA AAACTGACTACAGCTGAAGCTTCGTACGC
3 Cur1 KO	CAATTTGAA GACACACGGT AAATTCCGTA GCCCGTATTT CGCATAGGCCACTAGTGGATC
5 Cur1 KO check	CACACAAGCACAAA ATATGATAAA
3 Cur1 KO check	TT GATAGACGAT AGTGGATTTT T
5 Hsp82 KO	AGAGTCCTAT AAACAAAAGC ACAAACAAAC ACGCAAAGATCAGCTGAAGCTTCGTACGC
3 Hsp82 KO	ATGTTTTGTTTATAACCTATTCAAGGCCATGATGTTCT ACGCATAGGCCACTAGTGGATC
5 Hsp82 KO check	CAACACA GTAATCCATA AACCAG
3 Hsp82 KO check	TCGAAGACTTATGGTCTTCTTC
5 Ssa1 KO	GTATTACAAG AAACAAAAAT TCAAGTAAAT AACAGATAATCAGCTGAAGCTTCGTACGC
3 Ssa1 KO	AAAGACATTTTCGTTATTATCAATTGCCGCACCAATTG GCGCATAGGCCACTAGTGGATC
5 Ssa1 KO check	CAACGGCATT TTCGTTCT
3 Ssa1 KO check	GAGCCAAAAGCAATCTGAC
5 Ssa2 KO	CCAACAGATC AAGCAGATTT TATACAGAAA TATTTATACACAGCTGAAGCTTCGTACGC
3 Ssa2 KO	AGTAAAACTTTTCGGATATTTTACAGGGCGATCGCTA AGCGCATAGGCCACTAGTGGATC
5 Ssa2 KO check	CCTTGAATTG AGTTACTCAA CC
3 Ssa2 KO check	GGTTTCGACGGTATAGATGAA
5 Ssa4 KO	AATAACAAAA ACAAGAAAAA AAATAAACAA AACAATAATCCAGCTGAAGCTTCGTACGC
3 Ssa4 KO	GAAATTCGATGCTGCTACTTCATCGCATCTTTGTATTT ATGCATAGGCCACTAGTGGATC
5 Ssa4 KO check	AGATATCTCA ACTCTAGCCG C
3 Ssa4 KO check	AGATTGAGGTGTTAAACTCCG
5 Sse2 KO	TTTTTTACCT GTAACAGACG TAACCAAAGG ATATAATATACAGCTGAAGCTTCGTACGC

3 Sse2 KO	AGAATAAAGAGGGAACAATCCAAATAGACAAAAATTC CGAGCATAGGCCACTAGTGGATC
5 Sse2 KO check	TGGTTGGCAA ACGTTAGT
3 Sse2 KO check	GGACGGAACTGATTGGATA
5 Sti1 KO	TCCTCACTGTAGCTACTAAAACAACCTATACGCAAGA AAGCAGCTGAAGCTTCGTACGC
3 Sti1 KO	AAAAGAATTCAAGATAATAAAGTTATATTTCGTATTAT TTGCATAGGCCACTAGTGGATC
5 Sti1 KO check	GCGTATCCAGTAAATTCTATTG
3 Sti1 KO check	TGGTTTCTAGTTTCAGGC
Sis1-MFA1 F	TTATATGAAC GTTCCAGAAA CTTCTGGAAA AAGAATGGGA GAATTCGAGCTCGTTTAAAC
Sis1-MFA1 R	ATACTCCAAGTAAATCATAAAGTTTTGTCTCCTTGACC AT GGATCCTTCTATTCGATG
Sis1 -700	GA ATGTCATAAA GCCGTACGTT
RC Sis1 100	CCTGTTGGCTTATCTGGATG
Sse1-APQ12 F	AAATGTTTGA AGCCACATGA ATTGAGAAAG GTAAGCACAT GAATTCGAGCTCGTTTAAAC
Sse1-APQ12 R	AGTTATTGTTACCTAAATCTAAACCAAATGGAGTACTC AT TTTTGGGTTGCTCACTTT
Sse1 -700	AT TAATGACCCC TTGAGCTG
RC Sse1 100	AACAACAGATGGGGTGGA
Ydj1-APQ12 F	CCTATAATAT TTCGTACAAA ATTATAGAAG GCCATCGAAA GAATTCGAGCTCGTTTAAAC
Ydj1-APQ12 R	GAACACCTAGAATATCGTAAAACTTAGTTTCTTTAACC ATTTTTGGGTTGCTCACTTT
Ydj1 -700	C TCGAAGCTTT TCTTATCAAT GA
RC Ydj1 100	CAGCTTCCTCACTTGGATTC
Fes1-MFA1 F	TCGTTTGAAA TGATATACCT CTTGGACTGG AATCTTCTGG GAATTCGAGCTCGTTTAAAC
Fes1-MFA1 R	CTTGAGAATTCGCAATAGACCACTGTAATAGCTTTTC CAT GGATCCTTCTATTCGATG
Fes1 -700	TTCTACAGAT TGGATCAGTG GAC
RC Fes1 100	CCACCGAATAACTGCTGTAGC
Sti1-MFA1 F	TTAAGGTATC TTGTTTAAGC CCAAAAGTCT GCTCCCAAAT GAATTCGAGCTCGTTTAAAC
Sti1-MFA1 R	CGTTACCTTGTTGTTTGTATTCATCGGCTGTCAATGA CAT GGATCCTTCTATTCGATG
Sti1 -700	GAAGTAC CAAATAAGAG ATGTCGC
RC Sti1 100	GCTTTAGTGAAGAGCTCTATCGC
5 Ssa2 CORE	CCAACAGATC AAGCAGATTT TATACAGAAA TATTTATACAAGCTCGTTTTCGACACTG
3 Ssa2 CORE	TAAAACTTTTCGGATATTTTACAGGGCGATCGCTAAG CGTTGTTCCTTACCATTAAGTTG

5 Ssa1 ORFin Ssa2	CAACAGATC AAGCAGATTT TATACAGAAA TATTTATACAATGTCAAAAG CTGTCGGTAT T
3 Ssa1 ORFin Ssa2	TAAAACTTTTCGGATATTTTACAGGGCGATCGCTAAG CTTAATCAACTTCTTCAACGGTT
5 Ssa1 CORE	GTATTACAAG AAACAAAAAT TCAAGTAAAT AACAGATAATAGCTCGTTTTCGACACTG
3 Ssa1 CORE	AGACATTTTCGTTATTATCAATTGCCGCACCAATTGG CGTTGTTCCTTACCATTAAGTTG
5 Ssa2 ORFin Ssa1	ATTACAAG AAACAAAAAT TCAAGTAAAT AACAGATAATATGTCTAAAGCTGTCGGTATTG
3 Ssa2 ORFin Ssa1	GACATTTTCGTTATTATCAATTGCCGCACCAATTGGC TTAATCAACTTCTTCGACAGTTG

Table S3: Yeast Strains

Strain	Genotype	Plasmids Integrated	Figure	Reference
SLL2600	*MATa* [*PSI*+]Weak *ade1-14 his3Δ200 trp1-289 ura3-52 leu2-3, 112*	-	3, 4, 5, S2ABCDE, S3AB, S4AB	(Derkatch et al., 1996)
SY198 (W303)	*MATa* [*PSI*+]Strong *leu2-3,112 his3-11,-15 trip1-1 ura3-1 ade1-14 can1-100*	-	Materials and Methods	J. Weissman (YJW512)
SY199 (W303)	*MATα* [*PSI*+]Strong *leu2-3,112 his3-11,-15 trip1-1 ura3-1 ade1-14 can1-100*	-	Materials and Methods	J. Weissman (YJW508)
SY2373 (W303)	*MATa* [*PSI*+]Strong *leu2-3,112::LEU::P_{GAL}HSP104 his3-11,-15 trip1-1 ura3-1 ade1-14 can1-100*	SB598	1	This work
SY3667 (W303)	*MATa* [*PSI*+]Strong *leu2-3,112::LEU::P_{GAL}HSP104 his3-11,-15 trip1-1 ura3-1::URA::P_{GAL}SSA1 ade1-14 can1-100*	SB598 SB902	1	This work
SY3668 (W303)	*MATa* [*PSI*+]Strong *leu2-3,112::LEU::P_{GAL}HSP104 his3-11,-15 trip1-1 ura3-1::URA::P_{GAL}SSA1 ade1-14 can1-100 Δsis1::hphMX4 [P_{TET}-SIS1]*	SB598 SB902 SB880	1, S1	This work
SY3669 (W303)	*MATa* [*PSI*+]Strong *leu2-3,112::LEU::P_{GAL}HSP104 his3-11,-15::HIS::P_{SUP35}SUP35GFP trip1-1 ura3-1 ade1-14 can1-100*	SB598 SB808	2	This work
SY3670 (W303)	*MATa* [*PSI*+]Strong *leu2-3,112::LEU::P_{GAL}HSP104 his3-11,-15::HIS::P_{SUP35}SUP35GFP trip1-1 ura3-1::URA::P_{GAL}SSA1 ade1-14 can1-100*	SB598 SB902 SB808	2	This work
SY3671 (W303)	*MATa* [*PSI*+]Strong *leu2-3,112::LEU::P_{GAL}HSP104 his3-11,-15::HIS::P_{SUP35}SUP35GFP trip1-1 ura3-1::URA::P_{GAL}SSA1 ade1-14 can1-100 Δsis1::hphMX4 [P_{TET}-SIS1]*	SB598 SB902 SB880 SB808	2	This work

SY3672	*MATa* [*PSI*+]Weak *ade1-14 his3Δ200 trp1-289 ura3-52 leu2-3, 112 Δaha1::kanMX4*	-	3	This work
SY3673	*MATa* [*PSI*+]Weak *ade1-14 his3Δ200 trp1-289 ura3-52 leu2-3, 112 Δhch1::kanMX4*	-	3	This work
SY3674	*MATa* [*PSI*+]Weak *ade1-14 his3Δ200 trp1-289 ura3-52 leu2-3, 112 Δhsp26::kanMX4*	-	3	This work
SY3675	*MATa* [*PSI*+]Weak *ade1-14 his3Δ200 trp1-289 ura3-52 leu2-3, 112 Δbtn2::kanMX4*	-	3	This work
SY3676	*MATa* [*PSI*+]Weak *ade1-14 his3Δ200 trp1-289 ura3-52 leu2-3, 112 Δhsp42::kanMX4*	-	3	This work
SY3525	*MATa* [*PSI*+]Weak *ade1-14 his3Δ200 trp1-289 ura3-52 leu2-3, 112 Δapj1::kanMX4*	-	3	This work
SY3677	*MATa* [*PSI*+]Weak *ade1-14 his3Δ200 trp1-289 ura3-52 leu2-3, 112 Δcpr6::kanMX4*	-	3	This work
SY3230	*MATa* [*PSI*+]Weak *ade1-14 his3Δ200 trp1-289 ura3-52 leu2-3, 112 Δcur1::kanMX4*	-	3	This work
SY3634	*MATa* [*PSI*+]Weak *ade1-14 his3Δ200 trp1-289 ura3-52 leu2-3, 112 Δhsp82::kanMX4*	-	3	This work
SY3631	*MATa* [*PSI*+]Weak *ade1-14 his3Δ200 trp1-289 ura3-52 leu2-3, 112 Δssa1::kanMX4*	-	3	This work
SY3632	*MATa* [*PSI*+]Weak *ade1-14 his3Δ200 trp1-289 ura3-52 leu2-3, 112 Δssa2::kanMX4*	-	3, 5, S3AB	This work
SY3633	*MATa* [*PSI*+]Weak *ade1-14 his3Δ200 trp1-289 ura3-52 leu2-3, 112 Δssa4::kanMX4*	-	3	This work
SY3678	*MATa* [*PSI*+]Weak *ade1-14 his3Δ200 trp1-289 ura3-52 leu2-3, 112 Δsse2::kanMX4*	-	3	This work
SY2343	*MATa* [*PSI*+]Weak *ade1-14 his3Δ200 trp1-289 ura3-52 leu2-3, 112 Δsti1::kanMX4*	-	3, 5, S3AB	This work
SY3665	*MATa* [*PSI*+]Weak *ade1-14 his3Δ200 trp1-289 ura3-52*	-	4, S2A	This work

	leu2-3, 112 P_{MFA1}SIS1::KanMX4			
SY3639	*MATa* [*PSI*+]Weak *ade1-14 his3Δ200 trp1-289 ura3-52 leu2-3, 112 P_{APQ12}SSE1::KanMX4*	-	4, 5, S2C, S3AB	This work
SY3679	*MATa* [*PSI*+]Weak *ade1-14 his3Δ200 trp1-289 ura3-52 leu2-3, 112 P_{APQ12}YDJ1::KanMX4*	-	4, S2B	This work
SY3666	*MATa* [*PSI*+]Weak *ade1-14 his3Δ200 trp1-289 ura3-52 leu2-3, 112 P_{MFA1}FES1::KanMX4*	-	4, S2D	This work
SY3680	*MATa* [*PSI*+]Weak *ade1-14 his3Δ200 trp1-289 ura3-52 leu2-3, 112 P_{MFA1}STI1::KanMX4*	-	4, S2E	This work
SY3640	*MATa* [*PSI*+]Weak *ade1-14 his3Δ200 trp1-289 ura3-52 leu2-3, 112 SSA2::SSA1*	-	S4AB	This work
SY3641	*MATa* [*PSI*+]Weak *ade1-14 his3Δ200 trp1-289 ura3-52 leu2-3, 112 SSA1::SSA2*	-	S4AB	This work
SY2802	*MATa* [*PSI*+]Weak *ade1-14 his3Δ200 trp1-289 ura3-52::URA::P_{GPD}Firefly-mCherry leu2-3, 112 HSP104GFP::KANMX6*	SB1013	S5	(Klaips et al., 2014)
SY2125	*MATα* [*psi-*] *ade1-14 his3Δ200 trp1-289 ura3-52 leu2-3, 112 HSP104GFP::KANMX6*	-	Materials and Methods	(Klaips et al., 2014)
SY3485	*MATa* [*PSI*+]Weak *ade1-14 his3Δ200 trp1-289 ura3-52::URA::P_{GPD}Firefly-mCherry leu2-3, 112 Δsti1::kanMX4 HSP104GFP::KANMX6*	SB1013	S5	This work

References

Allen, K.D., Wegrzyn, R.D., Chernova, T. a, Müller, S., Newnam, G.P., Winslett, P. a, Wittich, K.B., Wilkinson, K.D., and Chernoff, Y.O. (2005). Hsp70 chaperones as modulators of prion life cycle: novel effects of Ssa and Ssb on the Saccharomyces cerevisiae prion [PSI+]. Genetics *169*, 1227–1242.

Aron, R., Higurashi, T., Sahi, C., and Craig, E.A. (2007). J-protein co-chaperone Sis1 required for generation of [RNQ+] seeds necessary for prion propagation. EMBO J. *26*, 3794–3803.

Astor, M.T., Kamiya, E., Sporn, Z.A., Berger, S.E., and Hines, J.K. (2018). Variant-specific and reciprocal Hsp40 functions in Hsp104-mediated prion elimination. Mol. Microbiol. *00*, 1–22.

Boy-Marcotte, E., Lagniel, G., Perrot, M., Bussereau, F., Boudsocq, A., Jacquet, M., and Labarre, J. (1999). The heat shock response in yeast: differential regulations and contributions of the Msn2p/Msn4p and Hsf1 regulons. Mol. Microbiol. *33*, 274–283.

Chernoff, Y.O., Lindquist, S.L., Ono, B., Inge-Vechtomov, S.G., and Liebman, S.W. (1995). Role of the chaperone protein Hsp104 in propagation of the yeast prion-like factor [psi+]. Science *268*, 880–884.

Chiti, F., and Dobson, C.M. (2006). Protein Misfolding, Functional Amyloid, and Human Disease. Annu. Rev. Biochem. *75*, 333–366.

Cox, B., and Tuite, M. (2018). The life of [PSI]. Curr. Genet. *64*, 1–8.

Derdowski, A., Sindi, S.S., Klaips, C.L., DiSalvo, S., and Serio, T.R. (2010). A size threshold limits prion transmission and establishes phenotypic diversity. Science *330*, 680–683.

Derkatch, I.L., Chernoff, Y.O., Kushnirov, V. V, Inge-Vechtomov, S.G., and Liebman, S.W. (1996). Genesis and variability of [PSI] prion factors in Saccharomyces cerevisiae. Genetics *144*, 1375–1386.

DiSalvo, S., Derdowski, A., Pezza, J.A., and Serio, T.R. (2011). Dominant prion mutants induce curing through pathways that promote chaperone-mediated disaggregation. Nat. Struct. Mol. Biol. *18*, 486–492.

Fan, Q., Park, K.-W., Du, Z., Morano, K. a, and Li, L. (2007). The role of Sse1 in the de novo formation and variant determination of the [PSI+] prion. Genetics *177*, 1583–1593.

Gasch, a P., Spellman, P.T., Kao, C.M., Carmel-Harel, O., Eisen, M.B., Storz, G., Botstein, D., and Brown, P.O. (2000). Genomic expression programs in the response of yeast cells to environmental changes. Mol. Biol. Cell *11*, 4241–4257.

Greene, L.E., Zhao, X., and Eisenberg, E. (2018). Curing of [PSI +] by Hsp104 Overexpression: Clues to solving the puzzle. Prion *12*, 9–15.

Higurashi, T., Hines, J.K., Sahi, C., Aron, R., and Craig, E.A. (2008). Specificity of the J-protein Sis1 in the propagation of 3 yeast prions. Proc. Natl. Acad. Sci. U. S. A. *105*, 16596–16601.

Jones, G., Song, Y., Chung, S., and Masison, D.C. (2004). Propagation of Saccharomyces cerevisiae [PSI+] prion is impaired by factors that regulate Hsp70 substrate binding. Mol. Cell. Biol. *24*, 3928–3937.

Jung, G., Jones, G., Wegrzyn, R.D., and Masison, D.C. (2000). A role for cytosolic hsp70 in yeast [PSI(+)] prion propagation and [PSI(+)] as a cellular stress. Genetics *156*, 559–570.

Klaips, C.L., Hochstrasser, M.L., Langlois, C.R., and Serio, T.R. (2014). Spatial quality control bypasses cell-based limitations on proteostasis to promote prion curing. Elife *3*, e04288.

Kryndushkin, D., and Wickner, R.B. (2007). Nucleotide exchange factors for Hsp70s are required for [URE3] prion propagation in Saccharomyces cerevisiae. Mol. Biol. Cell *18*, 2149–2154.

Kryndushkin, D.S., Alexandrov, I.M., Ter-Avanesyan, M.D., and Kushnirov, V. V (2003). Yeast [PSI+] prion aggregates are formed by small Sup35 polymers fragmented by Hsp104. J. Biol. Chem. *278*, 49636–49643.

Luke, M.M. (1991). Characterization of SIS1, a Saccharomyces cerevisiae homologue of bacterial dnaJ proteins. J. Cell Biol. *114*, 623–638.

Masison, D.C., Kirkland, P.A., and Sharma, D. (2010). Influence of Hsp70s and their regulators on yeast prion propagation. Prion *3*, 65–73.

Mathur, V., Hong, J.Y., and Liebman, S.W. (2009). Ssa1 overexpression and [PIN(+)] variants cure [PSI(+)] by dilution of aggregates. J. Mol. Biol. *390*, 155–167.

Matveenko, A.G., Barbitoff, Y.A., Jay-Garcia, L.M., Chernoff, Y.O., and Zhouravleva, G.A. (2018). Differential effects of chaperones on yeast prions: CURrent view. Curr. Genet. *64*, 317–325.

Moosavi, B., Wongwigkarn, J., and Tuite, M.F. (2010). Hsp70/Hsp90 co-chaperones are required for efficient Hsp104-mediated elimination of the yeast [PSI(+)] prion but not for prion propagation. Yeast *27*, 167–179.

Ness, F., Cox, B.S., Wongwigkarn, J., Naeimi, W.R., and Tuite, M.F. (2017). Over-expression of the molecular chaperone Hsp104 in *Saccharomyces cerevisiae* results in the malpartition of [*PSI* +] propagons. Mol. Microbiol. *00*.

Newnam, G.P., Wegrzyn, R.D., Lindquist, S.L., and Chernoff, Y.O. (1999). Antagonistic interactions between yeast chaperones Hsp104 and Hsp70 in prion curing. Mol. Cell. Biol. *19*, 1325–1333.

Park, Y.-N., Zhao, X., Yim, Y.-I., Todor, H., Ellerbrock, R., Reidy, M., Eisenberg, E., Masison, D.C., and Greene, L.E. (2014). Hsp104 overexpression cures yeast [PSI+] by causing dissolution of the prion seeds. Eukaryot. Cell.

Pei, F., DiSalvo, S., Sindi, S.S., and Serio, T.R. (2017). A dominant-negative mutant inhibits multiple prion variants through a common mechanism. PLoS Genet. *13*, e1007085.

Pezza, J. a, Villali, J., Sindi, S.S., and Serio, T.R. (2014). Amyloid-associated activity

contributes to the severity and toxicity of a prion phenotype. Nat. Commun. *5*, 4384.

Pezza, J.A., Langseth, S.X., Raupp Yamamoto, R., Doris, S.M., Ulin, S.P., Salomon, A.R., and Serio, T.R. (2009). The NatA acetyltransferase couples Sup35 prion complexes to the [PSI+] phenotype. Mol. Biol. Cell *20*, 1068–1080.

Reidy, M., and Masison, D.C. (2010). Sti1 regulation of Hsp70 and Hsp90 is critical for curing of Saccharomyces cerevisiae [PSI+] prions by Hsp104. Mol. Cell. Biol. *30*, 3542–3552.

Roth, M.E., Feng, L., McConnell, K.J., Schaffer, P.J., Guerra, C.E., Affourtit, J.P., Piper, K.R., Guccione, L., Hariharan, J., Ford, M.J., et al. (2004). Expression profiling using a hexamer-based universal microarray. Nat. Biotechnol. *22*, 418–426.

Sadlish, H., Rampelt, H., Shorter, J., Wegrzyn, R.D., Andréasson, C., Lindquist, S., and Bukau, B. (2008). Hsp110 chaperones regulate prion formation and propagation in S. cerevisiae by two discrete activities. PLoS One *3*, e1763.

Satpute-Krishnan, P., and Serio, T.R. (2005). Prion protein remodelling confers an immediate phenotypic switch. Nature *437*, 262–265.

Satpute-Krishnan, P., Langseth, S.X., and Serio, T.R. (2007). Hsp104-dependent remodeling of prion complexes mediates protein-only inheritance. PLoS Biol. *5*, e24.

Serio, T.R., Cashikar, A.G., Kowal, A.S., Sawicki, G.J., Moslehi, J.J., Serpell, L., Arnsdorf, M.F., and Lindquist, S.L. (2000). Nucleated conformational conversion and the replication of conformational information by a prion determinant. Science *289*, 1317–1321.

Shorter, J., and Lindquist, S. (2008). Hsp104, Hsp70 and Hsp40 interplay regulates formation, growth and elimination of Sup35 prions. EMBO J. *27*, 2712–2724.

Solís, E.J., Pandey, J.P., Zheng, X., Jin, D.X., Gupta, P.B., Airoldi, E.M., Pincus, D., and Denic, V. (2016). Defining the Essential Function of Yeast Hsf1 Reveals a Compact Transcriptional Program for Maintaining Eukaryotic Proteostasis. Mol. Cell *63*, 60–71.

Song, Y., Wu, Y., Jung, G., Tutar, Y., Eisenberg, E., Greene, L.E., and Masison, D.C. (2005). Role for Hsp70 chaperone in Saccharomyces cerevisiae prion seed replication. Eukaryot. Cell *4*, 289–297.

Storici, F., Lewis, L.K., and Resnick, M.A. (2001). In vivo site-directed mutagenesis using oligonucleotides. Nat. Biotechnol. *19*, 773–776.

Tipton, K., Verges, K., and Weissman, J. (2008). In vivo monitoring of the prion replication cycle reveals a critical role for Sis1 in delivering substrates to Hsp104. Mol. Cell *32*, 584–591.

Verghese, J., Abrams, J., Wang, Y., and Morano, K. a (2012). Biology of the heat shock response and protein chaperones: budding yeast (Saccharomyces cerevisiae) as a model system. Microbiol. Mol. Biol. Rev. *76*, 115–158.

Wach, A., Brachat, A., Pöhlmann, R., and Philippsen, P. (1994). New Heterologous Modules for Classical or PCR-based Gene Disruptions. Yeast *10*, 1793–1808.

Werner-Washburne, M., Stone, D.E., and Craig, E.A. (1987). Complex interactions among members of an essential subfamily of hsp70 genes in Saccharomyces cerevisiae.

Mol. Cell. Biol. *7*, 2568–2577.

Winkler, J., Tyedmers, J., Bukau, B., and Mogk, A. (2012a). Hsp70 targets Hsp100 chaperones to substrates for protein disaggregation and prion fragmentation. J. Cell Biol. *198*, 387–404.

Winkler, J., Tyedmers, J., Bukau, B., and Mogk, A. (2012b). Chaperone networks in protein disaggregation and prion propagation. J. Struct. Biol. *179*, 152–160.

Zheng, X., Krakowiak, J., Patel, N., Beyzavi, A., Ezike, J., Khalil, A.S., and Pincus, D. (2016). Dynamic control of Hsf1 during heat shock by a chaperone switch and phosphorylation. Elife *5*, e18638.

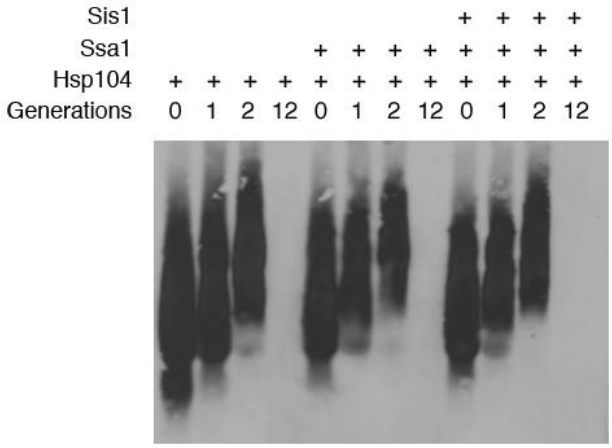

Figure 2. Prion aggregates undergo similar changes upon Hsp104 overexpression alone or with its co-factors.

Semi-native lysates of [*PSI+*]$_{Strong}$ pGal-Hsp104, pGal-Hsp104/Ssa1 and pGal-Hsp104/Ssa1/Tet-Sis1 cultures were analyzed by semi-denaturing detergent agarose gel electrophoresis (SDD-AGE) and immunoblotting for Sup35 following the indicated lengths of induction, 0 generation, 1 generation (~1.3 hr), 2 generations (~2.6 hr) and 12 generations (~15.6 hr).

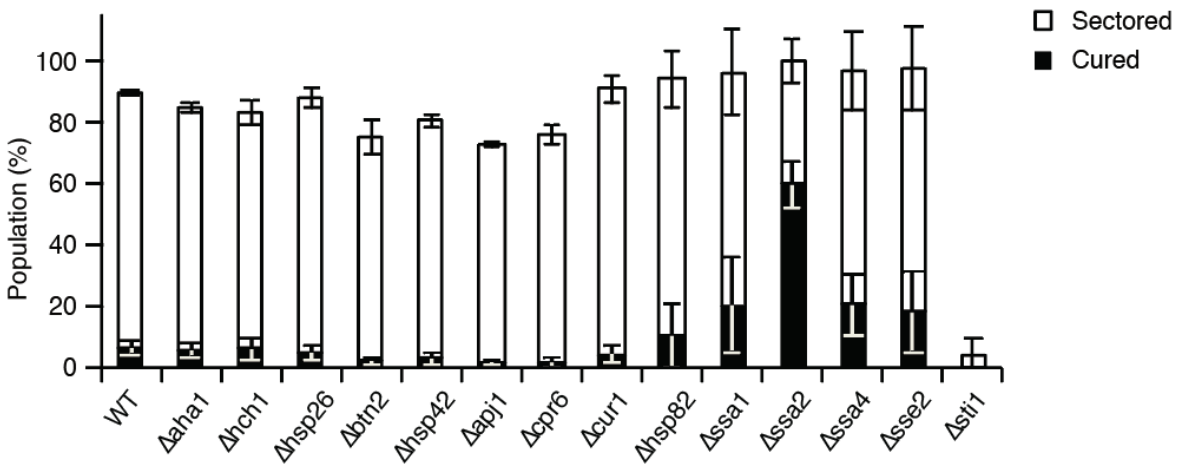

Figure 2. Examination of the non-essential heat shock proteins for their involvement in heat shock-mediated prion curing reveals two regulators, Ssa2 and Sti1.

[*PSI*+]Weak strains, WT or deleted for one of the indicated Hsf1-controlled genes, were incubated at 40°C for 30 min and then plated on rich medium to quantify prion loss by colony color phenotype. Data represent averages, and error bars represent standard deviations for biological replicates (n=3).

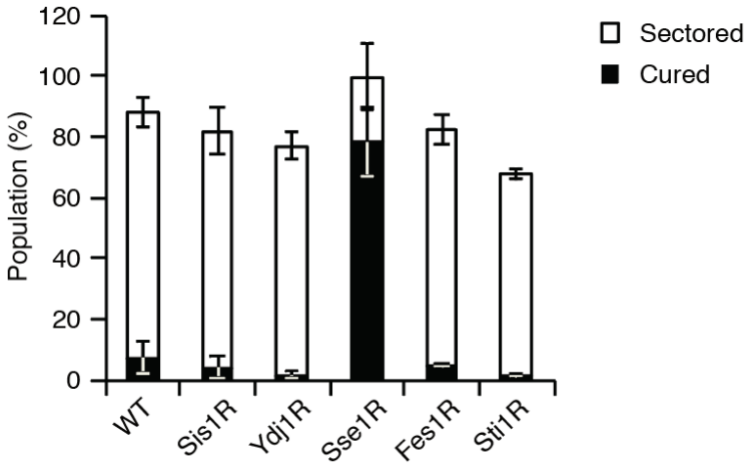

Figure 3. Examination of heat shock proteins for their involvement in heat-shock-mediated prion curing using promoter replaced strains reveals two regulators, Sse1 and Sti1.

[*PSI*+]$_{Weak}$ strains, WT or promoter replaced ("R"), were incubated at 40°C for 30 min and then plated on rich medium to measure prion loss by colony color phenotype. Data represent averages, and error bars represent standard deviations for biological replicates (n=3).

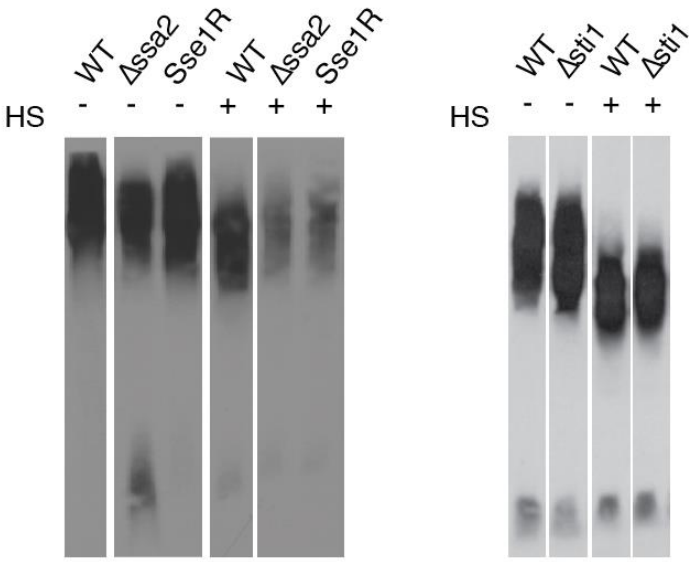

Figure 4. The impact of mutants on prion aggregates.

Semi-native lysates of [*PSI*+]$_{Weak}$ WT, Δ*ssa2*, Sse1R and Δ*sti1* cultures were analyzed by semi-denaturing detergent agarose gel electrophoresis (SDD-AGE) and immunoblotting for Sup35 at basal condition ("-") or after incubation at 40°C for 30 min ("+").

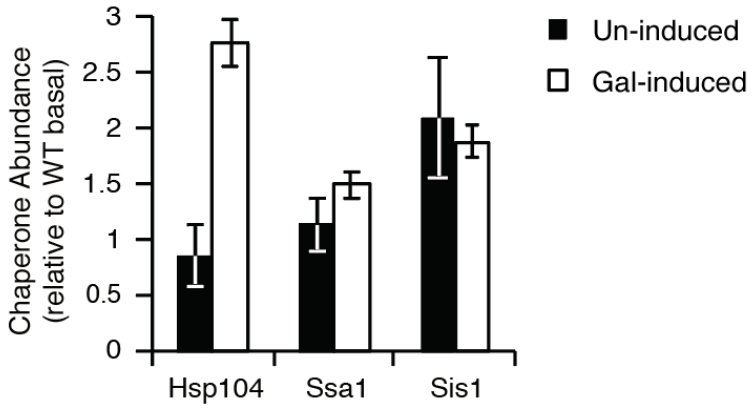

Figure S 1. Chaperone abundance in overexpression strains.

[*PSI*+]Strong pGal-Hsp104/Ssa1/Tet-Sis1 culture were incubated with (Gal-induced) or without (Un-induced) 3% Galactose for 15.6 h, and lysates were prepared and assayed by SDS-PAGE and quantitative immunoblotting for Hsp104, Ssa1, Sis1. Data represent averages, and error bars represent standard deviations for biological replicates (n=3).

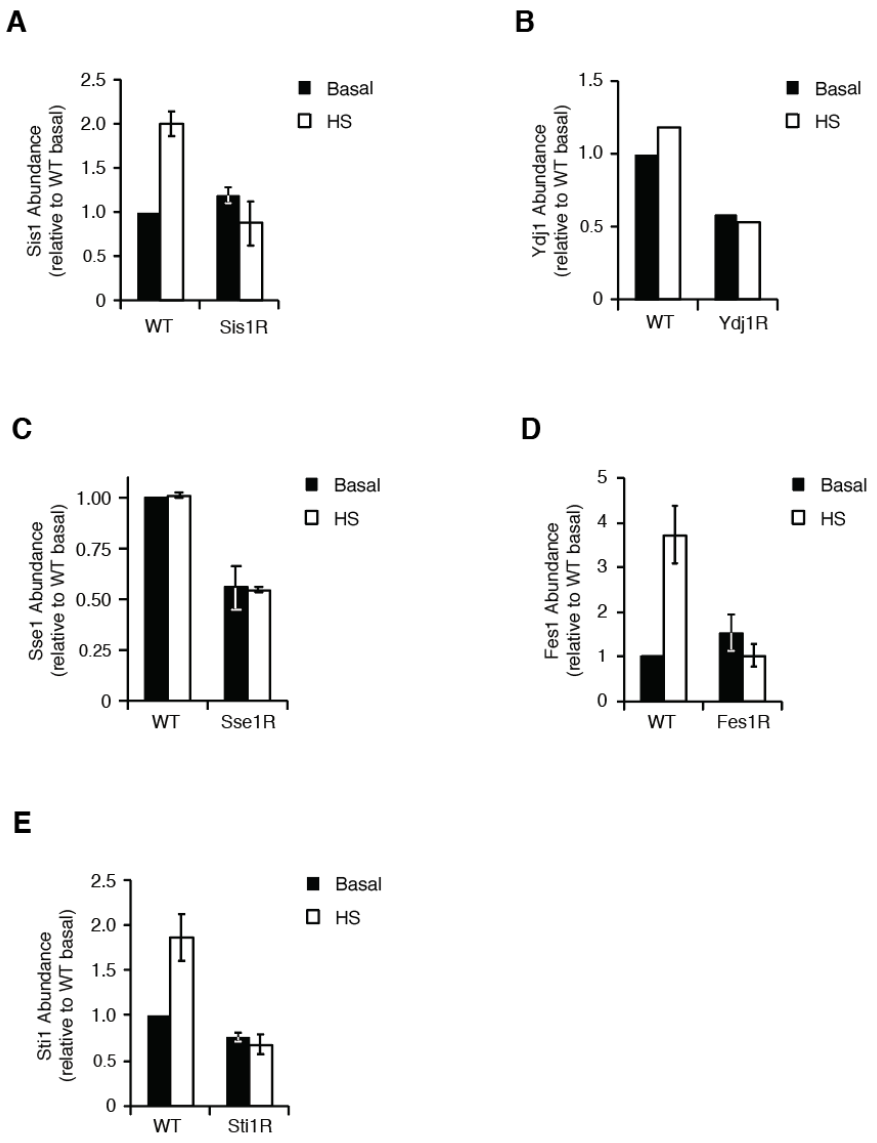

Figure S 2. Chaperone abundance in the promoter replaced strains at basal and HS conditions.

[*PSI*+]Weak cultures, WT or promoter replaced strains ("R"), were incubated at 30°C (Basal) or 40°C for 30 min (HS), and lysates were prepared and assayed by SDS-PAGE and quantitative immunoblotting for Sis1 (A), Ydj1 (B), Sse1 (C), Fes1 (D), Sti1 (E), respectively. Data represent averages, and error bars represent standard deviations for biological replicates (n=3, except for B, n=1).

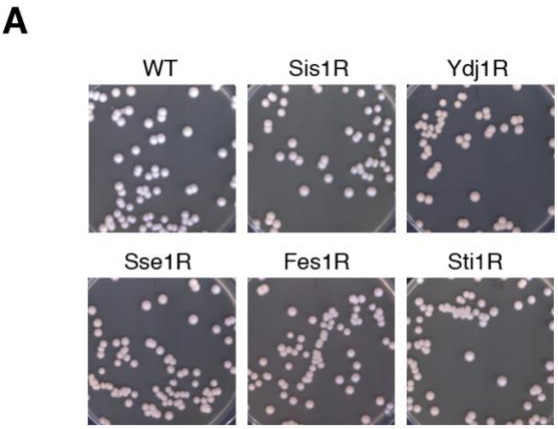

Figure S 3. Colonies of promoter replaced strains.

[*PSI*+]Weak strains with promoter replaced on the genes indicated ("R") were plated on rich medium at 30°C.

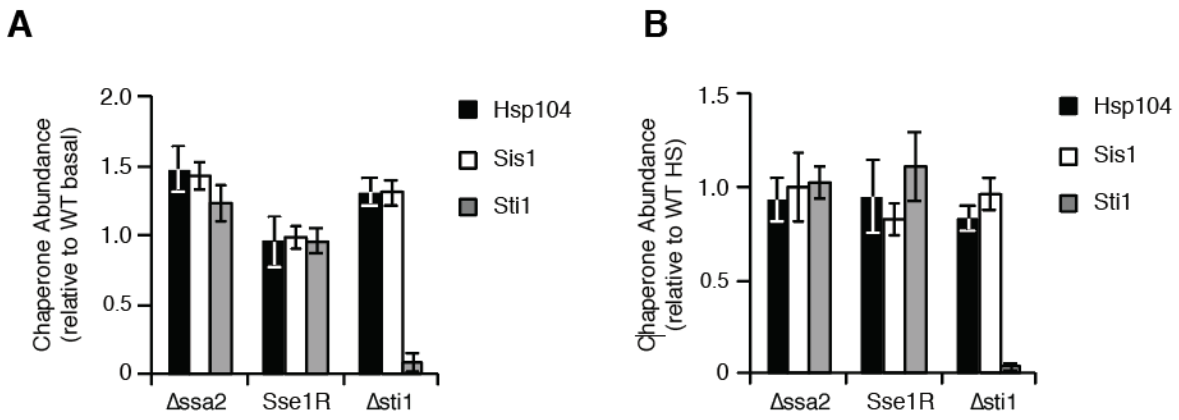

Figure S 4. Chaperone abundance in mutant strains.

(A) Lysates of [*PSI*+]Weak from exponentially growing cultures, WT or the indicated mutants, were prepared and assayed by SDS-PAGE and quantitative immunoblotting for Hsp104 (black), Sis1 (white) and Sti1 (grey). Data represent averages, and error bars represent standard deviations for biological replicates (n=3). (B) [*PSI*+]Weak cultures, WT or the mutants, were incubated at 40°C for 30 min, and lysates were prepared and assayed by SDS-PAGE and quantitative immunoblotting for Hsp104 (black), Sis1 (white) and Sti1 (grey). Data represent averages, and error bars represent standard deviations for biological replicates (n=3).

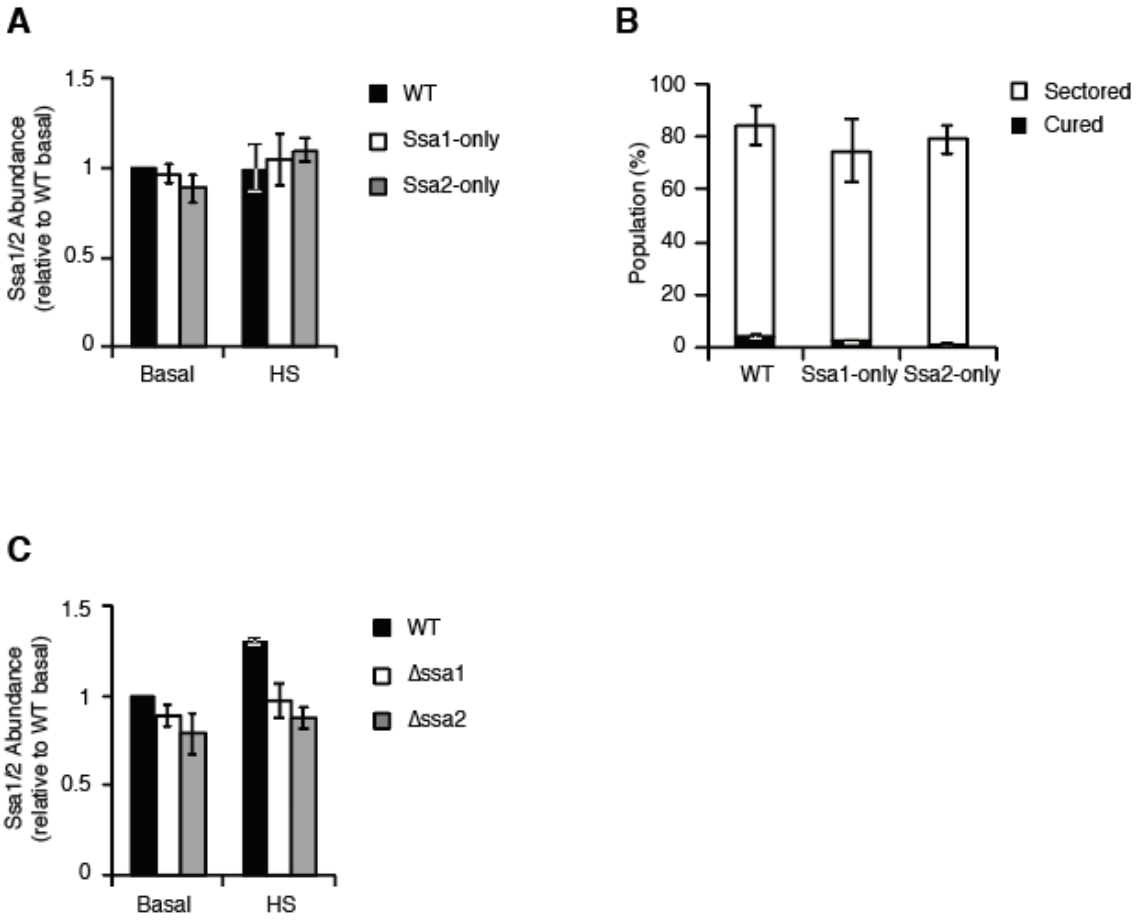

Figure S 5. Assessing the impact of Ssa1/2 on heat shock-mediated prion curing.

(A) [*PSI*+]Weak cultures of WT, Ssa1-only or Ssa2-only strains, were incubated at 40°C (HS) or 30°C (Basal) for 30 min, and lysates were prepared and assayed by SDS-PAGE and quantitative immunoblotting for Ssa1/2. Data represent averages, and error bars represent standard deviations for biological replicates (n=3). (B) [*PSI*+]Weak strains, WT, Ssa1-only or Ssa2-only, were incubated at 40°C for 30 min, and plated on rich medium to measure prion loss by colony color phenotype. Data represent averages, and error bars represent standard deviations for biological replicates (n=3). (C) [*PSI*+]Weak cultures of WT, Δ*ssa1* or Δ*ssa2*, were incubated at 40°C (HS) or 30°C (Basal) for 30 min, and lysates were prepared and assayed by SDS-PAGE and quantitative immunoblotting for Ssa1/2. Data represent averages, and error bars represent standard deviations for biological replicates (n=3).

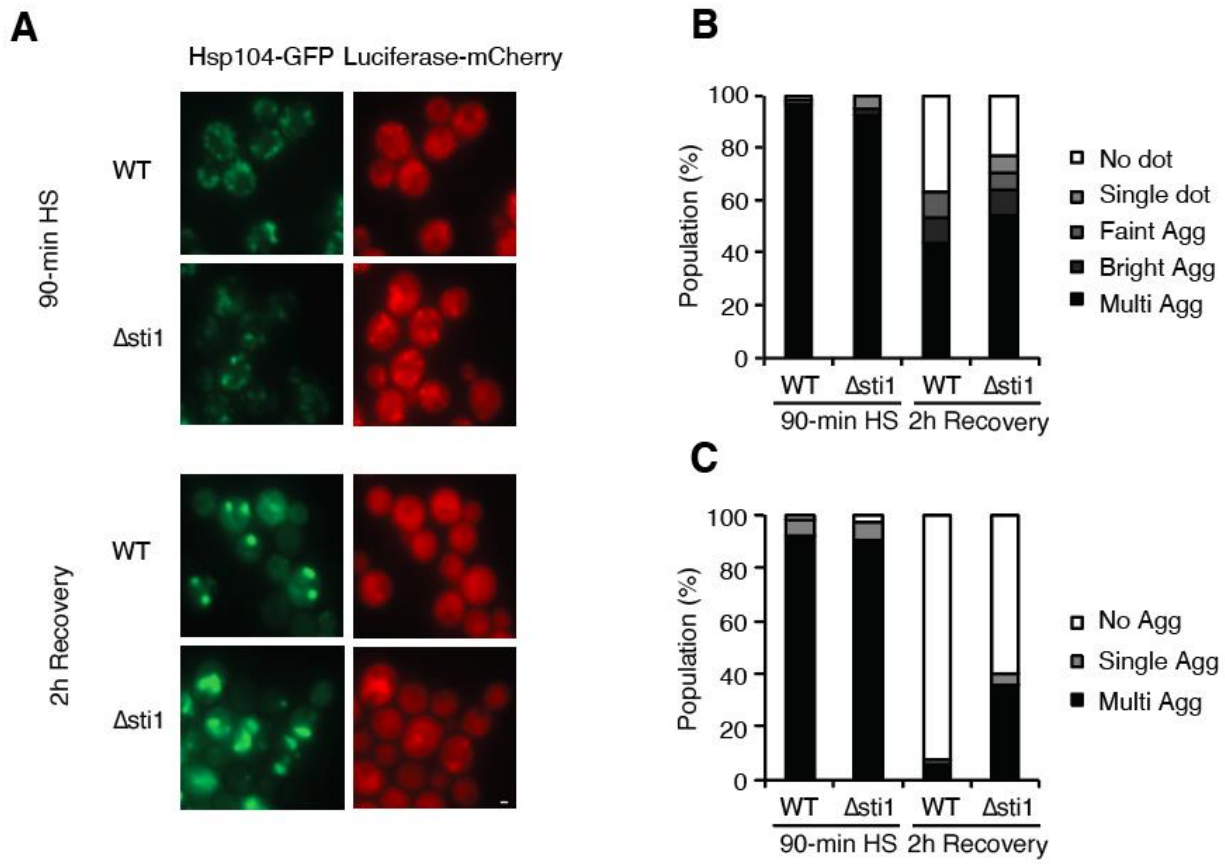

Figure S 6. Clearance of HS-induced misfolded aggregates is delayed in Δ*sti1* mutant relative to WT.

(A) WT or Δ*sti1* strains were incubated at 40°C for 90 min (90-min HS) or further followed by recovery at 30°C for 2 hours (2 h Recovery). The pattern of Hsp104-GFP and Luciferase-mCherry fluorescence was examined by fluorescence microscopy. Scale bar = 1 μm. (B) Quantification of Hsp104-GFP fluorescence pattern in (A): no dot (white); single dot (light gray); faint aggregate (medium gray); bright aggregate (dark gray); multiple bright aggregates (black); n>38. (C) Quantification of Luciferase-mCherry fluorescence pattern in (A): no aggregate (white); single aggregate (gray); multiple aggregates (black); n>42.

Chapter 3:

Decelerating chaperone-substrate dynamics promotes prion curing through amyloid clearance

Abstract

Amyloid promotes a dramatic transition in protein conformation that perpetuates, giving rise to a variety of distinct phenotypes, ranging from pathological disorders to dynamic heritable traits. Amyloid has long been thought to be resistant to clearance by the proteostasis network, but increasing evidence is challenging this view. For example, heat shock disassembles yeast prion amyloids, revealing *in vivo* solubilization of these aggregates. However, the exact proteostatic niche that promotes amyloid clearance is largely unknown. I identified several environmental stresses leading to prion curing via the same mechanism as heat shock and further showed that a shared characteristic was the activation of the transcription factor heat shock factor 1 (Hsf1). Strikingly, artificial Hsf1 activation interfered with heat shock-mediated prion curing, presumably due to overexpression of the nucleotide exchange factor Sse1. Limiting Sse1, which decelerates the Hsp70 cycle, promoted chaperone loading on prion aggregates and enabled artificial Hsf1 activation to resolve prion aggregates; in contrast, the same condition impaired resolution of stress-induced aggregates and cell growth at elevated temperature. Thus, our study demonstrates that the proteostasis network, fine-tuned for optimal dissolution of non-amyloid aggregates, can be reconfigured for solubilization of amyloid by modulating the Hsp70 cycle.

Introduction

Amyloid as a self-replicating protein conformation represents a unique conformational state of protein expanding the classic notion that the amino acid sequence of a protein predominantly dictates a particular shape and thereby function (Anfinsen, 1973). Remarkably, amyloid proteins have the capacity to adopt alternative conformations that are prone to self-assembly under physiological conditions. Given the high thermodynamic stability of these complexes and their unique capability to template the refolding of other conformers of the same protein into a like state (Chiti and Dobson, 2006), propagation of amyloid usually exceeds the capacity of protein quality control networks consisting of molecular chaperones and proteases that act to counteract it (Voisine et al., 2010). Thus, once arising, the amyloid state persists.

An increasing interest in amyloid has been seen for the past several decades, due to their intimate association with a range of debilitating neurodegenerative disorders and also the underappreciated functional roles in biological pathways (Chiti and Dobson, 2017; Chuang et al., 2018; Tuite and Serio, 2010). Amyloid appearance is usually accompanied by phenotypic switches for an organism resulting from the modulation of protein function (Satpute-Krishnan and Serio, 2005). Such amyloid-associated traits can be distinct and diverse, ranging from seemingly irreversible disease states, such as Alzheimer's Disease, Huntington's Disease and the Transmissible Spongiform Encephalopathies (prion diseases) (Chiti and Dobson, 2006; Chuang et al., 2018; Tuite and Serio, 2010), to dynamic functional states, such as hormone storage in vertebrates and transcriptional and translational regulation in fungi (Chiti and Dobson, 2006, 2017; Chuang et al., 2018;

Tuite and Serio, 2010). Given the structural similarities of amyloids formed by different proteins (Iadanza et al., 2018), these observations suggest that amyloid transitions may be reversible, finely tuned and accessible under physiological conditions.

Indeed, several lines of experimental evidence has demonstrated that a Hsp70-based chaperone complex consisting of specific J-proteins and nucleotide exchange factors (NEF) in mammalian systems can disaggregate amyloid fibers *in vitro*, and the biological relevance of this process has also been validated *in vivo* (Mogk et al., 2018; Scior et al., 2018). Furthermore, our studies on the [*PSI*$^{+}$] prion in *S. cerevisiae* revealed that existing Sup35 amyloid could be resolubilized in the distinct proteostatic niche created at elevated temperature (Klaips et al., 2014). Factors influencing the transition include the sequence and conformation of the amyloidogenic protein and the level and localization of the molecular chaperone Hsp104 (Klaips et al., 2014). These modifiers act to alter the balance between amyloid assembly and disassembly to induce amyloid disassembly under physiological conditions, allowing the energetic barrier between the amyloid and native states to be overcome.

While elevated growth temperature can induce amyloid disassembly, the factors defining this proteostatic niche are currently unknown. Here, we identify Sse1, a NEF for the Hsp70 chaperone, as a crucial regulator of chaperone activity in the resolution of Sup35 amyloid. Importantly, our studies suggest that the cellular protein quality control machinery is tuned to the resolution of stress-induced protein aggregates and that the efficient resolution of amyloid requires an alternative configuration of these factors.

Results

The [*PSI*+] prion in budding yeast, formed by the conformational conversion of a translation termination factor Sup35, is propagated as amyloid aggregates (Glover et al., 1997; Patino et al., 1996; Paushkin et al., 1996). Once Sup35 adopts the prion conformation, it is incorporated into amyloid aggregates, which can template the conversion of Sup35 of the native conformation into the prion conformation, concurrently leading to partial loss of Sup35 function (Pezza et al., 2014; Satpute-Krishnan and Serio, 2005). This change in protein state can be monitored as a switch in colony color from red to white in yeast strains encoding a premature stop codon in the *ADE1* or *ADE2* genes (Cox, 1965). The readily distinguishable phenotype makes the system amenable to evaluate the persistence of amyloid aggregates *in vivo*. Using this system, our previous work on the resolution of existing Sup35 amyloid following transient heat shock (HS) revealed a proteostatic niche created at elevated temperature that is incompatible with the self-perpetuating conformational state (Klaips et al., 2014). To explore the generality of this effect, we assessed the stability of the [*PSI*+] prion following other transient sub-lethal stresses.

A subset of environmental stresses promotes [*PSI*+] loss through a mechanism that parallels heat shock-mediated prion loss. I examined a range of environmental stress conditions, oxidative stress, ER stress, osmotic stress, protein folding stresses, including ethanol, methanol and the proline analog AZC. To ensure that the stress conditions were not causing substantial cell death, I optimized the concentrations of the stressors so that

yeast cell viability following stress exposure was over 70% (Figure S1). Applying these conditions to [*PSI*+] strains, we observed that several stress conditions including 6% ethanol, 0.5 mM AZC, and 9% methanol led to prion curing while others, including 1 mM H_2O_2, 0.5 M KCI or 2 mM DTT did not (Figure 1A). Thus, a subset of proteotoxic stresses leads to prion loss *in vivo*.

If the prion curing mechanism is through enhanced fragmentation as during HS, I would expect smaller aggregates upon the treatments and fewer aggregates during recovery. Using semi-denaturing detergent agarose gel electrophoresis (SDD-AGE) (Kryndushkin et al., 2003), I observed that the aggregates became smaller either upon stress (DTT, KCI, Ethanol, Methanol, HS) or during recovery (H_2O_2 and AZC) (Figure 1B). Notably, the slightly larger aggregates upon AZC treatment in comparison with cells growing in SD minimal medium are likely the consequence of temporal impaired chaperone function due to either extensive chaperone sequestration by misfolded protein aggregates (Escusa-Toret et al., 2013) or incorporation of AZC into newly formed chaperones, both of which will be alleviated upon stress relief. Consistent with that idea, smaller aggregates were seen upon AZC stress relief, indicating enhanced fragmentation. Remarkably, upon stress relief, fewer aggregates were observed only for the prion curing conditions, including ethanol, methanol, AZC and the HS positive control (Figure 1B). These findings indicate that a subset of stresses, including ethanol, methanol, AZC and heat shock, induces loss of the [*PSI*+] phenotype and Sup35 amyloid, likely through enhanced fragmentation.

Our previous studies revealed that heat-shock induced prion loss resulted from an elevation of Hsp104 expression, the accumulation of stress-induced protein aggregates, the binding of Hsp104 to these complexes, their asymmetric retention in mother cells due to this engagement, and their clearance after resolution of heat-induced aggregates due to the elevated levels of Hsp104 (Klaips et al., 2014). To determine if these basic principles apply to prion curing by other stresses, I assessed these characteristics for each of the environmental stresses. As expected, all of the prion curing conditions, including ethanol, methanol, AZC and HS, led to an upregulation of Hsp104 relative to normal conditions (Figure 2A), the presence of Hsp104 puncta (Figure 2B), which had been shown to co-localize with misfolded protein aggregates and can serve as an indicator of stress-induced aggregates (Klaips et al., 2014), and the accumulation of stress-induced aggregates (Figure 2C). In contrast, the conditions that do not induce prion curing, including H_2O_2, DTT and KCl, led to a mild upregulation of Hsp104 (Figure 2A), caused minimal Hsp104 puncta (Figure 2B), and failed to induce misfolded protein aggregates (Figure 2C). Therefore, all these prion curing conditions share the following characteristics: elevated expression of Hsp104 (Figure 2A), the accumulation of stress-induced protein aggregates (Figure 2C), the localization of Hsp104 to these stress-induced aggregates (Figure 2B), and a reduction in the size and accumulation of Sup35 aggregates (Figure 1B). Given the similarities among the stress conditions inducing [*PSI*$^+$] loss, I chose one condition, exposure to methanol, to further characterize mechanistically. I demonstrated that this process was dependent on the function of Hsp104 as transient treatment with the Hsp104 inhibitor GdnHCl (Ferreira et al., 2001), repressed prion curing (Figure 2D), as did expansion of the bud neck by Bni1 deletion (Kohno et al., 1996)

(Figure 2E), which had been shown to promote Hsp104 transmission into the daughter cell and reduce its asymmetric retention upon cell division (Klaips et al., 2014). Furthermore, upon stress relief from methanol treatment, I observed an increase in the amount of soluble Sup35 from 62% to 91% following cycloheximide (CHX) treatment, indicating the conversion of existing Sup35 from an amyloid form to a soluble form (Figure 2F). In summary, environmental stresses that induce Sup35 prion loss act through a mechanism paralleling HS-mediated prion loss.

Prion curing stresses are characterized by activation of the Heat Shock Response. Proteostatic niches incompatible with prion propagation may arise through changes in the complement of protein quality control factors present, a direct alteration to the structure of the amyloid itself induced by the stress, or both. Cytoplasmic stress responses in yeast are controlled by two major transcription programs, the Environmental Stress Response (ESR) and the Heat Shock Response (HSR) directed by the master regulators Msn2/4 and Hsf1, respectively (Verghese et al., 2012). To determine the contributions of these pathways to stress-induced prion clearance, I assessed the activation of each pathway in response to environmental stresses via transcriptional reporters. Using heat shock element (HSE) or stress response element (STRE)-based GFP reporters, I found that Hsf1 was activated significantly only for the prion-curing stresses (Figure 3A); on the contrary, Msn2/4 activation did not correlate with the prion curing phenotype (Figure 3B). To examine the contribution of Msn2/4 to HS-induced prion curing, I employed a Δ*msn2* strain, a Δ*msn4* strain, and a Δ*msn2/4* strain. Notably, a previous study reported that a premature stop codon (Q236TAA) exists in the *MSN4* ORF in yeast strain 74-D694

(Fitzpatrick et al., 2011), which could compromise the *MSN4* function and complicate the analysis. Therefore, I included strains having *MSN4* restored by removing the premature stop codon. Deletion of Msn2 (Δ*msn2MSN4*) or Msn4 (Δ*msn4*) moderately repressed prion curing, and deletion of Msn2/4 (Δ*msn2/4*) repressed prion curing from 92% to 32% (Figure 3C), suggesting the ESR is contributing to HS-mediated prion curing. However, pronounced curing of 80% was achieved in Δ*msn2/4* strain upon 90 min HS (Figure 3C), implying the Msn2/4 activation is dispensable for HS-mediated prion curing. In summary, Hsf1 activation appears to be a shared aspect of the prion curing stresses.

Artificial activation of Hsf1 is unable to induce prion loss and dominantly interferes with HS-mediated prion loss. Hsf1 is essential for cell viability in yeast (Sorger and Pelham, 1988); therefore, its necessity for stress-induced prion loss cannot be easily assessed. To determine if its contribution is sufficient to induce prion loss, I examined the impact of expressing a phospho-mimetic variant of Hsf1 (Hsf1-PO4*) on [*PSI*$^{+}$] stability (Zheng et al., 2016). A previous study showed that overexpression of this Hsf1 variant could fully activate Hsf1 activity to the same extent as heat shock (Zheng et al., 2016). Using a β-estradiol inducible system, I induced the overexpression of Hsf1-PO4* by adding estradiol and evaluated the status of Hsf1 activation using the HSE-GFP transcriptional reporter. The level of Hsf1 activation is comparable to that of HS (Figure 4A). However, such activation of Hsf1 failed to induce prion curing (Figure 4B).

Heat shock-induced prion loss is associated with a transient cessation in cell division and the asymmetric localization of chaperones, which is required for prion loss (Klaips et al.,

2014). I reasoned that artificial activation of Hsf1 would not create conditions to allow the concentration of chaperones in cells needed to induce prion loss. To circumvent this possibility, I arrested cells with α-factor following treatment (Amon, 2002). As a proof of principle, I first assessed the impact of α-factor treatment on heat-shock at 37°C, a condition that leads to only minor asymmetry in Hsp104 localization and to mild prion loss (Klaips et al., 2014). The prion loss was significantly increased with α-factor treatment (Figure 4B). However, α-factor treatment following Hsf1 activation did not cause any prion loss (Figure 4B). While I was unable to detect prion curing following artificial Hsf1 activation, we explored the possibility that expression of this variant might further promote prion loss following heat shock. Strikingly, this expression completely blocked HS-mediated prion curing (Figure 4C).

Sse1 levels limit Hsf1-induced and HS-induced prion curing. To explore the basis of this inhibitory effect of artificial Hsf1 activation, I sought to compare the chaperone profiles of HS, artificial Hsf1 activation and the combined condition. Hsp104, as the major fragmentase in yeast, plays an essential role in prion propagation and also heat shock-induced prion curing (Chernoff et al., 1995; Klaips et al., 2014). In addition, Hsp70 and its cofactors, including Hsp40s and NEFs, collaborate with Hsp104 to resolve protein aggregates and are linked to the maintenance of yeast prions (Fan et al., 2007; Higurashi et al., 2008; Sadlish et al., 2008; Song et al., 2005; Tipton et al., 2008). I found that Ssa1 and Sse1 were abnormally upregulated upon artificial Hsf1 activation and also the combined condition (Figure 5A).

To determine whether excess Ssa1 or Sse1 accounts for the inhibitory effect, I examined the effect of overexpressing Ssa1 or Sse1 on HS-mediated curing. When Ssa1 was overexpressed (Figure S2A), the HS-mediated prion curing was moderately repressed (Figure 5B). Therefore, excess Ssa1 could contribute to the inhibitory effect of artificial Hsf1 activation on prion curing but was not sufficient to block it. Sse1 overexpression has been reported to impair growth extraordinarily in budding yeast likely by perturbing the protein quality control network (Shaner et al., 2004). To minimize the undesired effects of Sse1 overexpression, I placed an extra copy of Sse1 under the control of *SSA4* promoter, whose expression is restricted to stress conditions (Boorstein and Craig, 1990). I observed pronounced overexpression of Sse1 upon HS (Figure S2B), and the HS-mediated prion loss was inhibited (Figure 5C), resembling the effect of artificial Hsf1 activation. Additionally, similar conditional overexpression of a Sse1 mutant (A280T, N281A, N572Y, and E575A) (sse1), which does not interact with Hsp70 and loses the nucleotide exchange function (Polier et al., 2008), did not affect HS-mediated prion curing (Figure S2B, 5C), suggesting the ability of excess Sse1 to interfere with HS-mediated prion curing is dependent on the nucleotide exchange function of Sse1. Therefore, excess Sse1 interferes with the prion curing pathway, which could mask the impact of artificial Hsf1 activation on prion propagation.

To revisit the effect of artificial Hsf1 activation on prion propagation, I replaced the promoter of Sse1 with that of *APQ12*, whose expression is not Hsf1 inducible (D. Pincus, personal communication). Such promoter replacement (SseR) led to the expression of Sse1 at 56% of the basal expression of a WT strain, and the expression did not change

significantly upon Hsf1 activation (Figure S2E). Activating Hsf1 in this strain resulted in mild prion curing, and α-factor treatment following Hsf1 activation induced significant prion curing of 44% (Figure 4B), implying that Hsf1 activation *per se* with a reduced level of Sse1 is sufficient to induce prion loss. Thus, the Sse1 level regulates Hsf1-induced prion curing.

Is prion curing by Hsf1 activation in the absence of HS the consequence of amyloid dissolution? To determine the mechanism of prion curing, we sought to examine prion aggregate size and the amount of soluble Sup35 under these conditions. Using SDD-AGE, I observed smaller aggregates upon Hsf1 activation both in WT and the SseR strain (Figure 5D). Despite the smaller aggregates observed for all strains upon inhibition of Sup35 synthesis by CHX treatment, the clearance of prion aggregates was only seen in the SseR strain, consistent with its prion curing phenotype (Figure 5D). Likewise, an increase in the amount of soluble Sup35 only occurred in the SseR strain (Figure 5E), in line with other observations. These findings suggest that the prion curing caused by artificial Hsf1 activation in the SseR strain is the result of amyloid clearance, reminiscent of heat shock-induced prion curing. Thus, activation of the heat shock response is sufficient to expand the capacity of the proteostasis network to resolve amyloids.

The observation that excess Sse1 inhibits prion curing motivated us to test whether limiting Sse1 promoted HS-mediated prion curing. Despite the fact that SseR does not change the expression of Hsp104 (Figure S2C), I observed more pronounced prion curing in the SseR strain compared to WT (Figure 5F), indicating that limiting Sse1 promotes

HS-mediated prion curing. To determine whether the effect is specific to Sse1, I tested the effect of limiting another cytosolic nucleotide exchange factor Fes1 on HS-mediated prion curing. Due to the fact that depletion of Fes1 weakens [*PSI*+] propagation (Jones et al., 2004), I sought to restrict the alteration in Fes1 expression to stress conditions and dramatically reduced its expression upon HS condition by replacing its promoter with that of *MFA1* (Figure S3A). This change did not interfere with HS-mediated prion curing (Figure S3B). Thus, the effect of modulating nucleotide exchange factor on HS-mediated prion curing is specific to Sse1.

Regulation of chaperone-substrate interaction by Sse1 is critical for the outcome of disaggregation. What is the mechanism by which Sse1 regulates the efficiency of amyloid clearance? Sse1, as a NEF, facilitates ADP release from Hsp70, thus weakening the Hsp70-substrate interaction and promoting the functional cycle of Hsp70 (Dragovic et al., 2006; Raviol et al., 2006). We reasoned when Sse1 is limited, the exchange of ADP for ATP should be delayed, which could decelerate substrate release from Hsp70 and result in extended Hsp70-substrate interaction, thus promoting amyloid remodeling. To determine the amount of chaperones bound to prion aggregates, the prion forming domain of Sup35 fused with HA (NM-HA) was employed to immunocapture aggregated Sup35 given that the fusion protein can be incorporated into Sup35 aggregates and immunocaptured by HA magnetic beads readily (Pezza et al., 2014). Consistent with the hypothesis, upon HS treatment, a 2.1-fold increase in Ssa1/2 bound to Sup35 aggregates was observed in the SseR strain relative to WT (Figure 6A). Notably, 4-fold more Hsp104 was also bound to Sup35 aggregates in the SseR strain relative to WT(Figure 6A), which

may account for enhanced fragmentation in former strain. Surprisingly, the amount of Ssb1/2, another class of Hsp70s whose functional cycle is also regulated by the nucleotide exchange activity of Sse1, bound to prion aggregates did not change significantly in the SseR strain relative to WT (Figure 6A). In contrast, when Sse1 was conditionally overexpressed upon HS, we observed less Ssa1 [0.67 fold], Ssb1/2 [0.54 fold], and Hsp104 [0.35 fold] bound to Sup35 aggregates in the Sse1 overexpressed strain relative to WT (Figure 6B). Such alteration was dependent on the nucleotide exchange function of Sse1 as overexpression of the Sse1 mutant (A280T, N281A, N572Y, and E575A) (sse1) did not affect the amount of Ssa1/2, Ssb1/2, or Hsp104 bound to Sup35 aggregates (Figure 6B). Thus, Sse1 levels appear to tune the efficiency of amyloid clearance by modulating the chaperone-prion aggregate interaction.

Is the regulation of chaperone-substrate interaction by Sse1 specific to amyloid aggregates? We sought to evaluate the association between chaperone and stress-induced protein aggregates and also the disaggregation efficiency. When Sse1 is limited, the chaperone-substrate dynamics are likely decelerated, thus yielding more ADP-bound Hsp70-substrate complex, which should reduce chaperone mobility. To determine the change in Hsp70 mobility, I applied florescence loss in photobleaching (FLIP) to strains expressing Ssa1-GFP. In the experiments, the daughter cells were constantly photobleached, while fluorescence loss in the mother cell was measured. The higher the mobility of Ssa1-GFP, the faster the fluorescence loss occurs. When there was no stress-induced aggregates present in normal conditions, the fluorescence loss curve was similar between WT and the SseR strains (Figure 6C), implying the mobility was unaffected by

the SseR allele in the absence of protein aggregates. However, in the presence of stress-denatured aggregates, the fluorescence drop was delayed significantly in the SseR strain relative to WT (Figure 6D), consistent with the hypothesis that SseR promotes the association between Hsp70 and stress-induced aggregates. Similarly, immunocapturing Ssa1-GFP-bound substrates revealed that 1.22-fold more substrates were interacting with Hsp70 in the SseR strain than in WT upon HS (Figure 6E).

Does SseR promote clearance of stress-denatured aggregates? Comparing strains with Hsp104-GFP upon stress relief showed that cells containing Hsp104 puncta persisted longer in SseR, even at 6h of recovery (Figure 6F), indicating a defect in dissolution of stress-denatured protein aggregates. Furthermore, the SseR strain exhibited a growth defect when grown at 37°C compared to WT while there was no difference in growth rate between the two strains at 30°C (Figure 6G). This result indicates in contrast to the effect on amyloid clearance, restricting Sse1 expression during HS in the SseR strain impairs the clearance of stress-denatured protein aggregates. Thus, the WT level of Sse1 is more favorable for non-amyloid aggregate dissolution, whereas a reduced level of Sse1 is more favorable for amyloid clearance.

Discussion

Our work has demonstrated that in addition to heat shock, a subset of environmental stresses can lead to prion curing through a shared mechanism. Hsf1 activation appears to correlate with prion loss, and with a proper level of Sse1, artificial Hsf1 activation *per*

se is sufficient to induce prion curing, implying that the upregulation of protein quality control factors is critical for amyloid resolution. Although this work cannot preclude the possibility that direction alteration to the amyloid conformations by these environmental stresses may contribute to amyloid disassembly, tuning the proteostasis network itself is capable of disassembling thermodynamically stable amyloid. This suggests that the primary limitation of the proteostasis network for amyloid clearance is the lack of sensing these aggregates since prion aggregates barely activate the stress response program (Eaglestone et al., 1999; Ross and Wickner, 2004). Additionally, our previous work showed that Hsp104-GFP localization in the [*PSI*$^{+}$] strain expressing Sup35 at its endogenous level was indistinguishable from the [*psi*$^{-}$] strain (Klaips et al., 2014), revealing poor chaperone engagement, which may account for lack of sensitivity for ordered amyloid aggregates by molecular chaperones.

Most of the research on the disaggregation machinery proposes that disaggregation of both amyloid and non-amyloid aggregates require the collaboration of Hsp104 and Hsp70 and are largely mechanistically equivalent processes (Doyle et al., 2013; Haslberger et al., 2010; Winkler et al., 2012b). Here, limiting Sse1 promotes chaperone-substrate engagement, enhancing amyloid resolubilization while impairing dissolution of stress-denatured aggregates, implying distinct requirements for the optimal disaggregation efficiency. In line with this idea, research using budding yeast showed that, in comparison to disaggregation of amorphous aggregates, fragmentation of amyloid fibrils requires a more cooperative mode of inter-subunit collaboration of Hsp104, implying an operational plasticity for amyloid and non-amyloid clients (DeSantis et al., 2012). These distinct

functional requirements represent another obstacle for amyloid disaggregation; that is, the configuration of the proteostasis network is primarily optimized to a more universal challenge - handling stress-induced aggregates - and therefore, is less favorable for amyloid clearance.

The Hsp70 functional cycle is critical for the refolding chaperone activity of Hsp70, whereas its significance in tuning the efficiency of amyloid resolution by Hsp104 is yet to be discovered. Previous work has linked factors regulating Hsp70 substrate binding to prion maintenance (Higurashi et al., 2008; Jones et al., 2004; Sadlish et al., 2008; Tipton et al., 2008), implying that the dynamics of the Hsp70 functional cycle affect the fragmentation activity essential for prion propagation; however, it is largely unexplored whether this regulation plays a role in potentiating the disaggregation machinery for resolubilizing prion amyloids. Here, we demonstrate that reconfiguring the chaperone complex by reducing nucleotide exchange for Hsp70 allows increased binding of Hsp70 and also Hsp104 recognition, enabling the solubilization of ordered amyloid aggregates. This critical requirement on the Hsp70 cycle for amyloid dissolution has also been shown in a mammalian disaggregation system; specifically, high nucleotide exchange of Hsp70 inhibits α-synuclein fibril disassembly (Gao et al., 2015), underscoring that this is a generic principle for resolving ordered aggregates.

We propose that the functional dynamics of Hsp70 tuned by the NEF Sse1 play a critical role in recruiting Hsp104, thus determining the disaggregation efficiency. However, an alternative explanation for the impact of altering NEF on Hsp104-prion aggregation

interaction could be inspired by a report on the *E. coli* Hsp104/Hsp70/NEF homolog, ClpB/DnaK/GrpE, showing that ClpB competes with GrpE for access to the DnaK ATPase domain (Doyle et al., 2015). Since the ability to interact with Hsp70 and the nucleotide exchange function is usually coupled, our findings cannot directly preclude the possibility that this mechanism is contributing to the outcome. However, the relative abundance of Hsp70 and Sse1, roughly 10:1, indicates that binding saturation and therefore competition is unlikely at physiological conditions. Furthermore, the increased Hsp70-prion aggregate interaction observed when the level of NEF (Sse1) is reduced cannot be explained by this proposed interplay between Hsp104, Hsp70 and NEF. And, this effect on Hsp70-substrate is likely the major contributor to the dramatic alteration to the Hsp104-substrate interaction, given the well-established interaction between Hsp70 and Hsp104 (Doyle et al., 2013; Haslberger et al., 2010; Winkler et al., 2012b).

Our studies identify Sse1 as a critical regulator of disaggregation of amyloid aggregates. Sse1 has previously been implicated in the appearance and curing of [*PSI*$^{+}$]; deletion of this factor disrupts [*PSI*$^{+}$] propagation (Sadlish et al., 2008), and overexpression promotes [*PSI*$^{+}$] appearance and variant determination (Fan et al., 2007). Two roles of Sse1 have been proposed to account for its involvement in the process: the leading function is nucleotide exchange and another is stimulating the nucleation of the Sup35 prion domain independent of its NEF function. Our observations suggest that the effect of altering Sse1 on amyloid clearance is intimately linked to its nucleotide exchange function rather than facilitating prion seed conversion. Complete depletion of Sse1 seems to extraordinarily inhibit fragment of prion aggregates indicated by larger prion aggregates in [*PSI*$^{+}$]$_{strong}$ and

loss of prion aggregates in [*PSI*$^{+}$]$_{weak}$ (Fan et al., 2007). However, our study suggests that an intermediate level of Sse1 could enhance fragment of prion aggregates, suggesting a narrow range of NEF levels for optimal fragmentation. The effect of excess Sse1 on [*PSI*$^{+}$] appearance and variant determination might be explained by affecting the dissolution of newly formed prion nucleates. Thus, the exact role of Sse1 in these processed is yet to be re-examined.

Materials and Methods

Plasmids and yeast strains. All plasmids used in this study are listed in Table S1; all oligonucleotides used in this study are listed in Table S2. All plasmids generated by PCR were confirmed by sequencing.

Plasmids:

SB1186 (pFA6a-KanMX4-P_{APQ12}) was constructed via assembling two fragments, FA6a-Kan and *APQ12* promoter, using DNA Assembly (NEB). FA6a-Kan fragment was amplified via PCR using primers FA6a-Kan-F and FA6a-Kan-R and pFA6a-KanMX4-P_{MFA1} (Pezza et al., 2014) as a template. The *APQ12* promoter was amplified via PCR using primers APQ12-F and APQ12-R. SB1185 (pRS306-P_{SSA4}SSE1) was constructed via assembling three fragments, pRS306, *SSA4* promoter and SSE1 ORF, using DNA Assembly (NEB). pRS306 (Sikorski and Hieter, 1989) was linearized by digestion with *Cla*I and *Not*I. The *SSA4* promoter and the *SSE1* ORF were amplified via PCR using primers Pssa4-F and Pssa4-R, SSE1 ORF F and SSE1 ORF R, respectively. SB1187 (pRS306-P_{SSA4}SSE1(A280T, N281A, N572Y, and E575A)) was generated via two rounds of site-directed mutagenesis on SB1185 using QuikChange (Agilent) and primers Sse1-572,575-F and Sse1-572,575-R, Sse1-280,281-F and Sse1-280,281-R, respectively.

Strains:

All yeast strains are derivatives of 74-D694 (Chernoff et al., 1995) and listed in Table S3. The HSE reporter strain (SY3635) was constructed by integration of *Pme*I-digested

SB1179 (a gift from D. Pincus) into SLL2600 and selection on medium lacking leucine. Expression was confirmed by fluorescence microscopy. The Δ*msn2* strain (SY2966), Δ*msn4* strain (SY2969), Δ*msn2/4* strain (SY2971) were generated by sporulation of a diploid strain containing Δ*msn2* and Δ*msn4*. Δ*msn2* was introduced to the strain by transforming a PCR-generated cassette using primers 5 Msn2 KO and 3 Msn2 KO and pFA6a-KanMX4 (Wach et al., 1994) as a template and selection on medium supplemented with G418. Δ*msn4* was introduced to the strain by transforming a PCR-generated cassette using primers 5 Msn4 KO and 3 Msn4 KO and pFA6a-HphMX4 (Wach et al., 1994) as a template and selection on medium supplemented with hygromycin B. Disruptions were verified by PCR using primer pairs, 5 Msn2(4) KO check/pTEFCH and 3 Msn2(4) KO check/pFA6a. The *MSN4* strain (SY2961) was constructed by targeting the core module of pCORE to the *MSN4* ORF by transformation of a PCR-generated fragment using primers Msn4 F DP and Msn4 R DP and SB583 (Storici et al., 2001) as a template into SLL2600 and selection on medium lacking uracil, followed by transformation of a W303-genomic PCR-generated fragment using primers Msn4 W303 F and Msn4 W303 R to replace the CORE cassette and selection on medium supplemented with 5-FOA. Disruption for *MSN4(TAA->CAA)* was confirmed by PCR amplification of genomic DNA and sequencing. The Δ*msn2MSN4* strain (SY3314) was constructed by mating SY2961 and an α mating-type Δ*msn2* strain sporulated from the Δ*msn2*Δ*msn4* diploid, sporulation and tetrad dissection. Disruption for *MSN4(TAA->CAA)* was confirmed by PCR amplification of genomic DNA and sequencing. The strain containing a chimeric transcription factor, GEM, comprised of Gal4 DNA binding domain, the estrogen receptor and the Msn2 activation domain (Zheng et al., 2016) (SY3636) was constructed by

integration of *Bst*XI-digested SB1178 (a gift from D. Pincus) into SY3635 and selection on medium lacking histidine. The Hsf1 induction strain (SY3629) was constructed by integration of *Fse*I-digested SB1181 (a gift from D. Pincus) into SY3636 and selection on medium lacking tryptophan. Expression was confirmed by fluorescence microscopy. The SseR Hsf1 induction strain (SY3630) was constructed by transformation of a PCR-generated fragment using primers Sse1-APQ12 F and Sse1-APQ12 R and SB1186 as a template. Promoter replacement was confirmed by PCR using primer pairs Sse1 -700/pFA6a and RC Sse1 100/pTEFCH and western blotting. The SseR strain (SY3639) was constructed by transformation of a PCR-generated fragment using primers Sse1-APQ12 F and Sse1-APQ12 R and SB1186 as a template. The [*psi-*] version (SY3655) was generated by curing the prion in SY3639 via growth on YPD plates containing 3 mM GdnHCI. The Sse1 inducible strain (SY3662) and the Sse1 mutant inducible strain (SY3663) were constructed by integration of *Ppu*MI-digested SB1185 and SB1187 respectively into SLL2600 and selection on medium lacking uracil. Expression was confirmed by western blotting. The *MAT*α [*PSI*+]$_{Weak}$ strain (SY3609) was constructed by mating type switching of SLL2600 with the pGAL-HO plasmid (Herskowitz and Jensen, 1991). The NMHA *SUP35*/Δ strain (SY3644) was constructed by mating SY1625 to SY3609, followed by transformation of a PCR-generated cassette using primers 5 SUP35 KO and 3 SUP35 KO and pFA6a-HphMX4 (Wach et al., 1994) as a template. Disruption was verified by PCR using primer pairs, 5 SUP35 KO CHK/pTEFCH and 3 SUP35 KO CHK/pFA6a. The NMHA SseR/SseR *SUP35*/Δ strain (SY3645) was constructed by introducing Sse1 promoter replacement to SY1625 and SY3609 as described, followed by mating and transformation of a PCR-generated cassette using primers 5 SUP35 KO

and 3 SUP35 KO and pFA6a-HphMX4 (Wach et al., 1994) as a template. The NMHA Sse1 inducible *SUP35*/Δ strain (SY3661) and NMHA Sse1 mutant inducible *SUP35*/Δ strain (SY3664) were constructed by integration of *Ppu*MI-digested SB1185 and SB1187 respectively into SY3644 and selection on medium lacking uracil. Expression was confirmed by western blotting. The *MAT*α Ssa1-GFP [*PSI*$^{+}$]$_{Weak}$ strain (SY3180) was constructed by mating SY2658 (Klaips et al., 2014) to SY3609, sporulation and tetrad dissection. The SseR Ssa1-GFP [*PSI*$^{+}$]$_{Weak}$ (SY3659) was constructed by mating SY3180 to SY3639, sporulation and tetrad dissection. Promoter replacement was confirmed by PCR, and GFP tagging was confirmed by fluorescence microscopy. The [*psi*$^{-}$] version (SY3660) was generated by curing the prion in SY3659 via growth on YPD plates containing 3 mM GdnHCl. The Hsp104-GFP [*psi*$^{-}$] (SY3656) was generated by curing the prion in SY2126 via growth on YPD plates containing 3 mM GdnHCl. The SseR Hsp104-GFP [*PSI*$^{+}$]$_{Weak}$ (SY3657) was constructed by introducing the *Sse1* promoter replacement into SY3609, followed by mating to SY2126, sporulation and tetrad dissection. Promoter replacement was confirmed by PCR, and GFP tagging was confirmed by fluorescence microscopy. The [*psi*$^{-}$] version (SY3658) was generated by curing the prion in SY3657 via growth on YPD plates containing 3 mM GdnHCl. The FesR strain (SY3666) was constructed by transformation of a PCR-generated fragment using primers Fes1-MFA1 F and Fes1-MFA1 R and SB526 as a template. Promoter replacement was confirmed by PCR using primer pairs Fes1 -700/pFA6a and RC Fes1 100/pTEFCH and western blotting.

Growth conditions and phenotypic analysis. Yeast cultures were grown in rich medium supplemented with 3 mM adenine (YPAD) unless otherwise specified. Cultures were kept at an OD_{600} of less than 0.5 at 30°C for at least 10 doublings to ensure exponential growth. To measure colony color phenotype, aliquots of cultures were diluted and plated on YPD plates. After growth at 30°C and a period of color development at room temperature, each colony was scored based on colony color phenotype: fully cured (red, [*psi-*]), sectored (mixture of red and white), uncured (white, [*PSI+*]$_{Weak}$). Fully cured and sectored colonies were combined in the "cured" category. For the proline analog AZC treatment experiment, cells were grown in minimal SD medium with only four supplements (His, Trp, Leu and Ura) to optimize the uptake of AZC. α-factor arrest was performed in YPD liquid medium containing a final concentration of 5 µg/ml α-factor for ~5 hr.

Protein analysis. Semi-denaturing detergent agarose gel electrophoresis (SDD-AGE), SDS-PAGE and quantitative immunoblotting were performed as previously described (Pezza et al., 2009). Quantification of western blots was done using Image Studio Lite (Li-Cor Biosciences). To analyze the fate of aggregated Sup35, the cycloheximide SDS-sensitivity assay was performed as previously described (Klaips et al., 2014). To quantify aggregate accumulation, the aggregate analysis assay was performed as previously described (Klaips et al., 2014). The Ssa1 immunocapture was performed adapted from the Hsp104 immunocapture as previously described (Klaips et al., 2014). Using Ssa1-GFP strains instead of Hsp104-GFP strains, this immunocapture isolated the proteins

interacting with Ssa1-GFP, and quantification of co-captured proteins was done using ImageQuant TL (GE Lifesciences).

Immunocapture. Native lysates were prepared as described (Klaips et al., 2014), and immunocapture was performed using anti-HA or anti-Myc magnetic beads (Thermo Scientific Pierce). Co-captured proteins were analyzed by SDS-PAGE and western blotting for Sup35, HA (Roche), Hsp104 (Abcam), Ssa1 (a gift from E. Craig), Sse1 (a gift from J. Brodsky) and Ssb1 (a gift from J. Frydman). The amount of each chaperone that was co-captured was normalized to the amount of captured aggregated Sup35.

Microscopy. Imaging was performed in complete SD medium supplemented with 2.5 mM adenine and 2% glucose. Images were obtained on a Zeiss Axio Imager M2 fluorescence light microscope with a 100x objective.

Flow cytometry. For measurement of HSE-GFP intensity, cells were grown in YPAD and treated with stressors as indicated, followed by washing and re-suspending in SD complete medium before flow cytometry. For measurement of STRE-GFP intensity, cells transformed with SB1166 (a gift from O. Brandman) were grown in SD medium lacking uracil and treated with stressors as indicated before flow cytometry. Flow cytometry was performed on a BD LSRFortessa using a 488 nm laser and a FITC filter to measure GFP fluorescence intensity in single cells. Data were collected at least in triplicate and population medians were computed with FlowJo (TreeStar Inc.).

Fluorescence Loss in Photobleaching (FLIP). FLIP experiments were performed on a Yokogawa Spinning Disk confocal microscope equipped with a 100x objective (NA=1.4) and a Bruker miniscanner. Frames were collected using 488-nm excitation and 500-560-nm emission wavelengths. Cells with buds of roughly 1/3 the size of their mothers were chosen for analysis, and average florescence pixel intensity was monitored in the mother cell, the bud, and a nearby cell as a control, with bleaching of the entire bud following each image acquisition. For each data set, a minimum of 20 cells was analyzed. Image analysis was performed using software NIS-Elements (Nikon), and specific values were normalized to background levels of fluorescence loss.

Table S1: Plasmids

Name	Description	Reference
SB1179	pNH605-4xHSEpr-YFP (pDP122)	(Zheng et al., 2016)
SB1166	pRS426-STRE-GFP	(Brandman et al., 2012)
SB1178	pRS303-GEM (pDP030)	(Zheng et al., 2016)
SB1181	pNH604-P_{GAL1}-HSF1PO4*-mKate (pDP726)	(Zheng et al., 2016)
SB1186	pFA6a-KanMX4-P_{APQ12}	This work
9026	pRS425	(Sikorski and Hieter, 1989)
SB763	pRS425-SSA1	(Newnam et al., 1999)
SB1185	pRS306-P_{SSA4}SSE1	This work
SB1187	pRS306-P_{SSA4}SSE1(A280T, N281A, N572Y, and E575A)	This work
SB653	pRS305-PSUP35PrD-HA3	(Pezza et al., 2014)
SB526	pFA6a-KanMX4-P_{MFA1}	(Pezza et al., 2014)

Table S2: Oligonucleotide Sequences

Description	Sequence (5'-3')
pTEFCH	GCACGTCAAGACTGTCAAGG
pFA6a	TGCCCAGATGCGAAGTTAAGTG
5 SUP35 KO	ACTTGCTCGGAATAACATCTATATCTGCCCACTAGCA ACACGGATCCCCGGGTTAATTAA
3 SUP35 KO	GGTATTATTGTGTTTGCATTTACTTATGTTTGCAAGAA ATGAATTCGAGCTCGTTTAAAC
5 SUP35 KO CHK	CACAAAAATCATACAACGAATGG
3 SUP35 KO CHK	CTAAATGATGTTGACAAACTTATG
5 Msn2 KO	TTTTTCAACTTTTATTGCTC ATAGAAGAAC TAGATCTAAACAGCTGAAGCTTCGTACGC
3 Msn2 KO	TTATGAAGAAAGATCTATCGAATTAAAAAAATGGGGT CTAGCATAGGCCACTAGTGGATC
5 Msn2 KO check	GTTTGTTGCCTGATATCAGC
3 Msn2 KO check	CTGACAGGCATATTGCACAG
5 Msn4 KO	TTCGGCTTTTTTTTCTTTTCTTCTTATTAA AAACAATATACAGCTGAAGCTTCGTACGC
3 Msn4 KO	TAGCTTGTCTTGCTTTTATTTGCTTTTGACCTTATTTTT TGCATAGGCCACTAGTGGATC
5 Msn4 KO check	CCGGATAAACCAAACCCACC
3 Msn4 KO check	TATTAAGAGTCATCACAGCAAC
Msn4 F DP	CAACAGGATTGAACGACAATGATTATAATCTAGACGA TACCAATAATGATGAGCTCGTTTTCGACACTGG
Msn4 R DP	CCGGCATGAACTTCAATGCTTCTTCTGAAGATACAAA ATCCTCTAAGATTTCCTTACCATTAAGTTGATC
Msn4 W303 F	ATGCTAGTCTTCGGACCTAA
Msn4 W303 R	TCAAAAATCACCGTGCTTT
Sse1-APQ12 F	AAATGTTTGAAGCCACATGA ATTGAGAAAG GTAAGCACATGAATTCGAGCTCGTTTAAAC
Sse1-APQ12 R	AGTTATTGTTACCTAAATCTAAACCAAATGGAGTACTC ATTTTTGGGTTGCTCACTTT
Sse1 -700	ATTAATGACCCCTTGAGCTG
RC Sse1 100	AACAACAGATGGGGTGGA
Pssa4-F	TGGAGCTCCACCGCGGTGGCCTTTTGCCCGGTGAGT TG
Pssa4-R	GAGTACTCATGATTATTGTTTTGTTTATTTTTTTTCTTG TTTTTG
SSE1 ORF F	AACAATAATCATGAGTACTCCATTTGGTTTAGATTTAG
SSE1 ORF R	CCTCGAGGTCGACGGTATCGTGGCATGTCCCCATTC ATG
Sse1-572,575-F	GAGACAGAAGACCGTAAGTATACTCTTGCAGAGTAC ATCTACACATTAC

Sse1-572,575-R	GTAATGTGTAGATGTACTCTGCAAGAGTATACTTACG GTCTTCTGTCTC
Sse1-280,281-F	GAAAAGTTGAAGAAAGTTTTGTCTACTGCTACTAATG CCCCATTCTCTGTTG
Sse1-280,281-R	CAACAGAGAATGGGGCATTAGTAGCAGTAGACAAAA CTTTCTTCAACTTTTC
FA6a-Kan-F	GATCCGTCGACCTGCAG
FA6a-Kan-R	TGTTTAGCTTGCCTCGTCC
APQ12-F	GGGACGAGGCAAGCTAAACAGGAAGCTTCC TTGAGAGTCC
APQ12-R	ACGCTGCAGGTCGACGGATCTTTTGGGTTGCTCACT TTGC
Fes1-MFA1 F	TCGTTTGAAA TGATATACCT CTTGGACTGG AATCTTCTGGGAATTCGAGCTCGTTTAAAC
Fes1-MFA1 R	CTTGAGAATTCGCAATAGACCACTGTAATAGCTTTTC CATGGATCCTTCTATTCGATG
Fes1 -700	TTCTACAGATTGGATCAGTG GAC
RC Fes1 100	CCACCGAATAACTGCTGTAGC

Table S3: Yeast Strains

Strain	Genotype	Plasmids Integrated	Figure	Reference
SLL2600	*MATa* [*PSI*+]Weak *ade1-14 his3Δ200 trp1-289 ura3-52 leu2-3, 112*	-	1AB, S1, 2ACDEF, S2ABCDE, 3B, S3AB, 4B, 5AB	(Derkatch et al., 1996)
SY2126	*MATa* [*PSI*+]Weak *ade1-14 his3Δ200 trp1-289 ura3-52 leu2-3, 112 HSP104GFP::KANMX6*	-	2B	(Klaips et al., 2014)
SY1888	*MATa* [*PSI*+]Weak *ade1-14 his3Δ200 trp1-289 ura3-52 leu2-3, 112 Δbni1::KANMX4*	-	2E	(Klaips et al., 2014)
SY3635	*MATa* [*PSI*+]Weak *ade1-14 his3Δ200 trp1-289 ura3-52 leu2-3, 112::LEU::HSE-YFP*	SB1179	3A, 4A	This work
SY2961	*MATa* [*PSI*+]Weak *ade1-14 his3Δ200 trp1-289 ura3-52 leu2-3,112 MSN4(TAA->CAA)*	-	3C	This work
SY2966	*MATa* [*PSI*+]*Weak ade1-14 his3Δ200 trp1-289 ura3-52 leu2-3, 112 Δmsn2::kanMX4*	-	3C	This work
SY3314	*MATa* [*PSI*+]Weak *ade1-14 his3Δ200 trp1-289 ura3-52 leu2-3,112 Δmsn2::kanMX4 MSN4(TAA->CAA)*	-	3C	This work
SY2969	*MATa* [*PSI*+]Weak *ade1-14 his3Δ200 trp1-289 ura3-52 leu2-3, 112 Δmsn4::hphMX4*	-	3C	This work
SY2971	*MATa* [*PSI*+]Weak *ade1-14 his3Δ200 trp1-289 ura3-52 leu2-3, 112 Δmsn2::kanMX4 Δmsn4::hphMX4*	-	3C	This work
SY3629	*MATa* [*PSI*+]Weak *ade1-14 his3Δ200::HIS::GEM trp1-289::TRP::Gal-Hsf1PO4* ura3-52 leu2-3, 112::LEU::HSE-YFP*	SB1178, SB1179, SB1181	4ABC, 5ADE	This work
SY3630	*MATa* [*PSI*+]Weak *ade1-14 his3Δ200::HIS::GEM trp1-289::TRP::Gal-Hsf1PO4* ura3-52 leu2-3, 112::LEU::HSE-YFP* P_{APQ12}*SSE1::KanMX4*	SB1178, SB1179, SB1181	S2E, 4B, 5DE	This work

SY3636	*MATa* [*PSI*+]Weak *ade1-14 his3Δ200::HIS::GEM trp1-289 ura3-52 leu2-3, 112::LEU::HSE-YFP*	SB1178, SB1179	4C, 5DE	This work
SY3662	*MATa* [*PSI*+]Weak *ade1-14 his3Δ200 trp1-289 ura3-52::URA3::P$_{SSA4}$SSE1 leu2-3, 112*	SB1185	S2B, 5C	This work
SY3663	*MATa* [*PSI*+]Weak *ade1-14 his3Δ200 trp1-289 ura3-52::URA3::P$_{SSA4}$SSE1 (A280T, N281A, N572Y, and E575A) leu2-3, 112*	SB1187	S2B, 5C	This work
SY3639	*MATa* [*PSI*+]Weak *ade1-14 his3Δ200 trp1-289 ura3-52 leu2-3, 112 P$_{APQ12}$SSE1::KanMX4*	-	S2CD, 5F	This work
SY1625	*MATa* [*psi*-] *ade1-14 his3Δ200 trp1-289 ura3-52 leu2-3, 112::LEU2::P$_{SUP35}$NMHA*	SB653	Materials and methods	(Pezza et al., 2014)
SY3609	*MATα* [*PSI*+]Weak *ade1-14 his3Δ200 trp1-289 ura3-52 leu2-3, 112*	-	Materials and methods	This work
SY3644	*MATa/α* [*PSI*+]Weak *ade1-14/ade1-14 his3Δ200/his3Δ200 trp1-289/ trp1-289 ura3-52/ura3-52 leu2-3, 112/ leu2-3, 112::LEU2::P$_{SUP35}$NMHA Δsup35::hphMX4*	SB653	S4AB, 6AB	This work
SY3645	*MATa/α* [*PSI*+]Weak *ade1-14/ade1-14 his3Δ200/his3Δ200 trp1-289/ trp1-289 ura3-52/ura3-52 leu2-3, 112/ leu2-3, 112::LEU2::P$_{SUP35}$NMHA Δsup35::hphMX4 P$_{APQ12}$SSE1::KanMX4*	SB653	S4A, 6A	This work
SY3661	*MATa/α* [*PSI*+]Weak *ade1-14/ade1-14 his3Δ200/his3Δ200 trp1-289/ trp1-289 ura3-52/ura3-52::URA3::P$_{SSA4}$SSE1 leu2-3, 112/ leu2-3, 112::LEU2::P$_{SUP35}$NMHA Δsup35::hphMX4*	SB1185	S4B, 6B	This work
SY3664	*MATa/α* [*PSI*+]Weak *ade1-14/ade1-14 his3Δ200/his3Δ200 trp1-289/ trp1-289 ura3-52/ura3-52::URA3::P$_{SSA4}$SSE1(A280T, N281A, N572Y, and E575A) leu2-3, 112/ leu2-3,*	SB1187	S4B, 6B	This work

	112::LEU2::P$_{SUP35}$NMHA Δsup35::hphMX4			
SY2657	*MATa* [*psi-*] *ade1-14 his3Δ200 trp1-289 ura3-52 leu2-3112 SSA1GFP::KANMX6*	-	6CE	(Klaips et al., 2014)
SY2658	*MATa* [*PSI+*]$_{Weak}$ *ade1-14 his3Δ200 trp1-289 ura3-52 leu2-3112 SSA1GFP::KANMX6*	-	6D	(Klaips et al., 2014)
SY3660	*MATa* [*psi-*] *ade1-14 his3Δ200 trp1-289 ura3-52 leu2-3112 SSA1GFP::KANMX6 P$_{APQ12}$SSE1::KanMX4*	-	6CE	This work
SY3659	*MATa* [*PSI+*]$_{Weak}$ *ade1-14 his3Δ200 trp1-289 ura3-52 leu2-3112 SSA1GFP::KANMX6 P$_{APQ12}$SSE1::KanMX4*	-	6D	This work
SY3180	*MATα* [*PSI+*]$_{Weak}$ *ade1-14 his3Δ200 trp1-289 ura3-52 leu2-3112 SSA1GFP::KANMX6*	-	Materials and methods	This work
SY3656	*MATa* [*psi-*] *ade1-14 his3Δ200 trp1-289 ura3-52 leu2-3, 112 HSP104GFP::KANMX6*	-	6F	This work
SY3657	*MATa* [*PSI+*]$_{Weak}$ *ade1-14 his3Δ200 trp1-289 ura3-52 leu2-3, 112 HSP104GFP::KANMX6 P$_{APQ12}$SSE1::KanMX4*	-	Materials and methods	This work
SY3658	*MATa* [*psi-*] *ade1-14 his3Δ200 trp1-289 ura3-52 leu2-3, 112 HSP104GFP::KANMX6 P$_{APQ12}$SSE1::KanMX4*	-	6F	This work
SLL2119	*MATa* [*psi-*] *ade1-14 his3Δ200 trp1-289 ura3-52 leu2-3, 112*	-	6G	(Chernoff et al., 1995)
SY3655	*MATa* [*psi-*] *ade1-14 his3Δ200 trp1-289 ura3-52 leu2-3, 112 P$_{APQ12}$SSE1::KanMX4*	-	6G	This work
SY3666	*MATa* [*PSI+*]$_{Weak}$ *ade1-14 his3Δ200 trp1-289 ura3-52 leu2-3, 112 P$_{MFA1}$FES1::KanMX4*	-	S3AB	This work

References

Amon, A. (2002). Synchronization procedures. Methods Enzymol. *351*, 457–467.

Anfinsen, C.B. (1973). Folding of Protein Chains. Science (80-.). *181*, 223–230.

Boorstein, W.R., and Craig, E. a (1990). Structure and regulation of the SSA4 HSP70 gene of Saccharomyces cerevisiae. J. Biol. Chem. *265*, 18912–18921.

Brandman, O., Stewart-Ornstein, J., Wong, D., Larson, A., Williams, C.C., Li, G.-W., Zhou, S., King, D., Shen, P.S., Weibezahn, J., et al. (2012). A Ribosome-Bound Quality Control Complex Triggers Degradation of Nascent Peptides and Signals Translation Stress. Cell *151*, 1042–1054.

Chernoff, Y.O., Lindquist, S.L., Ono, B., Inge-Vechtomov, S.G., and Liebman, S.W. (1995). Role of the chaperone protein Hsp104 in propagation of the yeast prion-like factor [psi+]. Science *268*, 880–884.

Chiti, F., and Dobson, C.M. (2006). Protein Misfolding, Functional Amyloid, and Human Disease. Annu. Rev. Biochem. *75*, 333–366.

Chiti, F., and Dobson, C.M. (2017). Protein Misfolding, Amyloid Formation, and Human Disease: A Summary of Progress Over the Last Decade. Annu. Rev. Biochem. *86*, 27–68.

Chuang, E., Hori, A.M., Hesketh, C.D., and Shorter, J. (2018). Amyloid assembly and disassembly. J. Cell Sci. *131*, jcs189928.

Cox, B.S. (1965). Ψ, A cytoplasmic suppressor of super-suppressor in yeast. Heredity (Edinb). *20*, 505–521.

Derkatch, I.L., Chernoff, Y.O., Kushnirov, V. V, Inge-Vechtomov, S.G., and Liebman, S.W. (1996). Genesis and variability of [PSI] prion factors in Saccharomyces cerevisiae. Genetics *144*, 1375–1386.

DeSantis, M.E., Leung, E.H., Sweeny, E.A., Jackrel, M.E., Cushman-Nick, M., Neuhaus-Follini, A., Vashist, S., Sochor, M.A., Knight, M.N., and Shorter, J. (2012). Operational plasticity enables hsp104 to disaggregate diverse amyloid and nonamyloid clients. Cell *151*, 778–793.

Doyle, S.M., Genest, O., and Wickner, S. (2013). Protein rescue from aggregates by powerful molecular chaperone machines. Nat. Rev. Mol. Cell Biol. *14*, 617–629.

Doyle, S.M., Shastry, S., Kravats, A.N., Shih, Y.H., Miot, M., Hoskins, J.R., Stan, G., and Wickner, S. (2015). Interplay between E. coli DnaK, ClpB and GrpE during protein disaggregation. J. Mol. Biol. *427*, 312–327.

Dragovic, Z., Broadley, S. a, Shomura, Y., Bracher, A., and Hartl, F.U. (2006). Molecular chaperones of the Hsp110 family act as nucleotide exchange factors of Hsp70s. EMBO J. *25*, 2519–2528.

Eaglestone, S.S., Cox, B.S., and Tuite, M.F. (1999). Translation termination efficiency can be regulated in Saccharomyces cerevisiae by environmental stress through a prion-mediated mechanism. Eur. Mol. Biol. Organ. J. *18*, 1974–1981.

Escusa-Toret, S., Vonk, W.I.M., and Frydman, J. (2013). Spatial sequestration of misfolded proteins by a dynamic chaperone pathway enhances cellular fitness during stress. Nat. Cell Biol. *15*, 1231–1243.

Fan, Q., Park, K.-W., Du, Z., Morano, K. a, and Li, L. (2007). The role of Sse1 in the de novo formation and variant determination of the [PSI+] prion. Genetics *177*, 1583–1593.

Ferreira, P.C., Ness, F., Edwards, S.R., Cox, B.S., and Tuite, M.F. (2001). The elimination of the yeast [PSI+] prion by guanidine hydrochloride is the result of Hsp104 inactivation. Mol. Microbiol. *40*, 1357–1369.

Fitzpatrick, D.A., O'Brien, J., Moran, C., Hasin, N., Kenny, E., Cormican, P., Gates, A., Morris, D.W., and Jones, G.W. (2011). Assessment of inactivating stop codon mutations in forty Saccharomyces cerevisiae strains: implications for [PSI] prion- mediated phenotypes. PLoS One *6*, e28684.

Gao, X., Carroni, M., Helen, R., Mayer, M.P., and Bukau, B. (2015). Human Hsp70 Disaggregase Reverses Parkinson ' s-Linked a -Synuclein Amyloid Fibrils. Mol. Cell *59*, 781–793.

Glover, J.R., Kowal, A.S., Schirmer, E.C., Patino, M.M., Liu, J.-J., and Lindquist, S. (1997). Self-Seeded Fibers Formed by Sup35, the Protein Determinant of [PSI+], a Heritable Prion-like Factor of S. cerevisiae. Cell *89*, 811–819.

Haslberger, T., Bukau, B., and Mogk, A. (2010). Towards a unifying mechanism for ClpB/Hsp104-mediated protein disaggregation and prion propagation. Biochem. Cell Biol. *88*, 63–75.

Herskowitz, I., and Jensen, R.E. (1991). [8] Putting the HO gene to work: Practical uses for mating-type switching. In Methods in Enzymology, pp. 132–146.

Higurashi, T., Hines, J.K., Sahi, C., Aron, R., and Craig, E.A. (2008). Specificity of the J-protein Sis1 in the propagation of 3 yeast prions. Proc. Natl. Acad. Sci. U. S. A. *105*, 16596–16601.

Iadanza, M.G., Jackson, M.P., Hewitt, E.W., Ranson, N.A., and Radford, S.E. (2018). A new era for understanding amyloid structures and disease. Nat. Rev. Mol. Cell Biol. *19*, 755–773.

Jones, G., Song, Y., Chung, S., and Masison, D.C. (2004). Propagation of Saccharomyces cerevisiae [PSI+] prion is impaired by factors that regulate Hsp70 substrate binding. Mol. Cell. Biol. *24*, 3928–3937.

Klaips, C.L., Hochstrasser, M.L., Langlois, C.R., and Serio, T.R. (2014). Spatial quality control bypasses cell-based limitations on proteostasis to promote prion curing. Elife *3*, e04288.

Kohno, H., Tanaka, K., Mino, A., Umikawa, M., Imamura, H., Fujiwara, T., Fujita, Y., Hotta, K., Qadota, H., Watanabe, T., et al. (1996). Bni1p implicated in cytoskeletal control is a putative target of Rho1p small GTP binding protein in Saccharomyces cerevisiae. EMBO J. *15*, 6060–6068.

Kryndushkin, D.S., Alexandrov, I.M., Ter-Avanesyan, M.D., and Kushnirov, V. V (2003).

Yeast [PSI+] prion aggregates are formed by small Sup35 polymers fragmented by Hsp104. J. Biol. Chem. *278*, 49636–49643.

Mogk, A., Bukau, B., and Kampinga, H.H. (2018). Cellular Handling of Protein Aggregates by Disaggregation Machines. Mol. Cell *69*, 214–226.

Newnam, G.P., Wegrzyn, R.D., Lindquist, S.L., and Chernoff, Y.O. (1999). Antagonistic interactions between yeast chaperones Hsp104 and Hsp70 in prion curing. Mol. Cell. Biol. *19*, 1325–1333.

Patino, M.M., Liu, J.J., Glover, J.R., and Lindquist, S. (1996). Support for the prion hypothesis for inheritance of a phenotypic trait in yeast. Science *273*, 622–626.

Paushkin, S. V, Kushnirov, V. V, Smirnov, V.N., and Ter-Avanesyan, M.D. (1996). Propagation of the yeast prion-like [psi+] determinant is mediated by oligomerization of the SUP35-encoded polypeptide chain release factor. EMBO J. *15*, 3127–3134.

Pezza, J. a, Villali, J., Sindi, S.S., and Serio, T.R. (2014). Amyloid-associated activity contributes to the severity and toxicity of a prion phenotype. Nat. Commun. *5*, 4384.

Pezza, J.A., Langseth, S.X., Raupp Yamamoto, R., Doris, S.M., Ulin, S.P., Salomon, A.R., and Serio, T.R. (2009). The NatA acetyltransferase couples Sup35 prion complexes to the [PSI+] phenotype. Mol. Biol. Cell *20*, 1068–1080.

Polier, S., Dragovic, Z., Hartl, F.U., and Bracher, A. (2008). Structural basis for the cooperation of Hsp70 and Hsp110 chaperones in protein folding. Cell *133*, 1068–1079.

Raviol, H., Sadlish, H., Rodriguez, F., Mayer, M.P., and Bukau, B. (2006). Chaperone network in the yeast cytosol: Hsp110 is revealed as an Hsp70 nucleotide exchange factor. EMBO J. *25*, 2510–2518.

Ross, E.D., and Wickner, R.B. (2004). Prions of yeast fail to elicit a transcriptional response. Yeast *21*, 963–972.

Sadlish, H., Rampelt, H., Shorter, J., Wegrzyn, R.D., Andréasson, C., Lindquist, S., and Bukau, B. (2008). Hsp110 chaperones regulate prion formation and propagation in S. cerevisiae by two discrete activities. PLoS One *3*, e1763.

Satpute-Krishnan, P., and Serio, T.R. (2005). Prion protein remodelling confers an immediate phenotypic switch. Nature *437*, 262–265.

Scior, A., Buntru, A., Arnsburg, K., Ast, A., Iburg, M., Juenemann, K., Pigazzini, M.L., Mlody, B., Puchkov, D., Priller, J., et al. (2018). Complete suppression of Htt fibrilization and disaggregation of Htt fibrils by a trimeric chaperone complex. EMBO J. *37*, 282–299.

Shaner, L., Trott, A., Goeckeler, J.L., Brodsky, J.L., and Morano, K.A. (2004). The function of the yeast molecular chaperone Sse1 is mechanistically distinct from the closely related Hsp70 family. J. Biol. Chem. *279*, 21992–22001.

Sikorski, R.S., and Hieter, P. (1989). A system of shuttle vectors and yeast host strains designed for efficient manipulation of DNA in Saccharomyces cerevisiae. Genetics *122*, 19–27.

Song, Y., Wu, Y., Jung, G., Tutar, Y., Eisenberg, E., Greene, L.E., and Masison, D.C. (2005). Role for Hsp70 chaperone in Saccharomyces cerevisiae prion seed replication.

Eukaryot. Cell *4*, 289–297.

Sorger, P.K., and Pelham, H.R.B. (1988). Yeast heat shock factor is an essential DNA-binding protein that exhibits. Cell *54*, 855–864.

Storici, F., Lewis, L.K., and Resnick, M.A. (2001). In vivo site-directed mutagenesis using oligonucleotides. Nat. Biotechnol. *19*, 773–776.

Tipton, K., Verges, K., and Weissman, J. (2008). In vivo monitoring of the prion replication cycle reveals a critical role for Sis1 in delivering substrates to Hsp104. Mol. Cell *32*, 584–591.

Tuite, M.F., and Serio, T.R. (2010). The prion hypothesis: from biological anomaly to basic regulatory mechanism. Nat. Rev. Mol. Cell Biol. *11*, 823–833.

Verghese, J., Abrams, J., Wang, Y., and Morano, K. a (2012). Biology of the heat shock response and protein chaperones: budding yeast (Saccharomyces cerevisiae) as a model system. Microbiol. Mol. Biol. Rev. *76*, 115–158.

Voisine, C., Pedersen, J.S., and Morimoto, R.I. (2010). Chaperone networks: Tipping the balance in protein folding diseases. Neurobiol. Dis. *40*, 12–20.

Wach, A., Brachat, A., Pöhlmann, R., and Philippsen, P. (1994). New Heterologous Modules for Classical or PCR-based Gene Disruptions. Yeast *10*, 1793–1808.

Winkler, J., Tyedmers, J., Bukau, B., and Mogk, A. (2012). Chaperone networks in protein disaggregation and prion propagation. J. Struct. Biol. *179*, 152–160.

Zheng, X., Krakowiak, J., Patel, N., Beyzavi, A., Ezike, J., Khalil, A.S., and Pincus, D. (2016). Dynamic control of Hsf1 during heat shock by a chaperone switch and phosphorylation. Elife *5*, e18638.

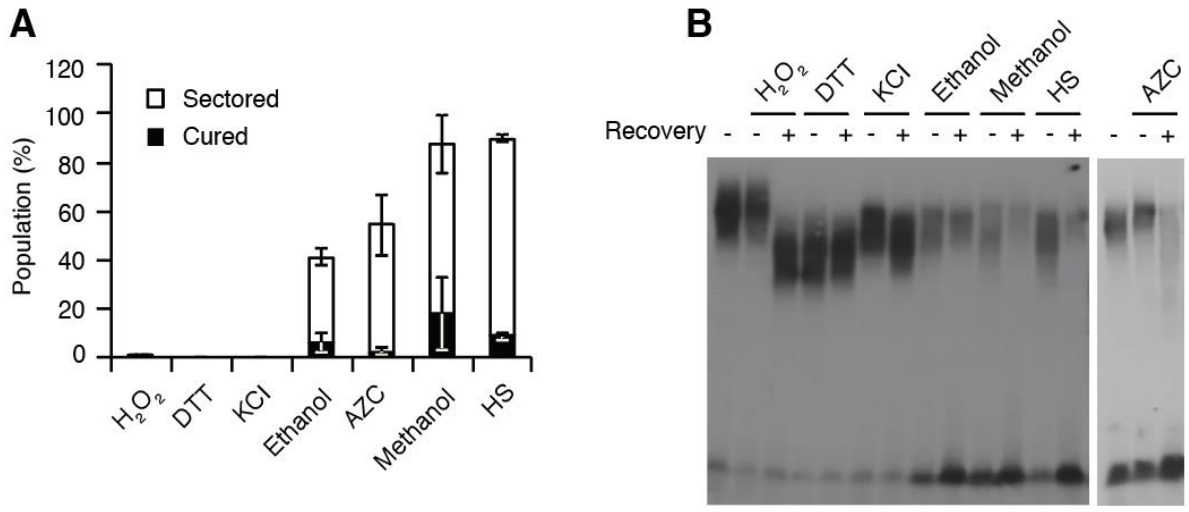

Figure 1. A subset of environmental stresses promotes [*PSI*+] loss through a mechanism that parallels heat-shock mediated protein loss.

(A) [*PSI*+] (SLL2600) cultures were incubated with one of the following stressors as indicated for 60 min, 1 mM H_2O_2, 2 mM DTT, 0.5 M KCl, 6% EtOH, 0.5 mM AZC, or 9% MeOH or were incubated at 40°C for 30 min as HS before plating on rich medium at 30°C to quantify curing. Quantification of colony color phenotypes are shown. Red colonies were categorized as cured (black) while colonies with mixed red and white sectors were categorized as sectored (white). Data represent averages, and error bars represent standard deviations for biological replicates (n=3). (B) Prion aggregate size upon stress treatments as described in (A) and during recovery from stress was assayed by semi-denaturing detergent agarose gel electrophoresis (SDD-AGE). Lysates from cells recovering for two hours following stresses were prepared as recovery samples (left panel). The right panel represents cells growing in SD minimal medium without or with AZC, and the recovery time for AZC treatment is 16 hours.

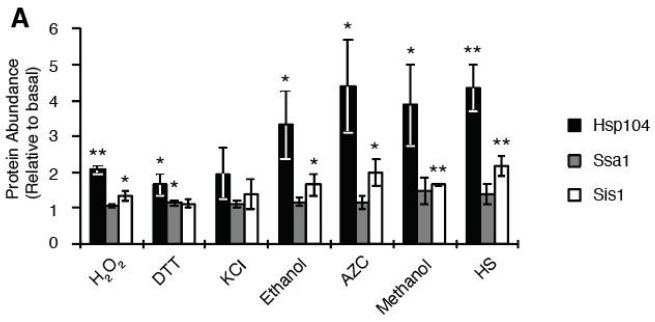
A
Protein Abundance (Relative to basal)
Hsp104
Ssa1
Sis1
H2O2
DTT
KCl
Ethanol
AZC
Methanol
HS

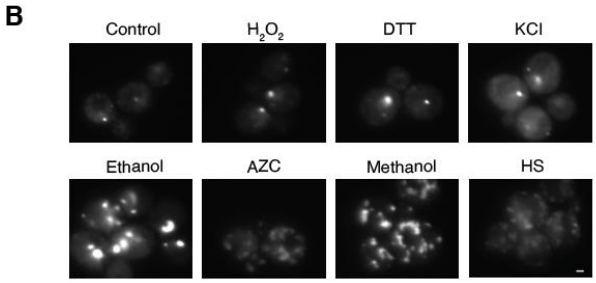
B
Control
H2O2
DTT
KCl
Ethanol
AZC
Methanol
HS

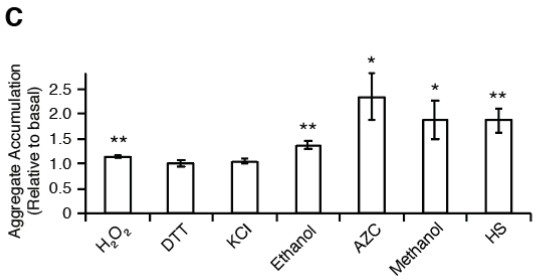
C
Aggregate Accumulation (Relative to basal)
H2O2
DTT
KCl
Ethanol
AZC
Methanol
HS

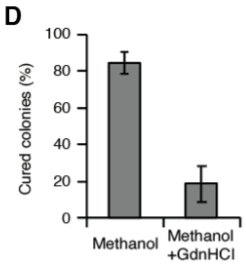
D
Cured colonies (%)
Methanol
Methanol +GdnHCl

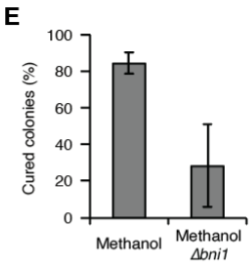
E
Cured colonies (%)
Methanol
Methanol Δbni1

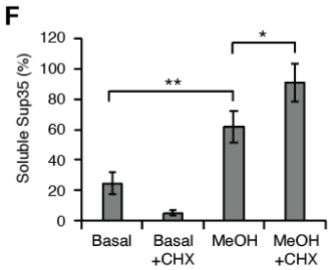
F
Soluble Sup35 (%)
Basal
Basal +CHX
MeOH
MeOH +CHX

Figure 2. Environmental stresses induce [*PSI*$^+$] loss through a common mechanism.

(A) [*PSI*$^+$] (SLL2600) cultures were incubated with one of the following stressors as indicated for 60 min, 1 mM H_2O_2, 2 mM DTT, 0.5 M KCl, 6% EtOH, 0.5 mM AZC, or 9% MeOH or were incubated at 40°C for 30 min as HS, and lysates were prepared and assayed by SDS-PAGE and quantitative immunoblotting for Hsp104 (black), Ssa1 (gray), Sis1 (white). Data represent averages, and error bars represent standard deviations for biological replicates (n=3, *p<0.05, **p<0.005 by unpaired t-test). (B) [*PSI*$^+$] HSP104GFP strain (SY2126) was stress-treated as described in (A), and the pattern of Hsp104-GFP fluorescence was examined by fluorescence microscopy. Representative images were shown. Scale bar = 1 μm. (C) Aggregates from lysates of a [*PSI*$^+$] strain (SLL2600) following treatment as described in (A) were prepared and analyzed by differential centrifugation and Bradford assay. Data represent averages, and error bars represent standard deviations for biological replicates (n≥3, *p<0.05, **p<0.005 by unpaired t-test). (D) [*PSI*$^+$] cultures (SLL2600) were incubated with 9% MeOH for 60 min in the absence or presence of 3 mM guanidine HCl (GdnHCl) and plated on rich medium to quantify prion loss by colony color phenotype. Data represent averages, and error bars represent standard deviations for biological replicates (n=3, p=0.0005 by unpaired t-test). (E) [*PSI*$^+$] WT (SLL2600) or Δ*bni1* (SY1888) strains were incubated with 9% MeOH for 60 min and plated on rich medium to quantify prion loss by colony color phenotype. Data represent averages, and error bars represent standard deviations for biological replicates (n=3, p=0.0139 by unpaired t-test). (F) Sup35 released from amyloid aggregates in a [*PSI*$^+$] strain (SLL2600) following MeOH treatment and recovery in the presence of cycloheximide was determined by treating lysates with 2% SDS at 53°C, followed by SDS-PAGE and immunoblotting for Sup35. Data represent averages, and error bars represent standard deviations for biological replicates (n≥4, *p<0.05, **p<0.005 by unpaired t-test).

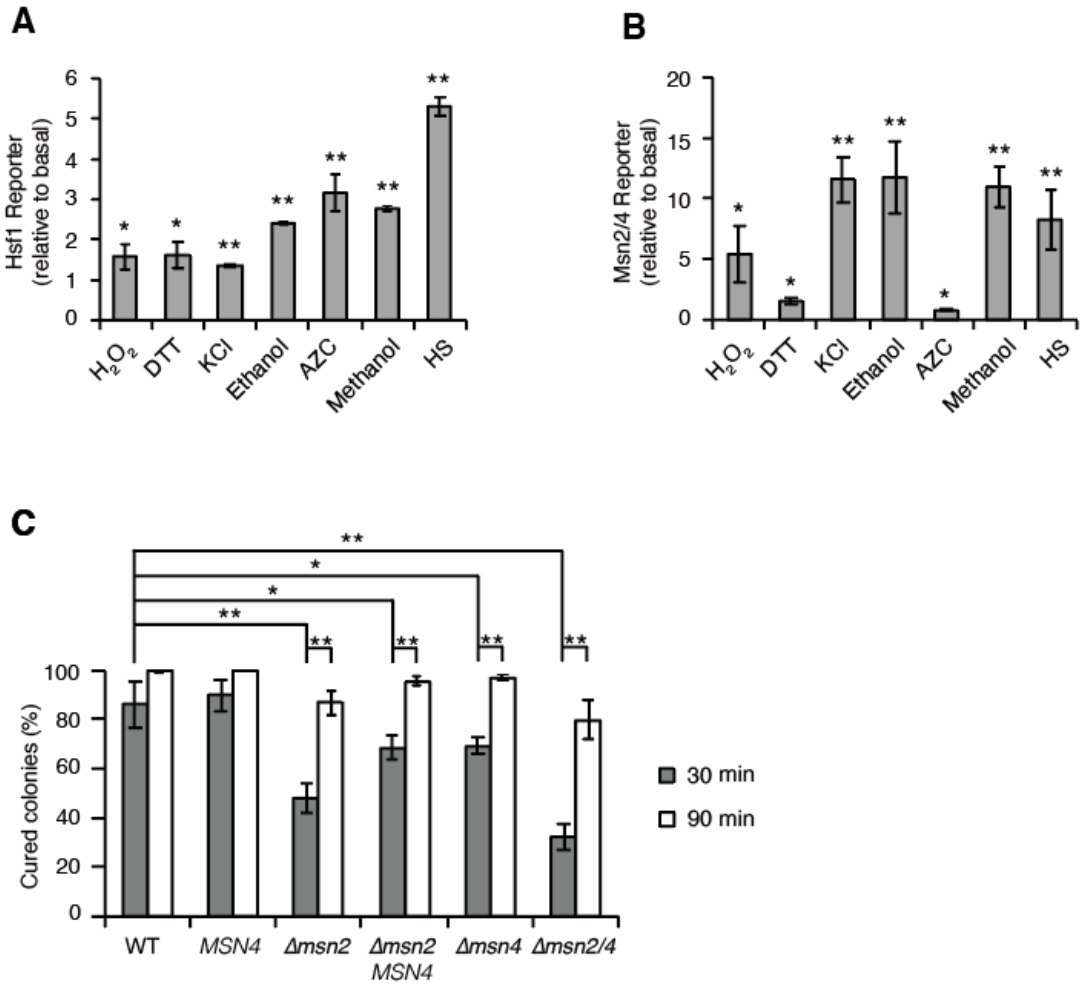

Figure 3. Activation of the Heat Shock Response but not the Environmental Stress Response correlates with the prion curing phenotype.

[*PSI*+] strains containing HSE-YFP reporter (A) or STRE-GFP reporter (B) were incubated with one of the following stressors as indicated for 60 min, 1 mM H_2O_2, 2 mM DTT, 0.5 M KCl, 6% EtOH, 0.5 mM AZC, or 9% MeOH or were incubated at 40°C for 30 min followed by recovery at 30°C for 30 min as HS, and fluorescence intensities were measured by flow cytometry. Data represent averages, and error bars represent standard deviations for biological replicates ($n \geq 3$, *$p<0.05$, **$p<0.005$ by unpaired t-test). (C) [*PSI*+] WT (SLL2600), *MSN4* (SY2961), Δ*msn2* (SY2966), Δ*msn2MSN4* (SY3314), Δ*msn4* (SY2969), and Δ*msn2/4* (SY2971) strains were incubated at 40°C for 30 min or 90 min and plated on rich medium to quantify prion loss by colony color phenotype. Data represent averages, and error bars represent standard deviations for biological replicates (n=3, *$p<0.05$, **$p<0.005$ by unpaired t-test).

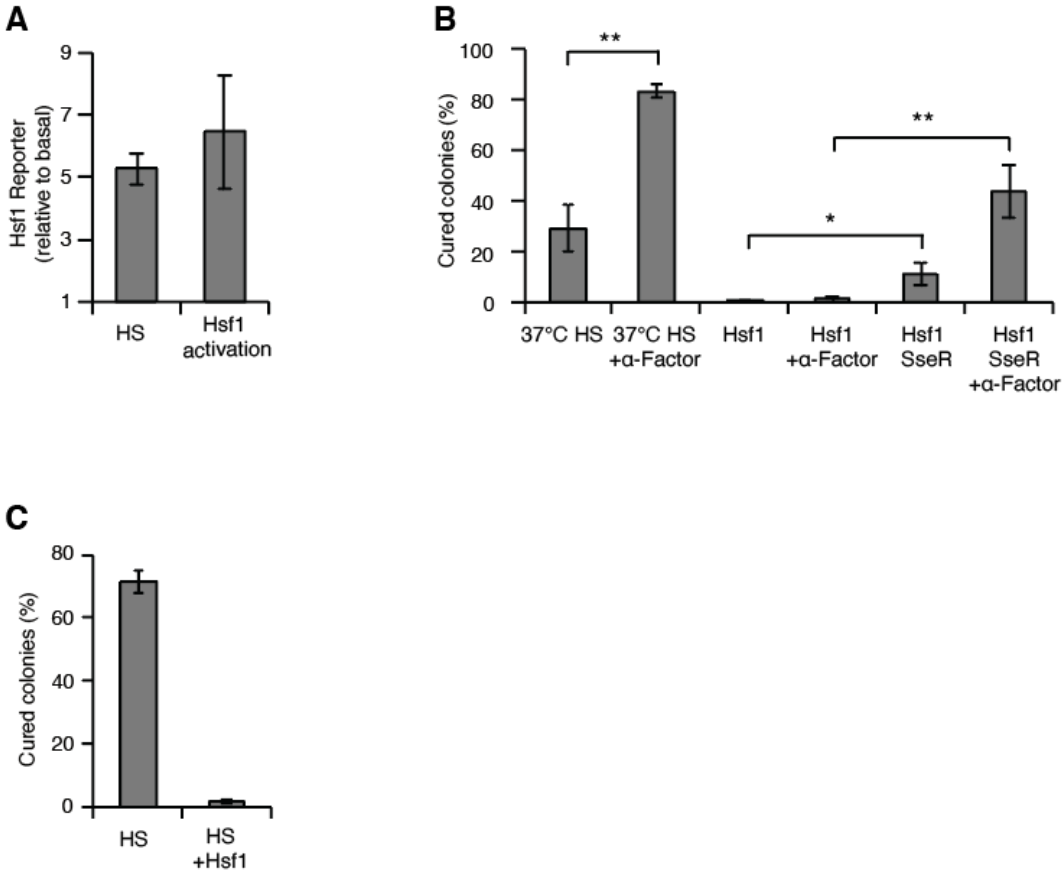

Figure 4. Artificial activation of Hsf1 is unable to induce prion loss and dominantly interferes with HS-mediated prion loss.

(A) [*PSI*+] strains containing HSE-GFP reporter were either incubated at 40°C for 30 min followed by recovery at 30°C for 30min or incubated with 1 μM estradiol for 5 hours to induce Hsf1-PO4*. Fluorescence intensities were measured by flow cytometry. Data represent averages, and error bars represent standard deviations for biological replicates ($n \geq 3$). (B) [*PSI*+] WT (SLL2600) strain was incubated at 37°C for 30 min and plated on rich medium to quantify prion loss by colony color phenotype. [*PSI*+] Hsf1-inducible strains were incubated with 1 μM estradiol for 5 hours to induce Hsf1-PO4* and plated on rich medium to quantify prion loss. If indicated, cells were also arrested for 5 hours by α factor following HS or Hsf1 activation before plated. Data represent averages, and error bars represent standard deviations for biological replicates (n=3, *$p<0.05$, **$p<0.005$ by unpaired t-test). (C) [*PSI*+] strains (SY3636, HS) and (SY3629, HS+Hsf1) were first incubated with 1 μM estradiol for 4.5 hours, then incubated at 40°C for 30 min and plated on rich medium to quantify prion loss by colony color phenotype. Data represent averages, and error bars represent standard deviations for biological replicates (n=3, $p<0.0001$ by unpaired t-test).

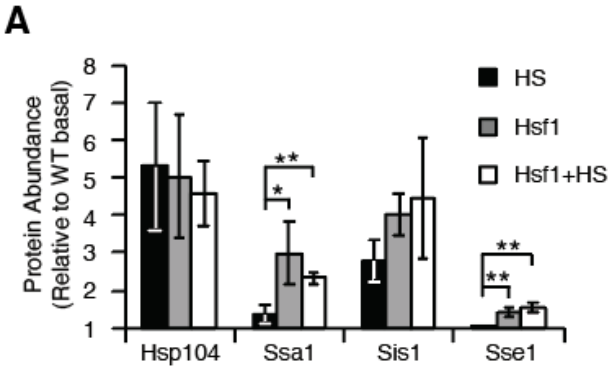
A
Protein Abundance (Relative to WT basal)
HS
Hsf1
Hsf1+HS
Hsp104
Ssa1
Sis1
Sse1

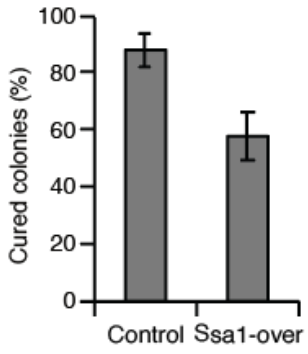
B
Cured colonies (%)
Control
Ssa1-over

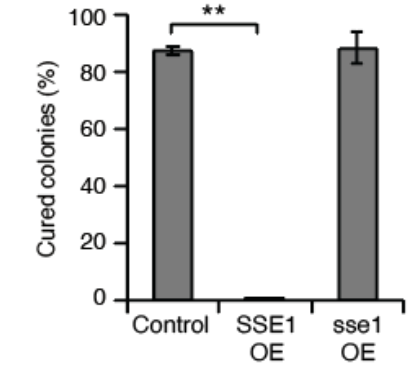
C
Cured colonies (%)
Control
SSE1 OE
sse1 OE

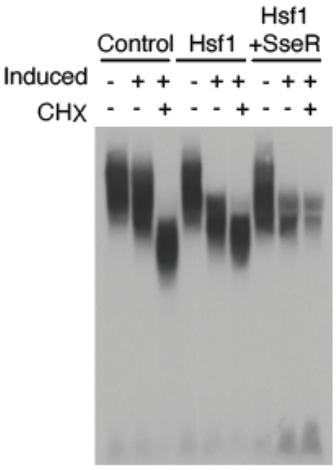
D
Control
Hsf1
Hsf1 +SseR
Induced
CHX

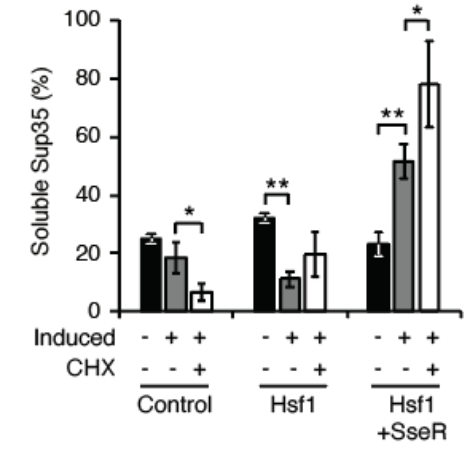
E
Soluble Sup35 (%)
Induced
CHX
Control
Hsf1
Hsf1 +SseR

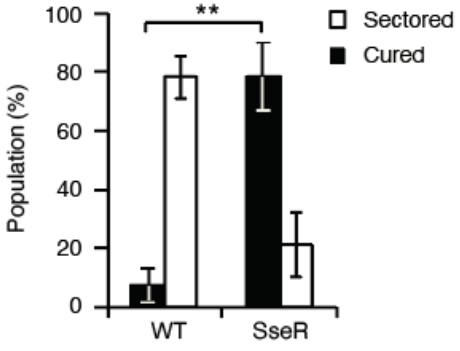
F
Population (%)
Sectored
Cured
WT
SseR

Figure 5. Sse1 levels limit Hsf1-induced and HS-induced prion curing.

(A) [*PSI*+] cultures were incubated at 40°C for 30 min (HS, black), incubated with 1 µM estradiol for 5 hours (Hsf1, grey), or incubated with 1 µM estradiol for 4.5 hours and then at 40°C for 30 min (Hsf1+HS, white), and lysates were prepared and assayed by SDS-PAGE and quantitative immunoblotting for Hsp104, Ssa1, Sse1 and Sis1. Data represent averages, and error bars represent standard deviations for biological replicates (n=3, p*<0.05, p**<0.005 by unpaired t-test). (B) [*PSI*+] strains containing empty vector (control) or Ssa1 expression plasmid (Ssa1-OE) were incubated at 40°C for 60 min and plated on rich medium to quantify prion loss by colony color phenotype. Data represent averages, and error bars represent standard deviations for biological replicates (n=3, p=0.0076 by unpaired t-test). (C) [*PSI*+] strains, WT (SLL2600), SSE1 OE (SY3662), and sse1 OE (SY3663), were incubated at 40°C for 30 min and plated on rich medium to quantify prion loss by colony color phenotype. Data represent averages, and error bars represent standard deviations for biological replicates (n=3, p**<0.0001 by unpaired t-test). (D) Prion aggregate size was assayed by SDD-AGE. Cultures were incubated with 1 µM estradiol for 5 hours when indicated (induced) and then incubated with CHX for 2 hours when indicated (CHX). (E) Sup35 released from amyloid aggregates following Hsf1 activation in the presence of cycloheximide was determined by treating lysates with 2% SDS at 53°C, followed by SDS-PAGE and immunoblotting for Sup35. Cultures were incubated with 1 µM estradiol for 5 hours when indicated (induced) and then incubated with CHX for 2 hours when indicated (CHX). Data represent averages, and error bars represent standard deviations for biological replicates (n=3, p*<0.05, p**<0.005 by unpaired t-test). (F) [*PSI*+] WT (SLL2600) or SseR (3639) strains were incubated at 40°C for 30 min as indicated and plated on rich medium to quantify prion loss by colony color phenotype. Data represent averages, and error bars represent standard deviations for biological replicates (n=3, p**=0.0007 by unpaired t-test).

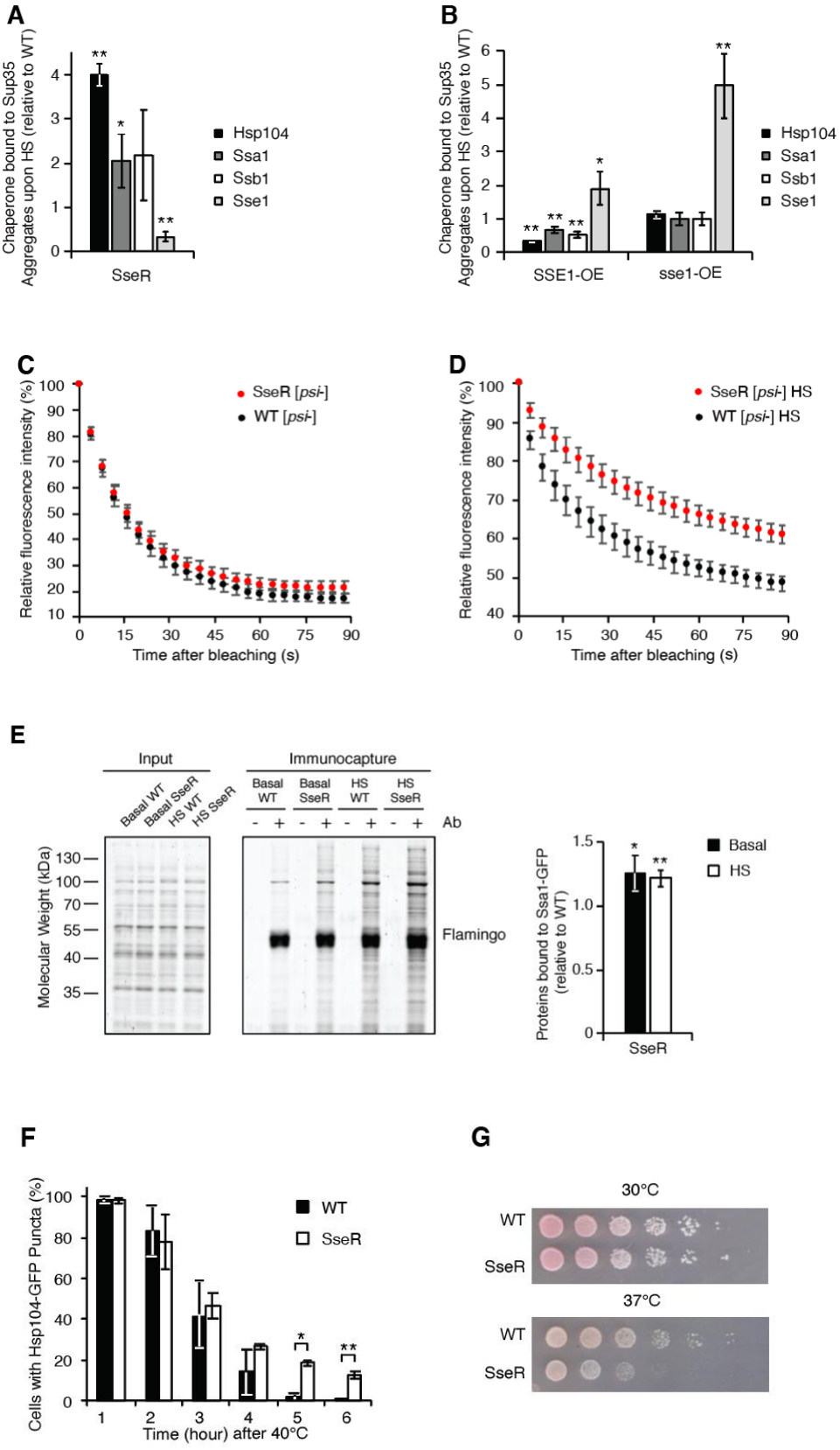
A
Chaperone bound to Sup35
Aggregates upon HS (relative to WT)
Hsp104
Ssa1
Ssb1
Sse1
SseR
B
Chaperone bound to Sup35
Aggregates upon HS (relative to WT)
Hsp104
Ssa1
Ssb1
Sse1
SSE1-OE
sse1-OE
C
Relative fluorescence intensity (%)
SseR [psi-]
WT [psi-]
Time after bleaching (s)
D
Relative fluorescence intensity (%)
SseR [psi-] HS
WT [psi-] HS
Time after bleaching (s)
E
Input
Immunocapture
Basal WT
Basal SseR
HS WT
HS SseR
Ab
Molecular Weight (kDa)
130
100
70
55
40
35
Flamingo
Proteins bound to Ssa1-GFP
(relative to WT)
Basal
HS
SseR
F
Cells with Hsp104-GFP Puncta (%)
WT
SseR
Time (hour) after 40°C
G
30°C
WT
SseR
37°C
WT
SseR

Figure 6. Changes in Sse1 levels alter the interactions between amyloid and non-amyloid substrates and chaperones, leading to distinct outcomes.

(A) [*PSI*$^{+}$] strains containing NM-HA, WT (SY3644) and SseR (SY3645), were incubated at 40°C for 30 min and aggregated Sup35 were immunocaptured and co-captured Hsp104 (black), Ssa1/2 (grey) and Sse1 (white) were assessed following SDS-PAGE and quantitative immunoblotting. The levels of bound chaperones were normalized to the precipitated Sup35 and compared with the levels isolated from the WT strain. Data represent averages, and error bars represent standard deviations for biological replicates (n=3, p*<0.05, p**<0.005 by unpaired t-test). (B) [*PSI*$^{+}$] strains containing NM-HA, WT (SY3644), Sse1-OE (SY3661) and sse1-OE (SY3664) were incubated at 40°C for 30 min, then recovered at 30°C for 60 min and the relative amounts of chaperone bound to Sup35 aggregates were determined as in (A). Data represent averages, and error bars represent standard deviations for biological replicates (n=3, p*<0.05, p**<0.005 by unpaired t-test). (C) FLIP time courses for Ssa1-GFP in WT [*psi*$^{-}$] (SY2657; black dots) and SseR [*psi*$^{-}$] (SY3660; red dots). Data represent averages, and error bars represent SEM for biological replicates (n=20). (D) FLIP time courses for Ssa1-GFP in WT [*PSI*$^{+}$] (SY2658; black dots) and SseR [*PSI*$^{+}$] (SY3659; red dots). Data represent averages, and error bars represent SEM for biological replicates (n=20). (E) [*psi*$^{-}$] strains with Ssa1-GFP WT (SY2657) and SseR (SY3660) were incubated at 30°C or 40°C for 30 min, and immunocapture in the presence (+) or absence (-) of anti-GFP antibodies (Ab) was performed on native lysates. Proteins were analyzed by SDS-PAGE and general protein staining (Flamingo). Quantification of the amount of proteins normalized to precipitated Ssa1 was shown on the right panel. Data represent averages, and error bars represent standard deviations for biological replicates (n=3, p*=0.0335, p**=0.0042 by unpaired t-test). (F) [*psi*$^{-}$] strains with Hsp104-GFP WT (SY3656) and SseR (SY3658) were incubated at 40°C for 90 min and then recovered at 30°C for the indicated time. The cells were analyzed by fluorescence microscopy and the percentage of cells containing Hsp104-GFP puncta were plotted. Data represent averages, and error bars represent standard deviations for biological replicates (n=3, p*=0.0002, p**=0.0006 by unpaired t-test). (G) [*psi*$^{-}$] cultures WT (SY2119) and SseR (SY3655) were spotted on YPD plates after 5-fold serial dilutions and grown at the temperature indicated.

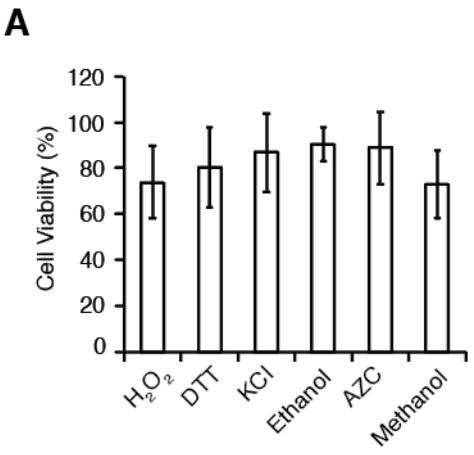

Figure S 1. Cell viability upon stress treatment.

Exponentially growing [*PSI+*] cultures (SLL2600) were incubated with one of the stressors (1 mM H_2O_2, 2 mM DTT, 0.5 M KCl, 6% Ethanol, 0.5 mM AZC, 9% Methanol) as indicated for 60 min and plated on rich medium at 30°C to quantify colony forming units. Data represent averages, and error bars represent standard deviations for biological replicates ($n \geq 3$).

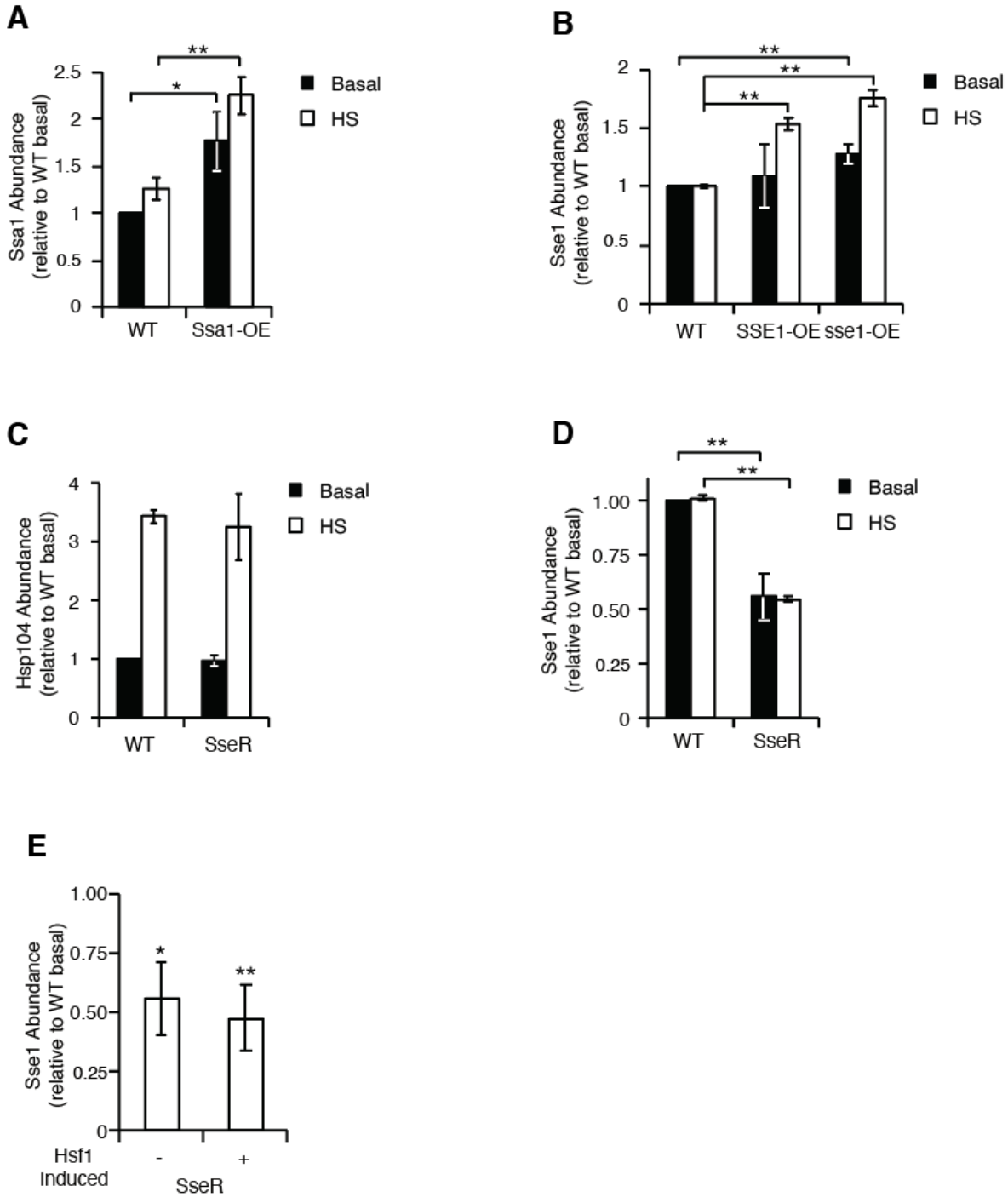

Figure S 2. Chaperone expression levels.

(A) [*PSI*+] cultures were incubated at 40°C for 30 min (HS, white) or not (Basal, black), and lysates were prepared and assayed by SDS-PAGE and quantitative immunoblotting for Ssa1. Data represent averages, and error bars represent standard deviations for biological replicates (n=3, p*<0.05, p**<0.005 by unpaired t-test). (B) [*PSI*+] cultures were

incubated at 40°C for 30 min (HS, white) or not (Basal, black), and lysates were prepared and assayed by SDS-PAGE and quantitative immunoblotting for Sse1. Data represent averages, and error bars represent standard deviations for biological replicates (n=3, p**<0.005 by unpaired t-test). (C) [*PSI*+] cultures were incubated at 40°C for 30 min (HS, white) or not (Basal, black), and lysates were prepared and assayed by SDS-PAGE and quantitative immunoblotting for Hsp104. Data represent averages, and error bars represent standard deviations for biological replicates (n=3). (D) [*PSI*+] cultures were incubated at 40°C for 30 min (HS, white) or not (Basal, black), and lysates were prepared and assayed by SDS-PAGE and quantitative immunoblotting for Sse1. Data represent averages, and error bars represent standard deviations for biological replicates (n=3, p**<0.005 by unpaired t-test). (E) [*PSI*+] cultures were incubated with 1 µM estradiol for 5 hours (Induced+) or not (Induced-), and lysates were prepared and assayed by SDS-PAGE and quantitative immunoblotting for Sse1. Data represent averages, and error bars represent standard deviations for biological replicates (n=3, p*<0.05, p**<0.005 by unpaired t-test).

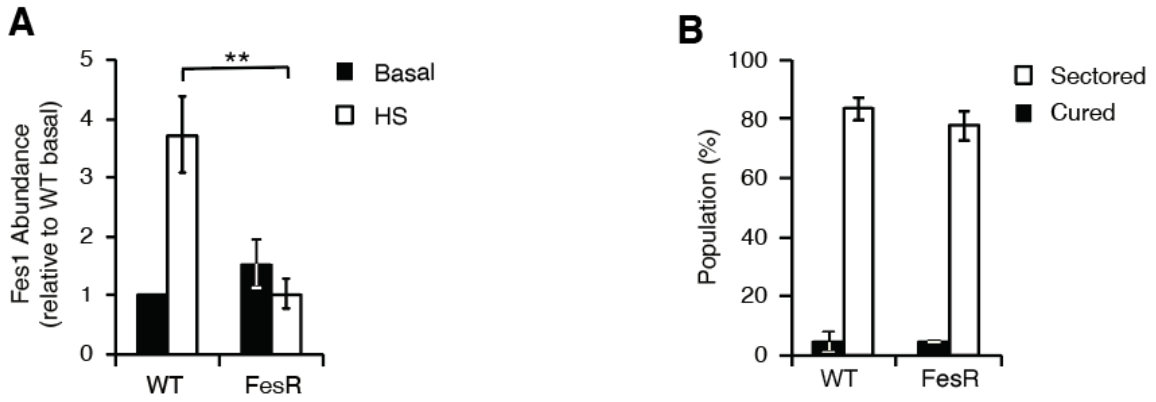

Figure S 3. Fes1 levels do not alter HS-mediated prion curing.

(A) [*PSI*+] cultures were incubated at 40°C for 30 min (HS, white) or not (Basal, black), and lysates were prepared and assayed by SDS-PAGE and quantitative immunoblotting for Fes1. Data represent averages, and error bars represent standard deviations for biological replicates (n=3, p**=0.0024 by unpaired t-test). (B) [*PSI*+] strains were incubated at 40°C for 30 min and plated on rich medium to quantify prion loss by colony color phenotype. Data represent averages, and error bars represent standard deviations for biological replicates (n=3).

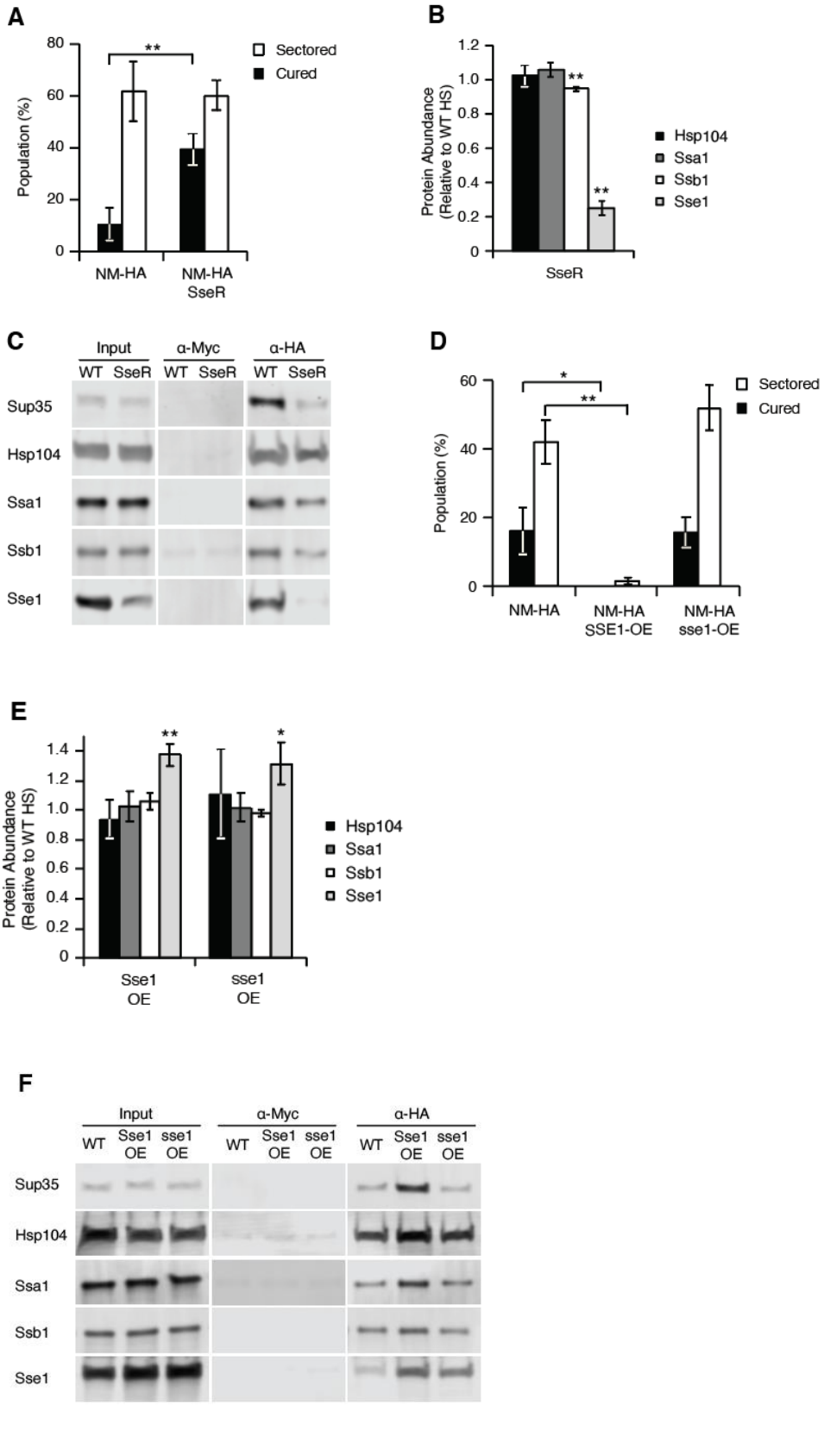
A
Population (%)
80
60
40
20
0
**
Sectored
Cured
NM-HA
NM-HA SseR
B
Protein Abundance (Relative to WT HS)
1.2
1.0
0.8
0.6
0.4
0.2
0
**
**
Hsp104
Ssa1
Ssb1
Sse1
SseR
C
Input
α-Myc
α-HA
WT SseR WT SseR WT SseR
Sup35
Hsp104
Ssa1
Ssb1
Sse1
D
Population (%)
60
40
20
0
*
**
Sectored
Cured
NM-HA
NM-HA SSE1-OE
NM-HA sse1-OE
E
Protein Abundance (Relative to WT HS)
1.4
1.2
1.0
0.8
0.6
0.4
0.2
0
**
*
Hsp104
Ssa1
Ssb1
Sse1
Sse1 OE
sse1 OE
F
Input
α-Myc
α-HA
WT Sse1 OE sse1 OE WT Sse1 OE sse1 OE WT Sse1 OE sse1 OE
Sup35
Hsp104
Ssa1
Ssb1
Sse1

Figure S 4. The colony color phenotypes and chaperone expression of strains expressing NM-HA.

(A) [*PSI*+] strains, WT (SY3644) and SseR (SY3645), containing NM-HA were incubated at 40°C for 30 min and plated on rich medium to quantify prion loss by colony color phenotype. Data represent averages, and error bars represent standard deviations for biological replicates (n=3, p**=0.0048 by unpaired t-test). (B) Immunocapture inputs for WT (SY3644) and SseR (SY3645) were assayed by SDS-PAGE and quantitative immunoblotting for Hsp104, Ssa1, Ssb1, Sse1. Data represent averages, and error bars represent standard deviations for biological replicates (n=3, p**<0.005 by unpaired t-test). (C) Representative gel from experiment quantified in Figure 6A. Aggregates in WT (SY3644) and SseR (SY3645) strains expressing NM-HA and full length Sup35 were immunocaptured using anti-HA magnetic beads and assayed by SDS-PAGE, and the amount of bound chaperone proteins was determined by immunoblotting. Panels shown are non-consecutive lanes run on the same gel. (D) [*PSI*+] strains containing NM-HA, WT (SY3644), SSE1-OE (SY3661) and sse1-OE (SY3664), were incubated at 40°C for 30 min and plated on rich medium to measure prion loss by colony color phenotype. Data represent averages, and error bars represent standard deviations for biological replicates (n=3, p*<0.05, p**<0.005 by unpaired t-test). (E) Immunocapture inputs for WT (SY3644), SSE1-OE (SY3661) and sse1-OE (SY3664) were assayed by SDS-PAGE and quantitative immunoblotting for Hsp104, Ssa1, Ssb1, Sse1. Data represent averages, and error bars represent standard deviations for biological replicates (n=3, p*<0.05, p**<0.005 by unpaired t-test). (F) Representative gel from experiment quantified in Figure 6B. Aggregates in WT (SY3644), SSE1-OE (SY3661), and sse1-OE (SY3664) strains expressing NM-HA and full length Sup35 were immunocaptured using anti-HA magnetic beads and assayed by SDS-PAGE, and the amount of bound chaperone proteins was determined by immunoblotting.

Chapter 4:

Discussion

Cellular Limitations in Disassembling Prion Aggregates

Prion propagation in yeast via the processes of conversion, fragmentation, and transmission is contingent on chaperone activities. In yeast, most of the processes have been well-studied, revealing the broad involvement of chaperones in the prion life cycle. The first step - conversion - is primarily dependent on the physical characteristics of the amyloid aggregates formed by the prion protein (Tanaka et al., 2006). However, a few studies propose that chaperones may directly modulate conversion by stabilizing early folding intermediates leading to the prion conformation as they promote *in vitro* fibrillization (Sadlish et al., 2008; Kumar et al., 2015). The most significant contribution of chaperones to the process appears to be the generation of more ends for conversion by fragmenting existing prion aggregates (Sindi and Serio, 2009). The second step - fragmentation - is essentially the action of chaperones on prion aggregates. Hsp70 along with its cofactor Hsp40 (Sis1) targets the AAA+ ATPase Hsp104 to its substrates - prion aggregates. Then, Hsp104 fragments prion aggregates by threading the prion protein from the aggregates through its central channel, thereby breaking apart the aggregates and resulting in smaller aggregates and more templates (Tessarz et al., 2008; Tipton et al., 2008; Winkler et al., 2012a). Without the activity of Hsp104, prion aggregates become larger, limiting their transmission (Kawai-Noma et al., 2009; Kryndushkin et al., 2003; Satpute-Krishnan et al., 2007; Wegrzyn et al., 2001), and the amplification of heritable prion aggregates is stalled (Cox et al., 2003). The last step - transmission - can also benefit from chaperone activities. Transmission has been shown to be size-dependent; therefore, smaller aggregates as a result of chaperone fragmentation are easier to

transmit (Derdowski et al., 2010). Overall, ironically, despite the role of chaperones in preventing protein aggregation, yeast prions hijack the protein quality control network to self-replicate and propagate. Because the impact of chaperones on these aggregates does not normally lead to their clearance, it has been implied that the PN is limited in its ability to resolve prion amyloids.

Yet, prion metastability and persistence can be challenged by adaptation of the PN (Klaips et al., 2014), providing insight into the dynamic interplay between prion propagation and the PN. Strikingly, the capability of the PN to resolve prion amyloids can be unlocked by a transient heat shock (Klaips et al., 2014). Through the upregulation of the fragmentase Hsp104 and its asymmetrical retention in a subpopulation, the adapted PN releases soluble Sup35 from existing prion aggregates, leading to resolubilization of prion complexes (Klaips et al., 2014). This indicates that PN activated by elevated temperature has the potential to hyperactively fragment prion aggregates, shifting the balance between amyloid assembly and disassembly towards the latter. These previous studies indicate that the level of Hsp104 represents one major limitation of PN to resolve prion aggregates under normal growth conditions. Here, we demonstrate that in addition to heat shock, a variety of stress conditions can activate the PN and tip the balance between amyloid assembly and disassembly towards dissolution of prion aggregates (Chapter 3). The mechanism of prion curing caused by these stress conditions appears to parallel that of heat shock-induced prion curing, relying on elevated expression of Hsp104 and its asymmetrical retention. Therefore, the limitations of the PN to resolve prion amyloids can be bypassed by the adaptability of the PN.

However, despite extensive research on the interplay between the PN and prion maintenance, our understanding of the cellular limitations on the resolution of prion amyloids is still in its infancy. Here, I attempt to summarize the current knowledge of the major limitations imposed by the inherent properties of amyloid aggregates and the PN and shed light on potential strategies that could be used to combat protein conformational diseases.

The physical properties of amyloid aggregates

Physical characteristics of prion amyloid aggregates represent the primary contributor to their resistance to the protein quality control system. Amyloid fibrils formed by a wide range of proteins have extraordinary rigidities (Knowles et al., 2007), largely due to the formation of filaments rich in hydrogen-bonded β sheets, a characteristic of amyloid structure. Besides, amyloid fibrils have a remarkable ability to proliferate, converting like proteins of native conformation to the amyloid conformation, which can be further enhanced by fibril fragmentation and secondary nucleation (Chiti and Dobson, 2006). These two features together make amyloid aggregates frequently overwhelm the quality control system.

Despite the similarities, variations in the characteristics of prion amyloids can modulate the interplay between prion propagation and the PN, thus establishing distinct prion phenotypes (Figure 1A). Such variations even exist among prions formed by the same

protein, exhibiting varying kinetic stability and conversion efficiency. For example, Sup35 can form different [*PSI*+] prion fibers *in vitro* at different temperatures, Sc4 (formed at 4ºC) and Sc37 (formed at 37ºC), and these variants give rise to distinct prion phenotypes once introduced into yeast (Tanaka et al., 2004). Sc4, the variant with a stronger prion phenotype, is less efficient in polymerization *in vitro* but can be fragmented more efficiently compared to Sc37, the weak variant, due to an increased brittleness of amyloid aggregates (Tanaka et al., 2006).

Such phenotypic variations are essentially the manifestation of the structural differences of yeast prion variants. One crucial feature of the amyloid conformations is the size of amyloid cores. Researchers found that although Sc4 and Sc37 fibers have an overlapping amyloid core composed of tightly packed β-sheets, Sc37, the weak variant, has an expanded amyloid core, which accounts for the increased kinetic stability and decreased fragmentation rate (Toyama et al., 2007). A conformational change modulating the kinetic stability is predicted to alter the efficiency with which the amyloid aggregates are fragmented. Indeed, the introduction of the G58D mutant of Sup35 to the [*PSI*+] prion results in a reduction in kinetic stability of the amyloid aggregates and promotes Hsp104-mediated disassembly of aggregates (DiSalvo et al., 2011). This conformational characteristic also modulates the sensitivity of yeast prion strains to prion curing conditions. For example, the weak variant of [*PSI*+] is more sensitive to HS-induced prion curing than the strong variant of [*PSI*+], partially due to higher kinetic stability of aggregates and decreased ability to amplify the prion aggregates through fragmentation (Klaips et al., 2014).

Work from our lab revealed, through both mathematical modeling and *in vivo* biochemical assays, another crucial yet previously unappreciated feature of the prion amyloids - the size of the stable amyloid nucleus (Villali *et al.* submitted). Amyloid aggregates with a size below this threshold are cleared via disassembly, and thus, this parameter determines the sensitivity of a strain to clearance through enhanced fragmentation. Specifically, amyloid aggregates with a larger nucleus are cleared more readily because there is a higher probability that the aggregate will be fragmented and spontaneously disassemble before doubling in size, the minimum threshold for surviving a single fragmentation event. Consistent with this idea, the weak variant of [*PSI*$^{+}$] has a larger amyloid nucleus than the strong variant, contributing to the sensitivities of the former to both HS-mediated prion curing and heterozygous deletion of Hsp104 (Villali *et al.* submitted). In addition, incorporation of the G58D mutant of Sup35 into the strong variant of [*PSI*$^{+}$] increases the amyloid nucleus size and leads to its sensitivity to HS-mediated prion curing (Villali *et al.* submitted). Moreover, the R2E1 sequence variant of Sup35 leads to a smaller amyloid nucleus size, thus promoting a high frequency of spontaneous [*PSI*$^{+}$] appearance by reducing the probability of clearance by a single fragmentation event (Villali *et al.* submitted). Thus, mutations can alter the outcome of a fragmentation event and thereby the persistence of the prion state.

Variations in prion characteristics can also be derived from mutations of the prion protein, which modulate the efficiency of the fragmentation reaction. Studies show that Sup35 mutants eliminating the oligopeptide repeat region exhibit poor fragmentation presumably

due to weaker chaperone binding and processing by Hsp104, thereby affecting the prion phenotype and its stability (Liu et al., 2002; Langlois et al., 2016). Similarly, the G58D mutant of Sup35 lowers the kinetic stability of the aggregates, leading to resolubilizing of prion aggregates through fragmentation (DiSalvo et al., 2011). Likewise, a mammalian PrP study reveals that the conformational stabilities of prion isolates determined by sensitivity to GdnHCI-based denaturation correlate with incubation times in mice, implying that less stable prions propagate faster (Legname et al., 2006).

In addition to alterations to fragmentation efficiency, factors impacting the conversion step present another avenue for combating prion propagation *in vivo*. The Q24R mutant of Sup35 decelerates the prion assembly rate, therefore inhibiting prion propagation. Likewise, studies on mammalian prions also show that mutants that repress the *in vitro* conversion of native protein to prion forms exhibit scrapie resistance (Bossers et al., 1997). The lack of the prion protein expression in animals renders them resistant to scrapie, indicating prion protein supply, essential to conversion, is required for disease progression (Prusiner et al., 1993; Sailer et al., 1994). Furthermore, mammalian PrP studies using antibodies to inhibit the conversion of soluble PrP to scrapie PrP demonstrate reduced infectivity and scrapie prion protein accumulation in cultured cells (Enari et al., 2001; Gabizon et al., 1988; Horiuchi, 1999). Studies also show that a synthetic β-sheet breaker peptide can reverse PrP conformational change and reduce infectivity in mice with experimental scrapie (Soto et al., 2000). Therefore, slowing the conversion step holds the potential for therapeutic interventions for prion diseases.

Lack of sensing of amyloid aggregates

Lack of sensing amyloid aggregates may represent a major cellular limitation for combating prion aggregates (Figure 1B). The presence of misfolded protein aggregates triggers a stress response, indicating that these species are recognized by the cell as aberrant (Trotter et al., 2002). However, multiple studies suggest that this is not that case for yeast prions. The presence of [*URE3*] does not cause a change in the global transcriptional program, and the present of [*PSI*+] does not affect the expression of Hsp104 (Eaglestone et al., 1999; Ross and Wickner, 2004). Titrating Hsp70 away from Hsf1 has been shown to be the major mechanism of Hsf1 activation in yeast (Zheng et al., 2016), and it is plausible that the prion aggregates are less capable of titrating away Hsp70 than stress-denatured aggregates. As a result, chaperone levels are not induced, which allows the fragmentation activity to support prion propagation but not to disassemble amyloid. The studies here suggests that activation of the protein quality control network, especially the part controlled by Hsf1, is sufficient to shift the balance toward disassembly of prion aggregates (Chapter 3). Therefore, the absence of a stress response upon appearance of [*PSI*+] is likely protective for the prion state, including during the *de novo* formation of prions (Villali *et al.* submitted).

Therefore, approaches that activate the stress response pathway can be effective at combating the toxicity of amyloid aggregates. Indeed, studies show that activation of the stress response via Hsf1 inhibits huntingtin aggregation in cellular models, suppresses polyglutamine aggregate formation in cellular and mouse models, protects neurons from

Aβ-induced toxicity and protects against polyglutamine-induced toxicity in fly models (Sittler, 2001; Fujimoto et al., 2005; Ansar et al., 2007; Neef et al., 2010). Proteostasis regulators that increase the proteostasis network capacity have also shown potential to ameliorate age-related degenerative diseases (Balch et al., 2008; Powers et al., 2009).

Chaperone configuration

Imbalance of chaperones may impose limitations on chaperone activity. Chaperones have evolved to facilitate protein folding and prevent protein aggregation, and a major part of the stress response is to upregulate these factors (Gasch et al., 2000; Verghese et al., 2012). It has been thought that the overexpression of a chaperone will enhance its activity and have beneficial effects. However, the balance among chaperones can also influence the outcome of these perturbations. Constitutive expression of Hsp70 in *Drosophila* cells reduces the rate of cell growth, implying a detrimental effect (Feder et al., 1992). Overexpressing Sse1, a nucleotide exchange factor of Hsp70, causes a growth defect in yeast cells (Shaner et al., 2004). Hsp70 (Ssa1) overexpression causes some toxicity to yeast cells in the presence of [*PSI*+] presumably due to the competition for Hsp70 cofactors (Keefer and True, 2017). These results suggest that imbalance of chaperone factors could negatively impact the chaperone activity and cause cytotoxicity.

Hsp104 overexpression may also represent a case where imbalance of chaperones interferes with chaperone activity. There are studies suggesting that Hsp104 overexpression leads to inhibition of its activity as exemplified by an increase in prion

aggregate size and a decrease in prion aggregate mobility (Kryndushkin et al., 2003; Winkler et al., 2012a). The distinction between HS-mediated prion curing and Hsp104-mediated prion curing may be the interplay of Hsp104 and its cofactors, which is unbalanced in the latter. Here, we show that when Hsp104 is overexpressed within a network controlled by Hsf1, fragmentation is enhanced as shown by smaller aggregates, the opposite observation to Hsp104 overexpression (Chapter 3). Therefore, the co-overexpression of Hsp104 factors that are controlled by Hsf1 is responsible for preserving Hsp104 activity.

The specific configuration of chaperone components can limit disassembly of prion aggregates. For example, we demonstrate here that the protein quality control system can be robust in clearing amyloid fibrils as shown by the resolubilization of prion aggregates (Chapter 3). However, the level of a nucleotide exchange factor Sse1, critical for the outcome of disassembling prion fibrils, is primarily optimized for the dissolution of amorphous aggregates, thus limiting the efficiency of amyloid clearance (Figure 1C). Most studies tend to favor a universal model of Hsp104-mediated disaggregation for the two types of aggregates: amorphous aggregates and amyloid aggregates (Haslberger et al., 2010). Both involve the threading of polypeptides through its central channel and the collaboration of Hsp70. However, there are studies suggesting otherwise. Compared to disaggregation of amorphous aggregates, fragmentation of amyloid fibrils requires a more cooperative mode of inter-subunit collaboration within Hsp104, implying an operational plasticity for amyloid and non-amyloid clients (DeSantis et al., 2012). Here, we show that one critical difference between the disaggregation of the two types of aggregates is the

level of nucleotide exchange factor. Reduction of this factor prolongs the interaction between chaperones and substrate, which is required for processing of physically rigid amyloid aggregates.

Implications for Disaggregation Systems in Metazoa

In our work, reducing nucleotide exchange factors promotes chaperone-prion aggregate interaction and results in an increase in disassembly of prion aggregates. There have been several studies showing the Hsp70-based chaperone complex consisting of Hsp70/Hsc70, J proteins and Hsp110 as NEFs in metazoa has the ability to disaggregate amyloid fibers both *in vitro* and *in vivo* (Gao et al., 2015; Kirstein et al., 2017; Scior et al., 2018). Consistent with our finding, the level of nucleotide exchange factor is important for the outcome of disassembling amyloid fibers *in vitro* as increasing the amount of nucleotide exchange factors reduces the outcome of disaggregation of amyloid fibers (Gao et al., 2015). Some studies suggest that the Hsp70-based system disaggregates amyloid fibrils *in vivo* and resolves aggregate-induced toxicity (Kirstein et al., 2017; Scior et al., 2018). It is worthwhile to test whether the level of nucleotide exchange factor is crucial for the phenotype, especially when the factor is reduced instead of completely depleted, whether increased disaggregation activity could be observed.

It has been proposed that managing amyloid aggregates through enhancing the chaperone activity might be challenging. When the fragmentation activity is not strong enough to shift the balance between amyloid assembly and disassembly toward the latter,

an increase in fragmentation may favor amyloid assembly and aggravate amyloid toxicity by creating new templates. Increasing evidence suggests that the oligomers are the more toxic form of aggregates than amyloids (Chiti and Dobson, 2017), and an increase in fragmentation activity may increase the amount of toxic oligomers and aggravate the toxicity. Indeed, when Hsf1 is activated with Sse1 overexpressed, fragmentation is enhanced; however, it is not strong enough to solubilize prion aggregates, and the amount of soluble Sup35 is decreased, indicating that more Sup35 is in the prion conformation (Chapter 3). Thus, enhancing the PN may strengthen the prion phenotype. Therefore, it is important to modulate the dose of treatment to make sure the fragmentation is sufficient to tip the balance between amyloid assembly and disassembly towards the latter.

Future Directions

Unraveling the mechanism of Hsp104-mediated prion curing

The elusive mechanism of Hsp104-mediated prion curing has puzzled researchers in the field for decades. Despite several models that have been proposed, including fragmentation inhibition (Winkler et al., 2012a), malpartitioning of heritable prion aggregates in a subpopulation of cells (Ness et al., 2017), and dissolution of prion aggregates through a secondary trimming activity of Hsp104 (i.e. removing monomer from fibril ends) (Park et al., 2014), there is not a conclusive understanding that accounts for the various features of this phenomenon, nor can any model offer satisfactory

explanations regarding the increasing list of genetic modulators implicated in the phenomenon. The observation that heat shock leads to prion curing in a Hsp104-dependent manner appears to help unravel the complexity of Hsp104 overexpression but also raises new questions. It indicates that Hsp104 overexpression is not necessarily connected to fragmentation inhibition; instead, coupled with upregulation of other heat shock proteins or other events triggered by heat shock, Hsp104 activity cannot only be preserved but also enhanced. The initial hypothesis that we tested was that overexpression of the well-studied Hsp104 cofactors Hsp70 (Ssa1) and Hsp40 (Sis1) with Hsp104 overexpression could rescue or even enhance Hsp104 activity. However, this idea was disproved (Chapter 2), indicating that additional factors are required. Then, we showed that Hsf1 activation which activates Hsp104 to the extent compared to that of Hsp104 overexpression individually leads to smaller aggregates and resolubilization of prion aggregates (Chapter 3). This observation implies that the overexpression of other heat shock proteins controlled by Hsf1 allows Hsp104 to excessively fragment prion aggregates at a rate that exceeds that of amyloid assembly. However, a screening of Hsf1-controlled heat shock proteins has not identified putative factors, implying the possibility of alternative models for Hsp104-mediated prion curing.

Therefore, it is imperative to revisit the system of Hsp104 overexpression and thoroughly characterize it. Notably, there are undesired effects associated with the galactose-inducible system due to the carbon source switch (Roth et al., 2004). Most of the previous studies on Hsp104-mediated prion curing have been conducted using this system, which complicates the interpretation of the observations. To better understand the basis of

Hsp104-mediated prion curing, it is imperative to revisit the question of what the mechanism of Hsp104-mediated prion curing is using alterative induction systems, such as the tetracycline-inducible system. The tetracycline-inducible system achieves gene expression without changes in growth medium composition, therefore avoiding undesired pleiotropic effects on cell metabolism (Bellí et al., 1998). Semi-denaturing agarose gel electrophoresis (SDD-AGE) can be used to determine the size of prion aggregates upon Hsp104 overexpression and plating assay can be utilized to determine the curing dynamics. Co-IP can be employed to evaluate the amount of chaperones bound to prion aggregates. A premise for the chaperone inhibition model for Hsp104 overexpression that has not been biochemically tested is that excess Hsp104 out-competes Hsp70 (Ssa1) for binding to prion aggregates, leading to Hsp70 free non-productive binding. The expected outcome upon Hsp104 overexpression will be a dramatic reduction in the amount of Ssa1 bound to prion aggregates. A thorough characterization of Hsp104 overexpression will rule out the contributions of the galactose-inducible system *per se* to the observed effects and clarify the discrepancies from previous reports.

Determining the role of Hsp70s in heat shock-mediated prion curing

This study clearly demonstrates the level of Sse1 is key to the outcome of heat shock-induced prion curing (Chapter 3). Reducing it promotes curing while overexpressing it represses curing. These outcomes are dependent on the nucleotide exchange function of Sse1, as a Sse1 mutant devoid of this function fails to represses the curing upon overexpression. The effect of altering Sse1 on the interaction between Hsp70 (Ssa1) and

prion aggregates is pronounced, consistent with the role of Sse1 in regulating Hsp70-substrate interaction. Based on these observations, we propose that Sse1 modulates the outcome of heat shock-induced prion curing via regulating the interaction between Ssa1/Hs104 and prion aggregates. However, Sse1 has also been shown to be the NEF of another group of Hsp70 Ssb1/2 (Dragovic et al., 2006; Raviol et al., 2006), and compared with Ssa1/2, Ssb1/2 appears to have the opposite effect on prion propagation, that is, destabilizing prions (Allen et al., 2005). Therefore, altering Sse1 may affect the interaction between Ssb1/2 and prion aggregates as well, thus contributing to the phenotype. Indeed, when Sse1 is overexpressed, less Ssb1/2 binds to prion aggregates; however, when Sse1 is reduced, the amount of Ssb1/2 bound to prion aggregates does not change. It is unclear why a reduction in Sse1 level does not affect the interaction between Ssb1/2 and prion aggregates. One possibility is that more Ssa1/2 is bound to prion aggregates when Sse1 is reduced, and Ssa1/2 out-completes Ssb1/2 for binding to prion aggregates. Another possibility is that Ssb1/2 preferentially binds to newly synthesized Sup35 and upon heat shock, Sup35 synthesis is repressed, limiting Ssb1/2 binding. While Ssb1/2 is less likely to contribute to the phenotypic change upon Sse1 reduction given the binding observations, it is plausible that the reduction in Ssb1/2 bound to prion aggregates contributes to the inhibition of prion curing upon Sse1 overexpression. A recent study shows that depletion of Ssb1/2 decreases the [*PSI*$^{+}$] destabilization caused by heat shock (Howie et al., 2019). Notably, depletion of Ssb1/2 has pleiotropic effects, such as slowing cell growth (Holmes et al., 2014), which may complicate the result. Overall, it is worthwhile to test whether Ssb1/2 is involved in regulating the interaction between Hsp104 and prion aggregates and mediating the prion curing.

The proposal model that altering Sse1 mediates prion curing through regulating the interaction between Ssa1/Hsp104 and Sup35 aggregates is based on the current knowledge of the collaboration of Hsp104 and Hsp70. Hsp70 (Ssa1/2) is thought to target Hsp104 to its substrates, upstream of the fragmentation by Hsp104 (Winkler et al., 2012a). However, due to the overlapping regulation of Sse1 on Ssa1/2 and Ssb1/2, caution must be taken to rule out the possibility that Sse1 mediates prion curing through regulating the interaction between Ssb1/2 and Sup35 aggregates. Ideally, specifically perturbing the amount of Ssa/Ssb that binds to prion aggregates would allow us to determine the role of Ssa/Ssb in regulating the interaction between Hsp104 and prion aggregates. Traditional studies tend to utilize gene deletion to determine the role of Ssa/Ssb in prion maintenance; however, the pleiotropic effects of deletion of these chaperones have been reported (Holmes et al., 2014) and also observed here (Chapter 2). To rule out the contributions of these undesired events, manipulating the chaperone levels through promoter replaced might be superior to those approaches.

Our work here underscores the importance of Hsp70 chaperone cycle in heat shock-mediated prion curing, revealing the limitation of the chaperone system configuration in resolubilizing prion aggregates. Compared with normal levels of a nucleotide exchange factor Sse1, which is optimal for dissolution of stress-denatured aggregates, reduction in Sse1 levels promotes heat shock-mediated prion curing presumably through modulating chaperone-substrate interactions. Furthermore, limiting Sse1 enables Hsf1 activation to

shift the balance between amyloid assembly and disassembly toward resolubilization of prion aggregates.

References

Allen, K.D., Wegrzyn, R.D., Chernova, T. a, Müller, S., Newnam, G.P., Winslett, P. a, Wittich, K.B., Wilkinson, K.D., and Chernoff, Y.O. (2005). Hsp70 chaperones as modulators of prion life cycle: novel effects of Ssa and Ssb on the Saccharomyces cerevisiae prion [PSI+]. Genetics 169, 1227–1242.

Balch, W.E., Morimoto, R.I., Dillin, A., and Kelly, J.W. (2008). Adapting proteostasis for disease intervention. Science 319, 916–919.

Bellí, G., Garí, E., Piedrafita, L., Aldea, M., and Herrero, E. (1998). An activator/repressor dual system allows tight tetracycline-regulated gene expression in budding yeast. Nucleic Acids Res. 26, 942–947.

Bossers, A., Belt, P.B.G.M., Raymond, G.J., Caughey, B., de Vries, R., and Smits, M.A. (1997). Scrapie susceptibility-linked polymorphisms modulate the in vitro conversion of sheep prion protein to protease-resistant forms. Proc. Natl. Acad. Sci. 94, 4931–4936.

Chiti, F., and Dobson, C.M. (2006). Protein Misfolding, Functional Amyloid, and Human Disease. Annu. Rev. Biochem. 75, 333–366.

Chiti, F., and Dobson, C.M. (2017). Protein Misfolding, Amyloid Formation, and Human Disease: A Summary of Progress Over the Last Decade. Annu. Rev. Biochem. 86, 27–68.

Cox, B., Ness, F., and Tuite, M. (2003). Analysis of the generation and segregation of propagons: Entities that propagate the [PSI+] prion in yeast. Genetics 165, 23–33.

Derdowski, A., Sindi, S.S., Klaips, C.L., DiSalvo, S., and Serio, T.R. (2010). A size threshold limits prion transmission and establishes phenotypic diversity. Science 330, 680–683.

DeSantis, M.E., Leung, E.H., Sweeny, E.A., Jackrel, M.E., Cushman-Nick, M., Neuhaus-Follini, A., Vashist, S., Sochor, M.A., Knight, M.N., and Shorter, J. (2012). Operational plasticity enables hsp104 to disaggregate diverse amyloid and nonamyloid clients. Cell 151, 778–793.

DiSalvo, S., Derdowski, A., Pezza, J.A., and Serio, T.R. (2011). Dominant prion mutants induce curing through pathways that promote chaperone-mediated disaggregation. Nat. Struct. Mol. Biol. 18, 486–492.

Dragovic, Z., Broadley, S. a, Shomura, Y., Bracher, A., and Hartl, F.U. (2006). Molecular chaperones of the Hsp110 family act as nucleotide exchange factors of Hsp70s. EMBO J. 25, 2519–2528.

Eaglestone, S.S., Cox, B.S., and Tuite, M.F. (1999). Translation termination efficiency can be regulated in Saccharomyces cerevisiae by environmental stress through a prion-mediated mechanism. Eur. Mol. Biol. Organ. J. 18, 1974–1981.

Enari, M., Flechsig, E., and Weissmann, C. (2001). Scrapie prion protein accumulation by scrapie-infected neuroblastoma cells abrogated by exposure to a prion protein antibody. Proc. Natl. Acad. Sci. 98, 9295–9299.

Feder, J.H., Rossi, J.M., Solomon, J., Solomon, N., and Lindquist, S. (1992). The consequences of expressing hsp70 in Drosophila cells at normal temperatures. Genes Dev. 6, 1402–1413.

Gabizon, R., McKinley, M.P., Groth, D., and Prusiner, S.B. (1988). Immunoaffinity purification and neutralization of scrapie prion infectivity. Proc. Natl. Acad. Sci. 85, 6617–6621.

Gao, X., Carroni, M., Helen, R., Mayer, M.P., and Bukau, B. (2015). Human Hsp70 Disaggregase Reverses Parkinson ' s-Linked a -Synuclein Amyloid Fibrils. Mol. Cell 59, 781–793.

Gasch, a P., Spellman, P.T., Kao, C.M., Carmel-Harel, O., Eisen, M.B., Storz, G., Botstein, D., and Brown, P.O. (2000). Genomic expression programs in the response of yeast cells to environmental changes. Mol. Biol. Cell 11, 4241–4257.

Haslberger, T., Bukau, B., and Mogk, A. (2010). Towards a unifying mechanism for ClpB/Hsp104-mediated protein disaggregation and prion propagation. Biochem. Cell Biol. 88, 63–75.

Holmes, W.M., Mannakee, B.K., Gutenkunst, R.N., and Serio, T.R. (2014). Loss of amino-terminal acetylation suppresses a prion phenotype by modulating global protein folding. Nat. Commun. 5, 4383.

Horiuchi, M. (1999). Specific binding of normal prion protein to the scrapie form via a localized domain initiates its conversion to the protease-resistant state. EMBO J. 18, 3193–3203.

Howie, R.L., Jay-Garcia, L.M., Kiktev, D.A., Faber, Q.L., Murphy, M., Rees, K.A., Sachwani, N., and Chernoff, Y.O. (2019). Role of the Cell Asymmetry Apparatus and Ribosome-Associated Chaperones in the Destabilization of a Saccharomyces cerevisiae Prion by Heat Shock. Genetics 212, 757–771.

Kawai-Noma, S., Pack, C.-G., Tsuji, T., Kinjo, M., and Taguchi, H. (2009). Single mother-daughter pair analysis to clarify the diffusion properties of yeast prion Sup35 in guanidine-HCl-treated [PSI +] cells. Genes to Cells 14, 1045–1054.

Keefer, K.M., and True, H.L. (2017). A toxic imbalance of Hsp70s in Saccharomyces cerevisiae is caused by competition for cofactors. Mol. Microbiol. 105, 860–868.

Kirstein, J., Arnsburg, K., Scior, A., Szlachcic, A., Guilbride, D.L., Morimoto, R.I., Bukau, B., and Nillegoda, N.B. (2017). In vivo properties of the disaggregase function of J-proteins and Hsc70 in Caenorhabditis elegans stress and aging. Aging Cell 16, 1414–1424.

Klaips, C.L., Hochstrasser, M.L., Langlois, C.R., and Serio, T.R. (2014). Spatial quality control bypasses cell-based limitations on proteostasis to promote prion curing. Elife 3, e04288.

Knowles, T.P., Fitzpatrick, A.W., Meehan, S., Mott, H.R., Vendruscolo, M., Dobson, C.M., and Welland, M.E. (2007). Role of Intermolecular Forces in Defining Material Properties of Protein Nanofibrils. Science (80-.). 318, 1900–1903.

Kryndushkin, D.S., Alexandrov, I.M., Ter-Avanesyan, M.D., and Kushnirov, V. V (2003). Yeast [PSI+] prion aggregates are formed by small Sup35 polymers fragmented by Hsp104. J. Biol. Chem. 278, 49636–49643.

Kumar, N., Gaur, D., Gupta, A., Puri, A., and Sharma, D. (2015). Hsp90-Associated Immunophilin Homolog Cpr7 Is Required for the Mitotic Stability of [URE3] Prion in Saccharomyces cerevisiae. PLOS Genet. 11, e1005567.

Langlois, C.R., Pei, F., Sindi, S.S., and Serio, T.R. (2016). Distinct Prion Domain Sequences Ensure Efficient Amyloid Propagation by Promoting Chaperone Binding or Processing In Vivo. PLoS Genet. 12, 1–30.

Legname, G., Nguyen, H.-O.B., Peretz, D., Cohen, F.E., DeArmond, S.J., and Prusiner, S.B. (2006). Continuum of prion protein structures enciphers a multitude of prion isolate-specified phenotypes. Proc. Natl. Acad. Sci. 103, 19105–19110.

Liu, J.-J., Sondheimer, N., and Lindquist, S.L. (2002). Changes in the middle region of Sup35 profoundly alter the nature of epigenetic inheritance for the yeast prion [PSI+]. Proc. Natl. Acad. Sci. 99, 16446–16453.

Ness, F., Cox, B.S., Wongwigkarn, J., Naeimi, W.R., and Tuite, M.F. (2017). Over-expression of the molecular chaperone Hsp104 in Saccharomyces cerevisiae results in the malpartition of [PSI +] propagons. Mol. Microbiol. 00.

Park, Y.-N., Zhao, X., Yim, Y.-I., Todor, H., Ellerbrock, R., Reidy, M., Eisenberg, E., Masison, D.C., and Greene, L.E. (2014). Hsp104 overexpression cures yeast [PSI+] by causing dissolution of the prion seeds. Eukaryot. Cell.

Powers, E.T., Morimoto, R.I., Dillin, A., Kelly, J.W., and Balch, W.E. (2009). Biological and chemical approaches to diseases of proteostasis deficiency. Annu. Rev. Biochem. 78, 959–991.

Prusiner, S.B., Groth, D., Serban, A., Koehler, R., Foster, D., Torchia, M., Burton, D., Yang, S.L., and DeArmond, S.J. (1993). Ablation of the prion protein (PrP) gene in mice prevents scrapie and facilitates production of anti-PrP antibodies. Proc. Natl. Acad. Sci. U. S. A. 90, 10608–10612.

Raviol, H., Sadlish, H., Rodriguez, F., Mayer, M.P., and Bukau, B. (2006). Chaperone network in the yeast cytosol: Hsp110 is revealed as an Hsp70 nucleotide exchange factor. EMBO J. 25, 2510–2518.

Ross, E.D., and Wickner, R.B. (2004). Prions of yeast fail to elicit a transcriptional response. Yeast 21, 963–972.

Roth, M.E., Feng, L., McConnell, K.J., Schaffer, P.J., Guerra, C.E., Affourtit, J.P., Piper, K.R., Guccione, L., Hariharan, J., Ford, M.J., et al. (2004). Expression profiling using a hexamer-based universal microarray. Nat. Biotechnol. 22, 418–426.

Sadlish, H., Rampelt, H., Shorter, J., Wegrzyn, R.D., Andréasson, C., Lindquist, S., and Bukau, B. (2008). Hsp110 chaperones regulate prion formation and propagation in S. cerevisiae by two discrete activities. PLoS One 3, e1763.

Sailer, A., Büeler, H., Fischer, M., Aguzzi, A., and Weissmann, C. (1994). No propagation

of prions in mice devoid of PrP. Cell 77, 967–968.

Satpute-Krishnan, P., Langseth, S.X., and Serio, T.R. (2007). Hsp104-dependent remodeling of prion complexes mediates protein-only inheritance. PLoS Biol. 5, e24.

Scior, A., Buntru, A., Arnsburg, K., Ast, A., Iburg, M., Juenemann, K., Pigazzini, M.L., Mlody, B., Puchkov, D., Priller, J., et al. (2018). Complete suppression of Htt fibrilization and disaggregation of Htt fibrils by a trimeric chaperone complex. EMBO J. 37, 282–299.

Shaner, L., Trott, A., Goeckeler, J.L., Brodsky, J.L., and Morano, K.A. (2004). The function of the yeast molecular chaperone Sse1 is mechanistically distinct from the closely related Hsp70 family. J. Biol. Chem. 279, 21992–22001.

Sindi, S.S., and Serio, T.R. (2009). Prion dynamics and the quest for the genetic determinant in protein-only inheritance. Curr. Opin. Microbiol. 12, 623–630.

Soto, C., Kascsak, R.J., Saborío, G.P., Aucouturier, P., Wisniewski, T., Prelli, F., Kascsak, R., Mendez, E., Harris, D.A., Ironside, J., et al. (2000). Reversion of prion protein conformational changes by synthetic b-sheet breaker peptides. Lancet 355, 192–197.

Tanaka, M., Chien, P., Naber, N., Cooke, R., and Weissman, J.S. (2004). Conformational variations in an infectious protein determine prion strain differences. Nature 428, 323–328.

Tanaka, M., Collins, S.R., Toyama, B.H., and Weissman, J.S. (2006). The physical basis of how prion conformations determine strain phenotypes. Nature 442, 585–589.

Tessarz, P., Mogk, A., and Bukau, B. (2008). Substrate threading through the central pore of the Hsp104 chaperone as a common mechanism for protein disaggregation and prion propagation. Mol. Microbiol. 68, 87–97.

Tipton, K., Verges, K., and Weissman, J. (2008). In vivo monitoring of the prion replication cycle reveals a critical role for Sis1 in delivering substrates to Hsp104. Mol. Cell 32, 584–591.

Toyama, B.H., Kelly, M.J.S., Gross, J.D., and Weissman, J.S. (2007). The structural basis of yeast prion strain variants. Nature 449, 233–237.

Trotter, E.W., Kao, C.M.F., Berenfeld, L., Botstein, D., Petsko, G.A., and Gray, J. V. (2002). Misfolded proteins are competent to mediate a subset of the responses to heat shock in Saccharomyces cerevisiae. J. Biol. Chem. 277, 44817–44825.

Verghese, J., Abrams, J., Wang, Y., and Morano, K. a (2012). Biology of the heat shock response and protein chaperones: budding yeast (Saccharomyces cerevisiae) as a model system. Microbiol. Mol. Biol. Rev. 76, 115–158.

Wegrzyn, R.D., Bapat, K., Newnam, G.P., Zink, A.D., and Chernoff, Y.O. (2001). Mechanism of Prion Loss after Hsp104 Inactivation in Yeast. Mol. Cell. Biol. 21, 4656–4669.

Winkler, J., Tyedmers, J., Bukau, B., and Mogk, A. (2012). Hsp70 targets Hsp100 chaperones to substrates for protein disaggregation and prion fragmentation. J. Cell Biol. 198, 387–404.

Zheng, X., Krakowiak, J., Patel, N., Beyzavi, A., Ezike, J., Khalil, A.S., and Pincus, D.

(2016). Dynamic control of Hsf1 during heat shock by a chaperone switch and phosphorylation. Elife 5, e18638.

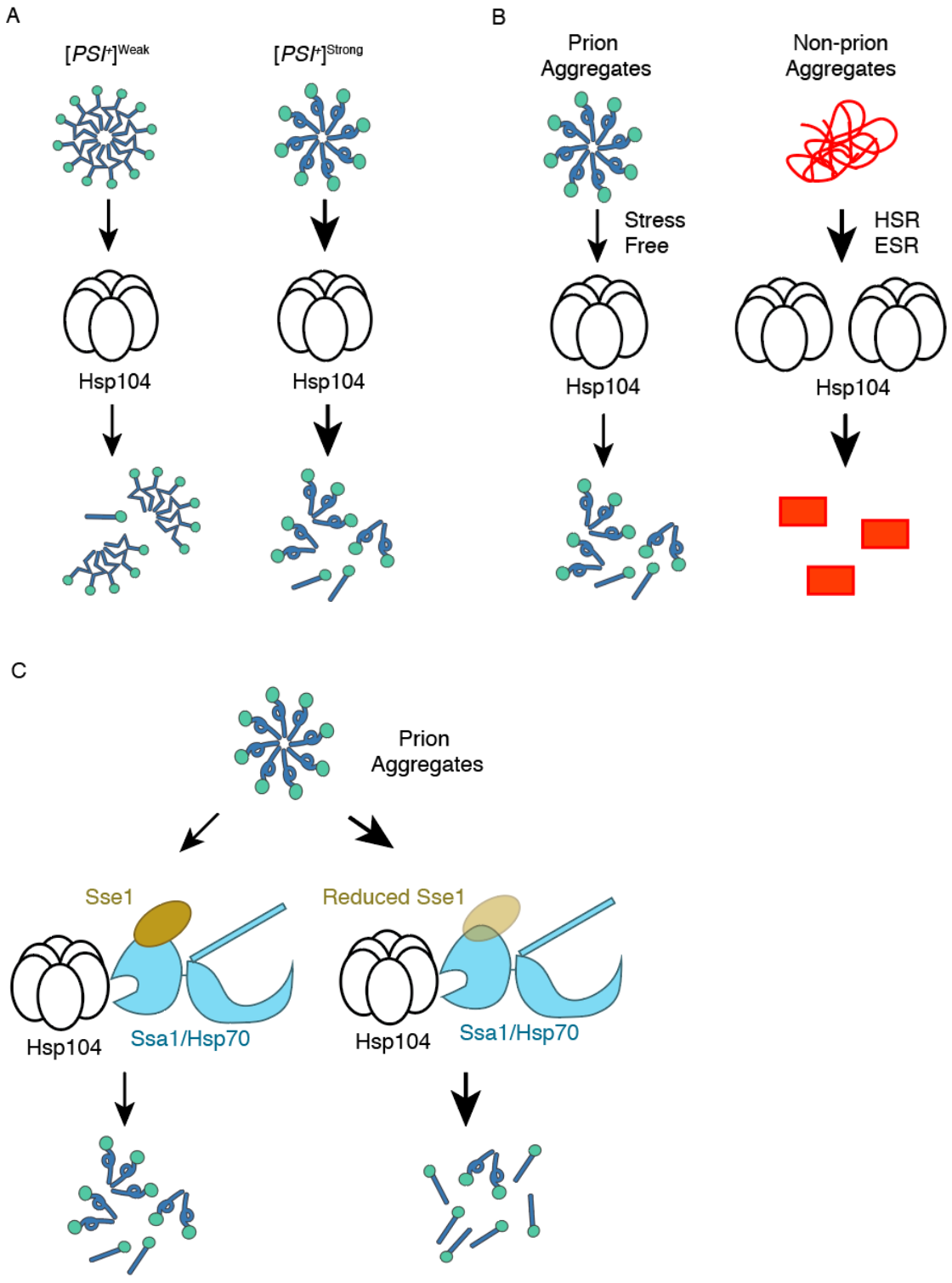

Figure 1. Cellular limitations in disassembling prion aggregates.

(A) The primary limitation of amyloid clearance lies in the physical properties of amyloid aggregates, which dictate their sensitivity to fragmentation and amplification efficiency. Compared to [*PSI*+]$_{Weak}$, [*PSI*+]$_{Strong}$ prion aggregates are fragmented by Hsp104 more efficiently. (B) The lack of sensing amyloid aggregates represents another major cellular limitation. Unlike non-prion aggregates, which can activate heat shock response (HSR) or environmental stress response (ESR) and are rapidly resolved thereafter, prion aggregates fail to trigger a stress response and are partially processed by the PN. (C) Chaperone configuration represents a potentially critical cellular limitation. Despite the normal level of the nucleotide exchange factor of Hsp70 - Sse1 supports the optimal resolution of non-amyloid aggregates, reducing its level reconfigures the fragmentation machinery to boost amyloid clearance.